

Styles of Deformation in Ishtar Terra and Their Implications

WILLIAM M. KAULA,¹ DUANE L. BINDSCHADLER,¹ ROBERT E. GRIMM,^{2,3}
VICKI L. HANSEN,² KARI M. ROBERTS,⁴ AND SUZANNE E. SMREKAR⁵

Ishtar Terra, the highest region on Venus, appears to have characteristics of both plume uplifts and convergent belts. Magellan imagery over longitudes 330°-30°E indicates a great variety of tectonic and volcanic activity, with large variations within distances of only a few 100 km. The most prominent terrain types are the volcanic plains of Lakshmi and the mountain belts of Maxwell, Freyja, and Danu. The belts appear to have marked variations in age. There are also extensive regions of tessera in both the upland and outboard plateaus, some rather featureless smooth scarps, flanking basins of complex extensional tectonics, and regions of gravitational or impact modification. Parts of Ishtar are the locations of contemporary vigorous tectonics and past extensive volcanism. Ishtar appears to be the consequence of a history of several 100 m.y., in which there have been marked changes in kinematic patterns and in which activity at any stage has been strongly influenced by the past. Ishtar demonstrates three general properties of Venus: (1) erosional degradation is absent, leading to preservation of patterns resulting from past activity; (2) many surface features are the responses of a competent layer less than 10 km thick to flows of 100 km or broader scale; and (3) these broader scale flows are controlled mainly by heterogeneities in the mantle. Ishtar Terra does not appear to be the result of a compression conveyed by an Earthlike lithosphere. But there is still doubt as to whether Ishtar is predominantly the consequence of a mantle upflow or downflow. Upflow is favored by the extensive volcanic plain of Lakshmi and the high geoid: topography ratio; downflow is favored by the intense deformation of the mountain belts and the absence of major rifts. Both could be occurring, or have recently occurred, with Lakshmi the most likely locus of upflow and Maxwell the main locus of downflow. But doubts about the causes of Ishtar will probably never be resolved without circularization of the Magellan orbit to obtain a more detailed gravity field.

1. INTRODUCTION

Ishtar Terra is of special interest as the most prominent departure from hydrostatic equilibrium on Venus. The peak of Maxwell Montes is 10 km above the mean planetary radius (MPR), which outstrips the second highest feature, Maat Mons in Atla Regio, by more than a kilometer. This promontory is part of a general uplands more than 3 km high in topography and more than 20 m high in geoid, with a horizontal extent of about 4000 km: about 1% of the planet's surface area. These uplands have sharply defined boundaries in most places and significant variations in character on scales of 200 to 1000 km. The variety of terrains is evident in the imagery, of which Figure 1 is a mosaic. The immediate causes of most of these variations are evident: lava flows for the smooth plains of Lakshmi Planum, convergent motions for the surrounding mountain belts of Maxwell, Freyja, Akna, and Danu [Masursky *et al.*, 1980; Barsukov *et al.*, 1986]. But there are differences among these physiographic provinces of varying subtlety, and for some features (e.g., the smoothness of the scarps bordering eastern Lakshmi) the proximate cause is not at all evident. Nearly all papers in this special issue are devoted to particular feature types; it is our belief that one directed to an area markedly anomalous, but widely ranging in character, would be a valuable complement.

The main physiographic provinces of western Ishtar Terra are shown in Figure 2. Our discussion will be confined, however, to the parts of Ishtar Terra between 330°E and 30°E: i.e., those imaged by the Magellan radar between the start of the mission and the start of the first

superior conjunction hiatus. If we take the 3-km elevation contour as the limit, then the latitudinal bounds would be about 55°N to 78°N. However, tectonic patterns associated with Ishtar Terra extend to superior conjunction hiatus. If we take the 3-km elevation contour as the limit, then the latitudinal bounds would be about 55°N to 78°N. However, tectonic patterns associated with Ishtar Terra extend to lower elevations in many places. Within these longitude and latitude boundaries, we identify seven major provinces: Lakshmi, Danu, Freyja, North Scarp and Basin, South Scarp and Basin, Maxwell, and Western Fortuna. Each province is named after its dominant feature, but the province includes other named features that have close relationship to the dominant feature: e.g., the province "Danu" includes not only Danu Montes but also Vesta Rupes, Clotho Tessera, and parts of Lakshmi Planum and Sedna Planitia.

Important to interpretation of the imagery are topographic altitudes and gravity variations. Figure 3 gives the Magellan altimetry for the area discussed in the form of contours at 0.5-km intervals. Superimposed on it is the geoid from the 36th degree field of Smith and Nerem [1992], based on Pioneer Venus tracking data. The spacecraft was 700-2200 km high at these latitudes, so the signal is bland, and the geoid high probably shifted toward the pericenter, i.e., southward. A regional gravity solution by Grimm and Phillips [1991] also obtains a geoid high to the south of Ishtar but somewhat west of that in Figure 3. For interpretation of Ishtar Terra, circularization of the Magellan orbiter to an altitude of about 250 km is required.

Ishtar Terra's great height, broad extent, and particularly its large geoid anomaly require appreciable support from mantle convection. But even the first-order nature of this dependence (upflow or downflow, or combinations thereof) is debated [Pronin, 1986; Bindshadler *et al.*, 1990; Grimm and Phillips, 1990, 1991; Roberts and Head, 1990a,b; Lenardic *et al.*, 1991]. Examination of the Magellan imagery should help to address these questions. Ideally, such an examination would result in a kinematic map of the surface, analogous to those inferred on Earth from remanent magnetism, dated offsets of interfaces, and other devices. The clues to motions on Venus are much more limited. Furthermore, the immediate causes of surface features often are quite indirect in their relationships to any mantle flow pattern. This indirectness is most evident for the lava

¹Department of Earth and Space Sciences, University of California, Los Angeles.

²Department of Geological Sciences, Southern Methodist University, Dallas, Texas.

³Now at Department of Geology, Arizona State University, Tempe.

⁴Department of Geological Sciences, Brown University, Providence, Rhode Island.

⁵Department of Earth, Atmospheric, and Planetary Sciences, Massachusetts Institute of Technology, Cambridge.

Copyright 1992 by the American Geophysical Union.

Paper number 92JE01643.
0148-0227/92/92JE-01643\$05.00

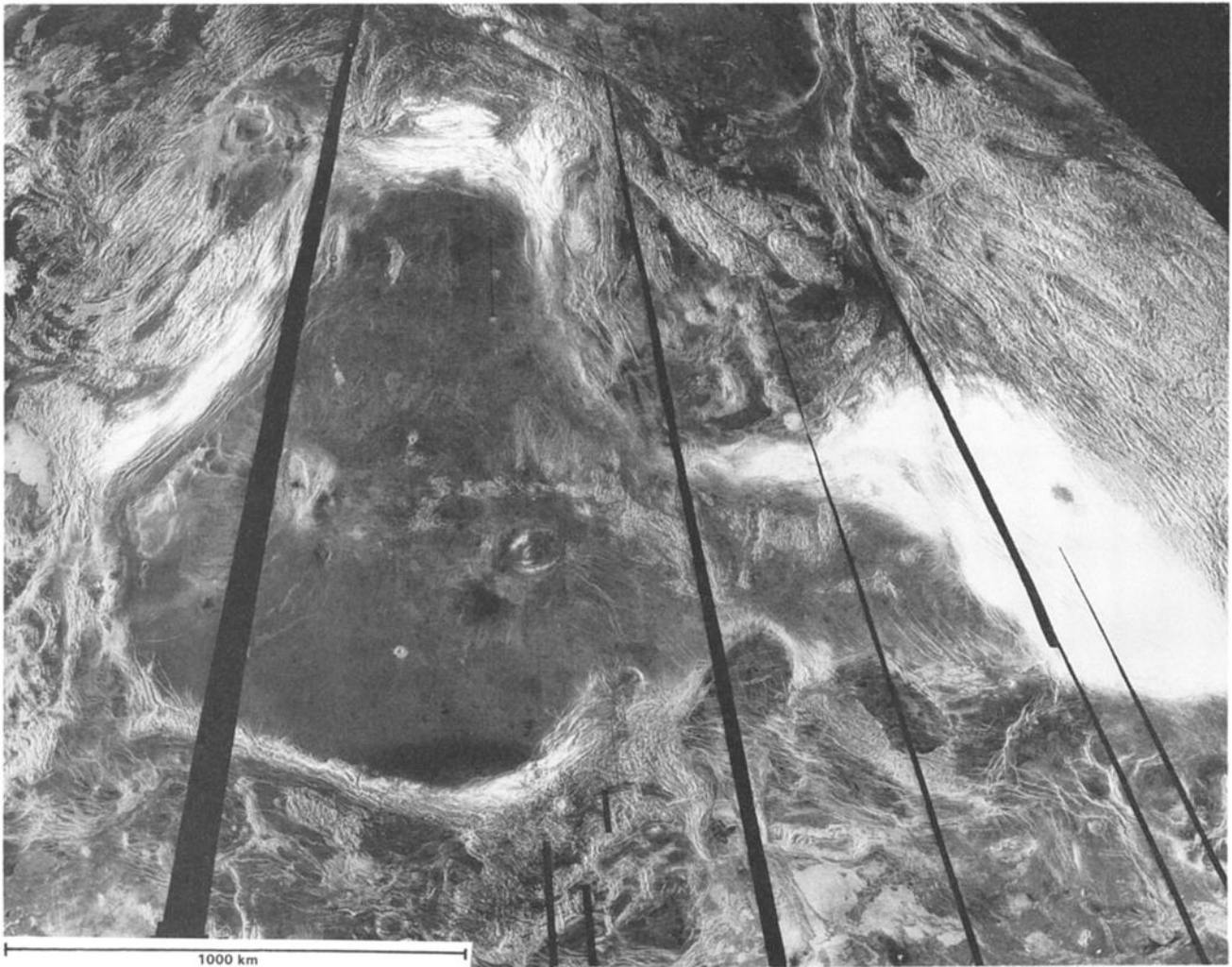


Fig. 1. Western Ishtar Terra. Latitudes 55°-80°N, longitudes 300°-30°E. From C2-MIDRP.60N333E.

flows covering the Lakshmi plateau, but it is also true for the variations on a 10-km scale in the mountain belts, arising from the weakness of the lower crust, as occurring in many parts of Venus [Zuber, 1987; Solomon *et al.*, this issue].

The variety of features in Ishtar Terra compels a somewhat segmented approach. Section 2 is the major part of this paper, which contains detailed description and interpretation for each of the seven provinces. Section 3 draws on section 2 to identify and interpret characteristic feature types. Section 4 attempts to infer the contemporary structure and kinematics of Ishtar Terra, plus the evolution leading thereto.

2. ANALYSES OF PHYSIOGRAPHIC PROVINCES

These analyses are varied in form not only because of the differences in character among the seven provinces (Figure 2) but also because the effort was necessarily divided among coauthors. For purposes of description, we divide the provinces into 28 regions, some of them evident in Figure 2, others defined on the geomorphic unit maps.

The following are principal data sources:

1. The radar imagery is conveyed through digital images or photo prints that are of the minimum scale at which the emulsion can carry the 75-meter resolution: 1:3,000,000. They are designated F-MIDRP.jkNlmn, where *jk* is the north latitude and *lmn* is the east longitude of the center point to the nearest integer degree. Their

projection is sinusoidal. Twenty-one F-MIDRPs are available for Ishtar Terra. The images printed in this paper are nearly all segments of F-MIDRPs. However, they offer a rather selective view, so the serious reader is urged to consult the original F-MIDRPs, obtainable on compact discs from the NSSDC at NASA Goddard Space Flight Center or from a Planetary Data Center.

2. The radar altimetry by Magellan is conveyed through 1:4,500,000 contour plots of 500-m interval; see Figure 3.

3. The gravimetry for Ishtar Terra is of low resolution but nonetheless has a strong influence on our interpretations; see Figure 3.

The main systematic products of these analyses are geomorphic units: characteristic combinations of features identified in the imagery and altimetry that cover sufficient areas to be represented on 1:5,000,000-1:20,000,000 scale maps. See Table 1.

For some areas, we present delineations of structural features and histories. But it is difficult to make a systematic map for as broad an area as Ishtar Terra, so they have been limited to selected areas. The ability to infer histories varies from one province to another, dependent on how overwhelming has been recent activity: tectonic, volcanic, or impact. Thus provinces with a variety of features of relatively mild relief, such as South Scarp and Basin and Danu montes, have more clues of the past than do Lakshmi Planum, which has been largely flooded by relatively recent flows, and Maxwell Montes, whose faults and folds appear to arise largely from contemporary tectonics.

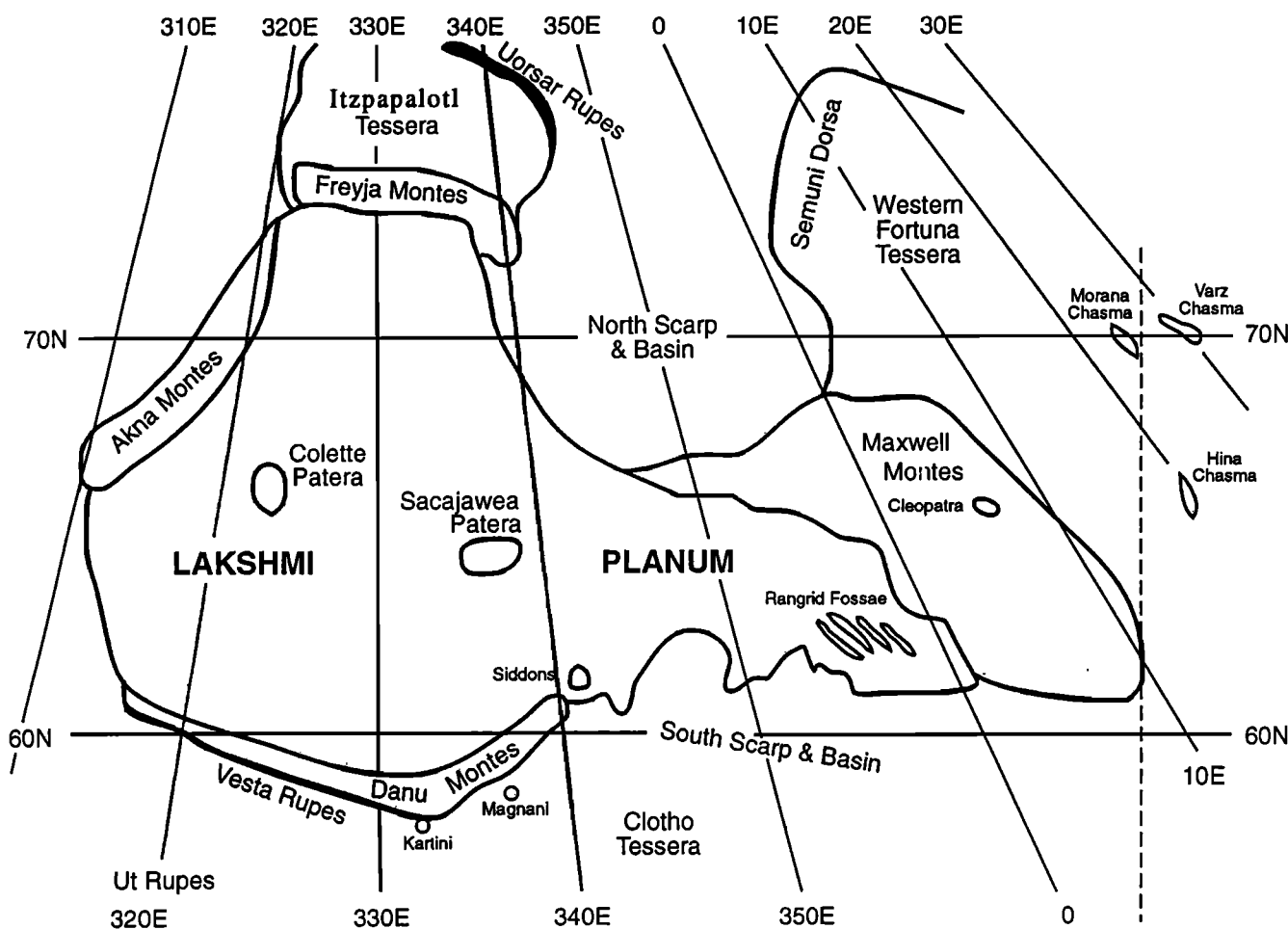


Fig. 2. Sketch map of western Ishtar Terra. A degree of latitude is 105.6 km long; in the latitudes of Ishtar Terra, a degree of longitude varies from 61 km to 22 km. The dashed line indicates the eastern limit of Figure 1.

2.1. Lakshmi

Lakshmi Planum is a broad, smooth area rising from a height of 2.5 km above mean planetary radius (MPR), just north of Danu Montes, around 60°N, 334°E, to almost 5.0 km along the edges of Freyja (73°N, 330°E) and Maxwell Montes (66°N, 355°E). Correlated with elevation is the frequency of appearance of ridged terrain. Lava flows dominate the entire plain, with relatively little to be inferred in the way of structural relationships. Hence, in Lakshmi Planum a description by geomorphic units, as given in Table 1, is appropriate; see Figures 4 and 5.

Sacajawea (Figures 6 and 7; F-MIDRPs 65N330, 65N342). Sacajawea (64.5°N, 336.5°E) is a volcanic caldera previously described from the Arecibo and Venera imagery [Barsukov *et al.*, 1986; Stofan *et al.*, 1987; Roberts and Head, 1990a] and most recently from the Magellan imagery [Head *et al.*, 1991, this issue]. It is a 260 x 175 km depression 2 km deep. The depression is enclosed by a zone of concentric troughs that extends 60-130 km from the caldera floor. Individual troughs are 1-2 km wide, are 4-100 km long, and spaced about 3 km apart. These features are thought to be related to broad sagging and downward warping of the plateau above a partially drained and solidified shallow crustal magma reservoir [Head *et al.*, 1991]. The floor of the caldera is covered by smooth, mottled plains (Sp). The brightest deposits are observed about the periphery and in the center of the caldera floor, where a ponded, leveed flow appears to have been one of the latest eruptions within the caldera. Linear to sinuous ridges and scarps (centered at 64°N, 340°E) extend up to 250 km from the eastern edge of the caldera, trending approximately N60°W (Figure

7). These structures are 1-3 km wide and spaced 3-10 km apart. A volcanic shield 11 km in diameter (63.95°N, 339.5°E) is situated along the trend of one of these features. The association of the ridges and scarps with the caldera and volcanic shield led Roberts and Head [1990a] and Head *et al.* [1991] to suggest that they represent a zone of dike intrusion along which magma has been injected and erupted at the surface.

Sacajawea appears to lack the distinctive apron of lobate flows that surrounds Colette, a large shield and caldera complex located in western Lakshmi [Stofan *et al.* 1987; Roberts and Head, 1990a]. A faint region of mottled, lobate flows (Pl) is associated with the ridges and scarps trending SE from the caldera. An additional region of mottled, lobate flows (Pl and P_{sd}) is located to the SW of the caldera (63.5°N, 333°E). This region was identified as a "vent complex" by Roberts and Head [1990a,b] from the Venera data, since it appeared to consist of a cluster of small volcanic shields. These shields are not all as clearly observed in the Magellan images, perhaps because of a higher incidence angle (22°) than that of the Venera orbiters (10°) [Pettingill *et al.*, this issue], and thus are less sensitive to slight slopes. These regions appear to contain the only lava flows associated with Sacajawea that are distinct from the general plains of Lakshmi.

Ridged terrain (Tr) (Figures 8 and 9; F-MIDRPs 65N330, 65N342, 65N354). The ridged terrain east of Sacajawea has an extremely complex structural fabric, with extensive embayments. It is hypothesized to be the exposed portions of tesserallike bedrock underlying the plains of Lakshmi [Roberts and Head, 1990a]. Exposures are found primarily at higher elevations than most of Lakshmi, in the area

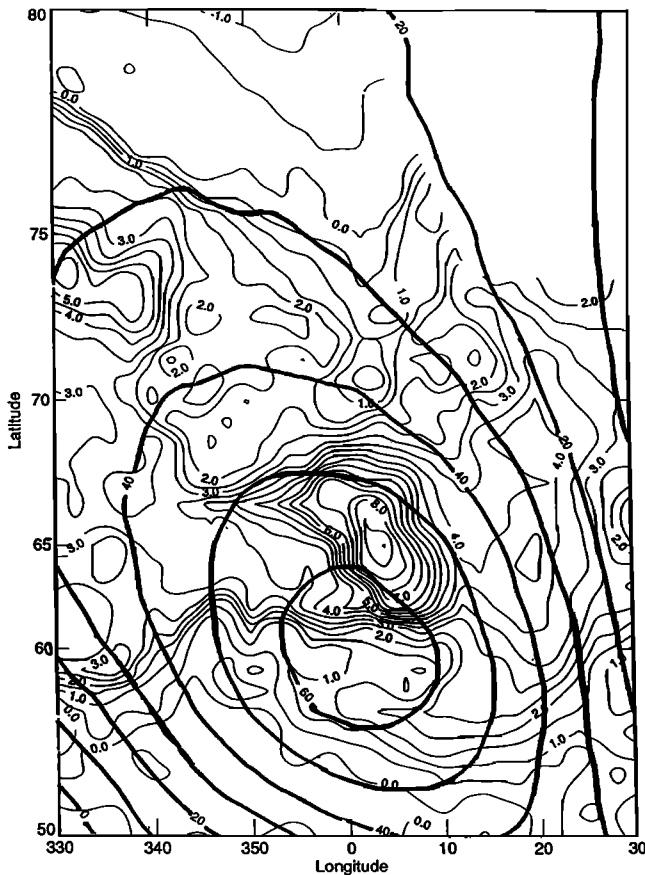


Fig. 3. Topographic altitudes in kilometers (fine lines, 0.5-km interval) and geoid heights in meters (heavy lines, 10-m interval). The altitudes are from Magellan altimetry with track spacing of 13 km or less (See also Figures 16 and 17 of *Solomon et al.* [this issue]). The geoid is obtained by analysis of Pioneer Venus tracking [Smith and Nerem, 1992]. The spacecraft altitude was 700 to 2200 km, south to north, over the latitudes of this map. The analysis technique ("a priori sigmas") tends to show any extremum closer to pericenter (i.e., more south) than its actual location.

63°-66°N, 330°-357°E. Magellan imagery shows more heavily flooded portions of ridged terrain than seen in the Venera data, consistent with the hypothesis that this unit forms the basement of the entire plateau. The two largest exposures of ridged terrain (Tr) are centered at 65°N, 343°E (Figure 8), and 65°N, 351°E (Figure 9). These exposures contain three major lineament orientations, also observed in the Venera imagery [Roberts and Head, 1990a].

1. The first is NW trending troughs. Troughs oriented N45°-50°W of variable width and spacing are observed in the eastern exposure (Figure 9). Broad troughs with grabenlike morphology are observed throughout the exposure, many of them extensively flooded by volcanism. They are 2-3 km wide, 5-25 km apart, and up to 130 km in length. The maximum lengths are obscured by flooding. Several of these troughs extend beyond the Tr unit boundary into the surrounding plains. Near 64.2°N, 351°E a trough is associated with a series of rounded "levees," similar in appearance to spatter ramparts observed along terrestrial basaltic fissure eruptions. This association suggests that some of the volcanic resurfacing on Lakshmi may have been fissure-fed, with fissures emplaced along preexisting zones of weakness in the bedrock tessera. Narrower troughs or fractures less than 1 km in width are also observed. These closely spaced structures are less than 1 km apart and form a pervasive fabric in the eastern exposure. East of 350°E many of these fractures extend into the surrounding plains, as do the broader troughs mentioned above.

Troughs and scarps oriented N50°-60°W are observed in the western large exposure of Tr. These structures are not as distinctive as those in the eastern exposure, possibly due to lower amounts of volcanic infill that highlights the grabenlike troughs to the east. This is consistent with the observation that this exposure of ridged terrain (Tr) is slightly higher, on the average, than the eastern exposure. The typical spacing and width of these structures are so narrow that they form a fine NW-trending linear fabric of scarps and lineaments, some of them clearly troughs. Their widths are from less than 1 km to 10 km, with spacings of 1 to 5 km. Their lengths are up to 180 km, but the maximum length is obscured by flooding. The wider troughs are often filled by lavas, suggesting that the minimum width is also obscured by flooding. Some of these structures extend into the region of fractured terrain (Tf) to the NW.

2. The second is NE trending lineaments. Ridges, scarps, and troughs oriented N20-30°E are observed in the eastern exposure of ridged terrain. These structures are 1-4 km in width and spacing. They appear to be highly degraded and flooded narrow troughs. Faint ridges with similar orientations and morphologies are observed partially buried in the surrounding plains and may represent more heavily flooded regions of the unit.

Troughs oriented N45°60°E are observed in the western exposure of ridged terrain (Tr). These structures are similar in morphology to the NW-trending troughs and scarps but are not as pervasively distributed. They are concentrated in the western end of the exposure, near 65.6°N, 341°E, where they are partially flooded by lavas. Widths and spacings are approximately 1-5 km.

3. The third is approximately N-S trending lineaments. Broad troughs (about 3 km wide, spaced 20-40 km, more than 100 km long and oriented N0°-10°W to N0°-10°E) are observed throughout the eastern exposure of ridged terrain. These troughs are heavily degraded, and appear to be crosscut by most of the other structures in this exposure. To the west, highly degraded troughs, scarps and ridges oriented N0-15°W are observed. Many of them appear to be flooded and crosscut or offset along strike (e.g., 65.8°N, 341°E). These structures are clustered in three locations (63.8°N, 346°E; 65.6°N, 344.5°E; 66°N, 339.5°E); Their spacings are 2-4 km; grabenlike troughs are less than about 4 km wide, while the ridges and scarps are 1-3 km wide. Lengths exceed 100 km. Some of these structures extend into the plains to the north and into the region of fractured terrain to the NW.

Orientations of structures within the smaller exposures of ridged terrain (Tr) are difficult to measure precisely, but they appear to be similar to those of the structures in the larger exposures.

Volcanism has flooded not only the margins but also the interior of ridged terrain. A few small pits and a chain of pits are observed that may be local volcanic sources (e.g., 65.15°N, 349.7°E).

Fractured Terrain (Tf) (Figure 8; F-MIDRPs 65N330, 65N342, 70N339). This terrain was originally mapped from Venera imagery as a "grooved plains" unit by Roberts and Head [1990a]. It was interpreted by Pronin [1986] to be a system of faults formed under tension: see Figure 8. The fractured terrain, concentrated 250 km north of Sacajawea (67°N, 338.5°E), consists of linear to curvilinear fractures and troughs trending along three dominant orientations: N25°-30°W, N25°-30°E, and N0°-5°E. These structures range in width from less than 1 km to 3 km; 1-1.5 km is typical. Their spacing varies from 1 to 25 km, but usually it is less than 5 km. Their lengths extend at least 150-225 km. The boundary between exposures of fractured terrain and ridged terrain is transitional. There is a gradual change from the rugged relief of the western large exposure of ridged terrain and the lower relief of fractured terrain, which is essentially characterized by plains cut by fractures and troughs.

TABLE 1. GEOMORPHIC UNITS

Name & Symbol	Definition	Interpretation	Archetype	
			Latitude	Longitude
Chasma (Ch)	canyon, 10-60 km wide, >1 km deep, >150 km long, steep walls and usually a rough floor, with anastomosing lineations	large scale extension, sometimes volcanically modified	64°N,	21°E
Impact crater (Im)	circular depression, raised hummocky rim, often multiple if radius >50 km; surrounded by irregular brightness to about three radii	bolide infall	66°N,	7°E
Mountain belt (Mb) Subtypes: With Deposits (Mbd) Troughs (Mbg)	parallel and subparallel ridges 10-30 km apart, very radar-bright alternating with less bright; some partly covered with deposit (Mbd), some with rectilinear troughs (Mbg)	large-scale compression with intense folding & overthrusting; chemical enhancement of brightness some gravitational modification	64°N, 65°N, 67°N,	2°E 7°E 0°E
Fractured plains (Pf)	smooth-appearing plains with bright lineations, < 0.5 km wide, up to 100 km long or more	volcanic flows with low strain fractures or joints	53°N,	336°E
Lobate plains (Pl)	plains with lobate deposits; ridges much less abundant than in Pr	volcanic flows	62.5°N,	332°E
Ridged plains (Pr) Subtype: Anastomosing (Pra)	smooth plains with many ridges that have broad, domical cross sections and crenulations along one side	mainly volcanic flows, followed by compression or fracturing	59°N, 60°N,	350°E 336°E
Smooth plains (Ps) Subtype: Dark (Psd)	smooth plains, in which individual flows are indistinguishable	low-viscosity, high-volume lava flows	70°N, 59°N,	334°E 331°E
Ridge belts (Rb)	Systems of roughly parallel ridges, sometimes intersecting, usually 20-40 km wide, 50-300 km, up to 1000 km long: radar bright against dark background	compression of pre-existing terrain, usually plains	73°N,	11°E
Plumose ridges (Rp)	narrow lineations at 2-3 km intervals against a darker background	moderate areal compression	62°N,	18°E
Caldera floor (Sp)	plains within a caldera	lava flows	64.5°N,	336°E
Chevron tessera (Tc) (=Tch)	tessera containing ridges 5-20 km spacing, but containing two distinct directions, intersecting at 50-100 km intervals, to make a chevron pattern	mainly compression, with a changing stress orientation	66°N,	25°E
Disrupted ridged terrain (Td) (=Tds)	many symmetric ridges, parallel to anastomosing; width 10-20 km, length < 4 times width; plus usually small (<6 km) troughs, intersecting ridges at many angles.	ridges by compression, troughs by extension.	58°N,	336°E
Fractured terrain (Tf)	complex ridged terrain dominated by two or more sets of steep-sided linear troughs or scarps	troughs by extension; scarps entail strike-slip, because of offsets	53°N,	336°E
Linear ridged terrain (Tl) (=Tlr=Tsr) Subtype: With deposits (Tlc)	many symmetric ridges, parallel to anastomosing; width 10-20 km, length well over 100 km. Usually paralleled by smaller ridges and troughs	compression, sometimes followed by surficial modification, by volcanic flow or impact ejecta	65°N, 66°N,	17°E 11°E
Ridged terrain (Tr)	complex structural fabric with two or more directions of lineaments; some with many embayments by smoother material.	varying tectonic stresses, both extensional and compressional; some followed by lava flooding.	65°N,	350°E

Some of the troughs in the fractured terrain (Tf) appear to continue up to 200 km beyond the mapped border of the unit into the northern plains, where they parallel the troughs at the NE border of the plateau (Figure 22). This extension suggests that fractured terrain may have once formed a more pervasive fabric on the plateau. The part preserved from flooding is a local topographic high, like the units of ridged terrain. Alternatively, these unusually long troughs may be related to the stresses associated with the unbuttressed plateau border and hence are not part of an underlying pervasive structural fabric.

Plains (Ps) (Figures 7, 8, 10, and 14; C1-MIDRPs 60N347, 75N338). The plains of Lakshmi are remarkably smooth and of generally uniform moderate radar brightness. Most of them lack distinctive lobate flows. Some local regions of brighter, lobate plains (Pl) are observed to the SE and SW of Sacajawea. In the central portion of the plateau (68°N, 330°E) these lobate plains perhaps are flows associated with Colette Patera. Near the edges of the plateau (e.g., 68°N, 341°E) they are associated with fractures that parallel the boundary. Regions of radar-dark, diffuse plains (Psd) are observed in

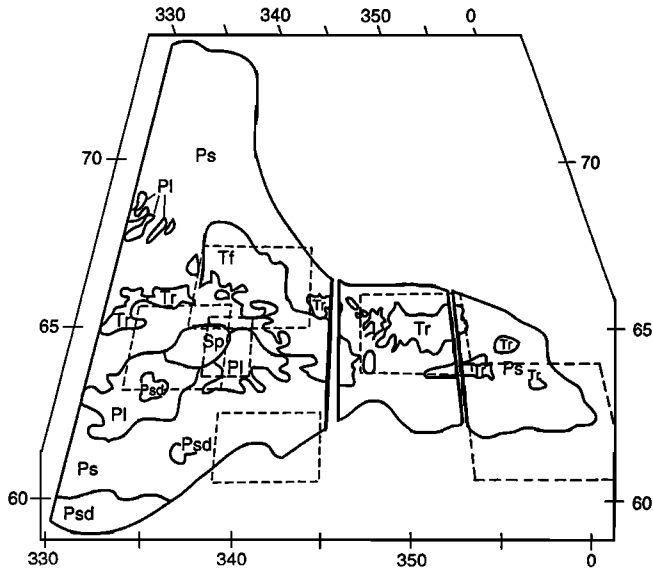


Fig. 4. Geomorphic map of Lakshmi Planum east of longitude 330°. Locations of Figures 6-11 are outlined. See Table 1 for definitions of geomorphic units.

association with the patch of lobate plains to the SW of Sacajawea and in the southern portion of the plateau, near the base of Danu montes (59.5°N, 330°336°E, Figure 14). The southern region of radar-dark plains appears to contain wind streaks trending NE-SW. These wind streaks may be soils from broken-down lavas blown into lows between ridges observed in this region.

Effusive volcanic eruptions are thought to produce the extensive regions of plains on Lakshmi. Recent analyses by *Head and Wilson [1992]* suggest that lavas erupted at the high elevations of Lakshmi may be highly vesicular and porous. Such flows may weather rapidly, producing relatively featureless (Ps) and radar-dark (Psd) plains as seen on Lakshmi. But there is no evidence in the radar reflection and emissivity of porosity from such vesiculation or from aeolian transport [*Pettengill et al., this issue*]. Hence the smoothness indicates low-viscosity flows.

Plains on Lakshmi have been deformed locally into ridges and troughs not only in the area of fractured terrain (Tf), which has been embayed and flooded by subsequent volcanic plains, but also along the plateau margins. Ridged plains were identified at the periphery of the plateau near the borders of Freyja, Maxwell, and Danu montes from the Venera data [*Roberts and Head, 1990a*]. Magellan data

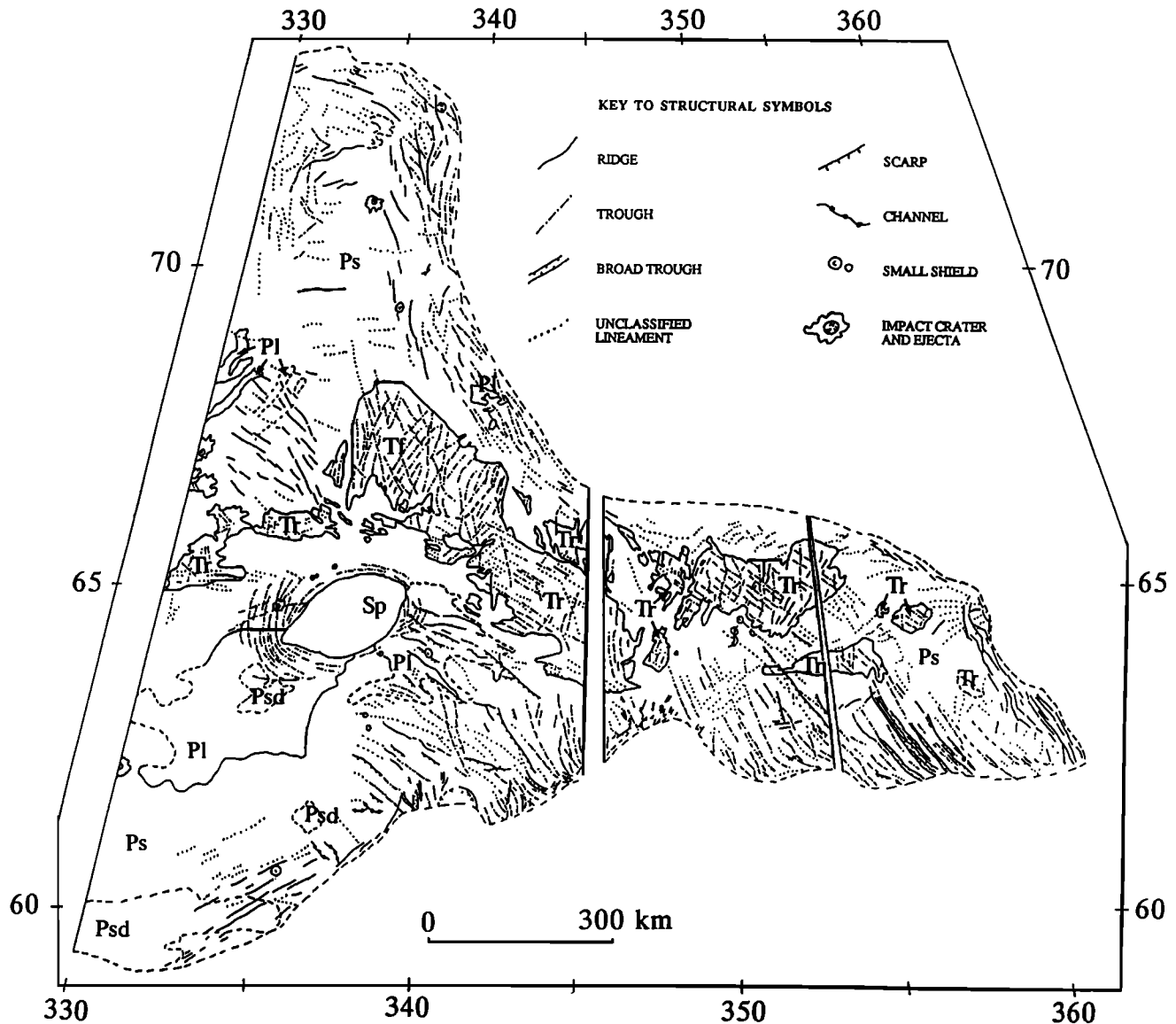


Fig. 5. Structural map of Lakshmi Planum east of longitude 330°.

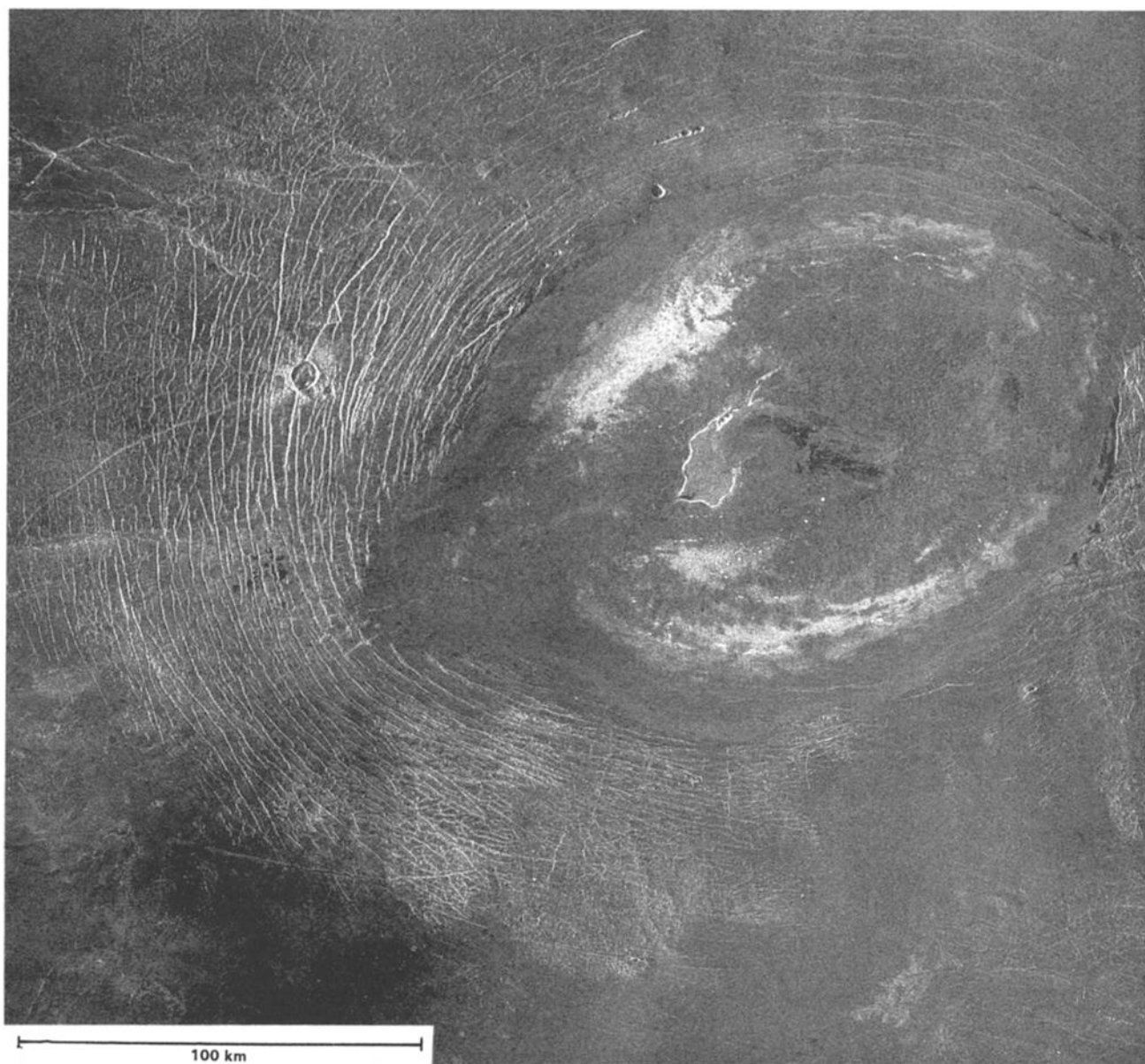


Fig. 6. Sacajewea Caldera. Latitude 63.1°-65.6°N, longitude 332.4°-338.3°E = 264 x 275 km. From F-MIDRPs 65N330 and 65N344.

reveal details of these features and the additional presence of troughs about the margins of Lakshmi (Figures 10 and 11). Ridges and troughs are observed south and west of Freyja Montes, west of Maxwell Montes, and north of Danu Montes and the southern edge of the plateau.

Broad arches and sinuous ridges parallel the mountains of Freyja from where the range trends eastwest (e.g., 73°N, 333°E) to where it curves more northsouth (71.4°N, 337°E). Widths range from less than 1 km to approximately 3 km. Spacing varies from 1-4 km to up to 10-20 km, decreasing toward the mountain belt. Ridges are up to 140 km in length. The most prominent ridges are observed where the altitude increases 0.5-1.0 km toward Freyja Montes. Troughs, many with grabenlike morphology, also parallel eastern Freyja and the border between Lakshmi and the North Basin and Scarp Province (e.g., 68°N, 341°E). These structures are 1-2 km wide, 40-200 km long, and spaced 3-10 km apart. They do not parallel northern Freyja, where the mountain range trends eastwest. There is a general transition from troughs nearest the edge of the plateau-North Basin boundary to ridges inboard of the plateau. The troughs may be the result of

relaxation of the plateau edge where it is unsupported by the North Basin, whereas ridges are probably related to compressional stresses associated with the formation of the mountain belt.

Faint EW trending lineaments similar to wrinkle ridges in morphology are observed in a zone extending south from Freyja to about 69°N, between longitudes 330°-337°E. These lineaments are characterized by broad arches up to 10 km in width and often have crenulated ridge crests about 600 m wide. They are spaced about 10 km apart and have lengths ranging from 50 to 200 km. Similar structures with more strongly developed ridge crests are observed south of 69.5°N, trending N30°-45°W. The origin of these structures is unclear but is thought to be related to some degree of crustal shortening.

Faint lineaments trending generally northsouth are observed in north central Lakshmi (71.2°N, 331°E). These structures are less than 1 km wide, up to 100 km long and spaced 1-5 km apart. The most prominent lineaments appear to be troughs. Shorter segments are often partially aligned, giving the appearance of an echelon fractures. The origin of these structures is also unclear. Sinuous ridges parallel the trend of Maxwell Montes at the western base of the mountain

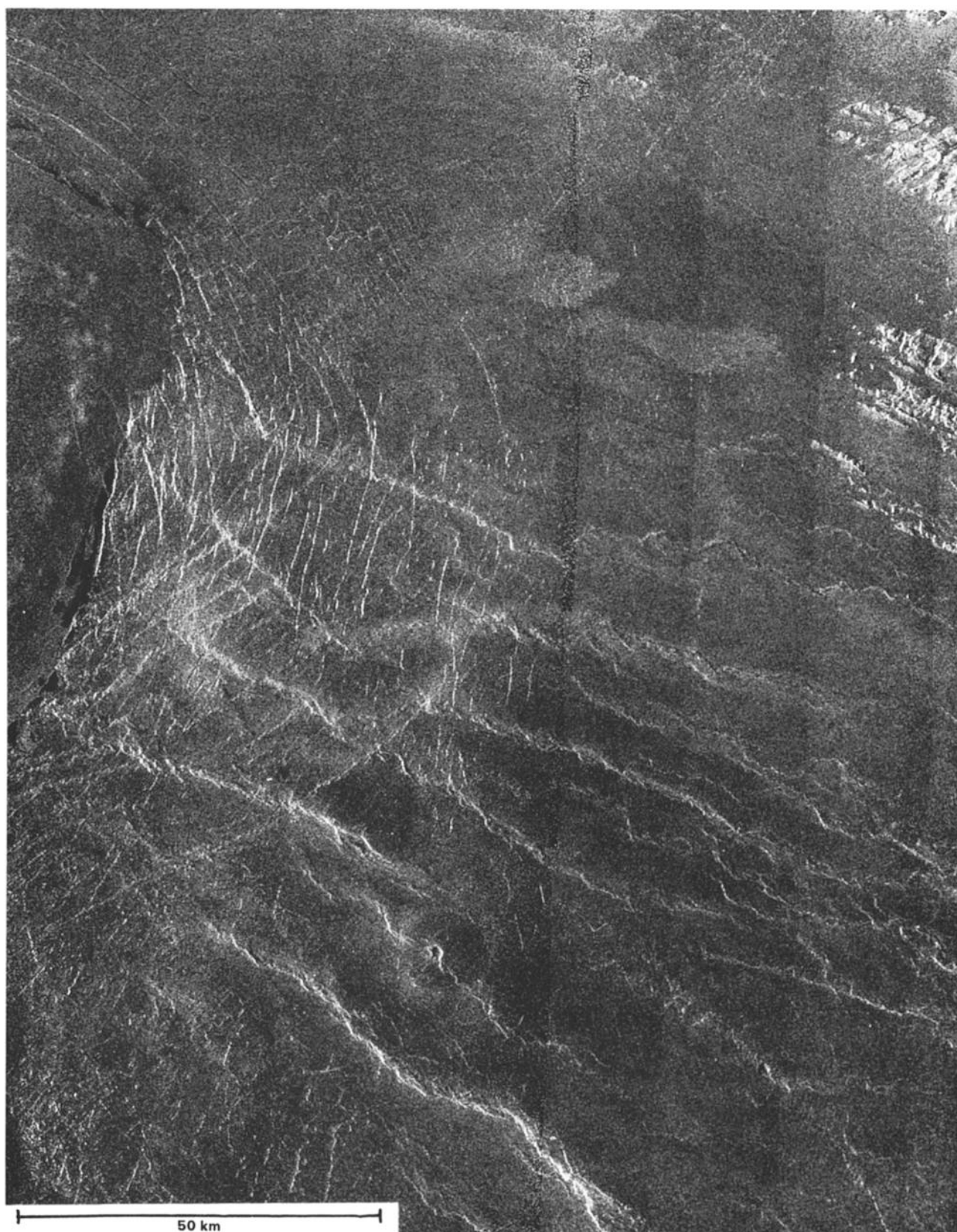


Fig. 7. Mottled lobate plains (Pl) and ridges and scarps trending SE of Sacajewea Caldera. Latitude 63.6°-65.2°N, longitude 337.5°-340.1°E = 170 x 119 km. From F-MIDRP.65N342.

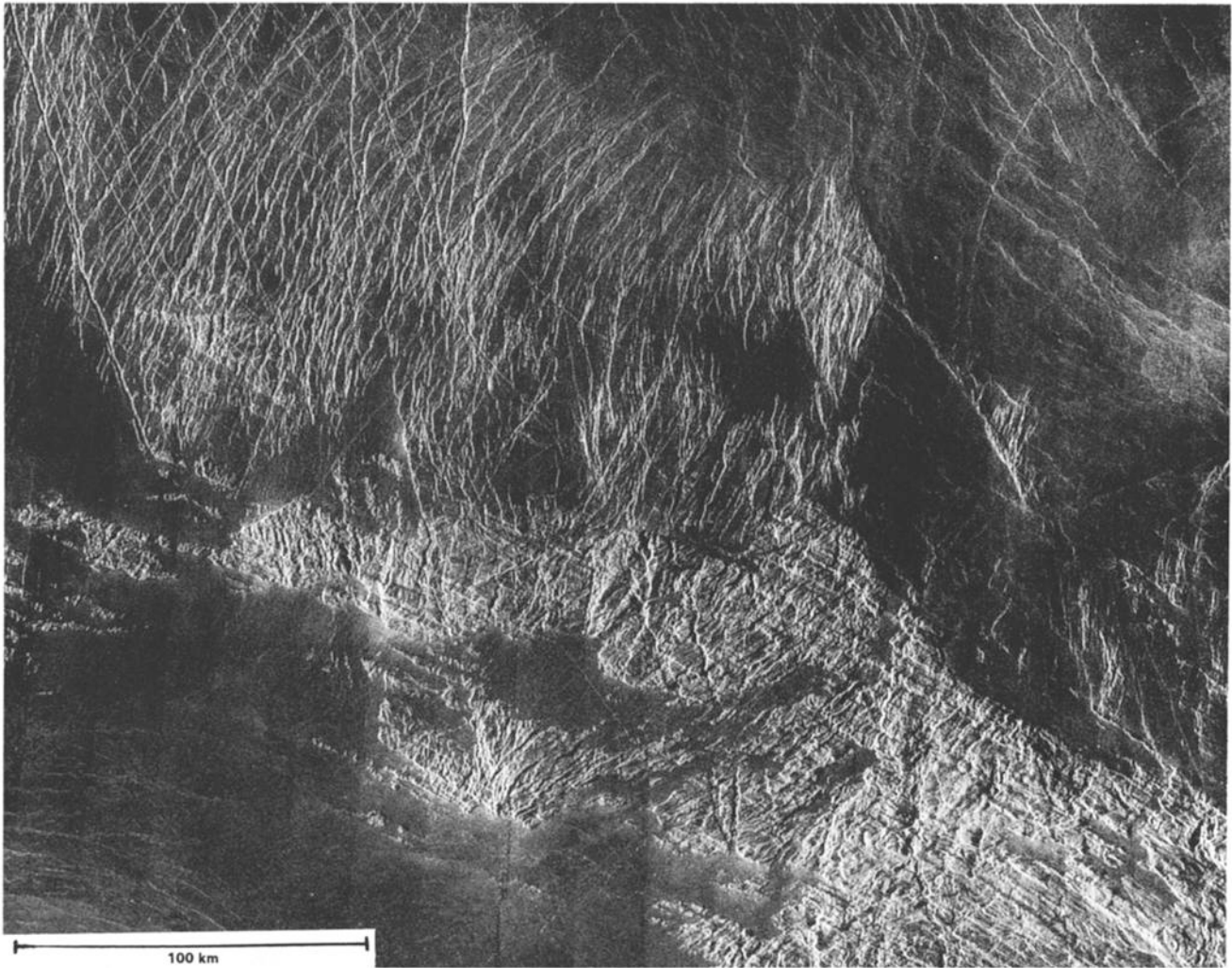


Fig. 8. Ridged terrain (Tr) in central Lakshmi Planum. Latitude 64.9°-67.5°N, longitude 336.0°-344.2°E = 275 x 352 km. From F-MIDRP.65N342.

range (Figure 10). These ridges are up to 4 km wide, 150-300 km long, and spaced 3-10 km apart. Their spacing decreases toward the mountain belt. These ridges are generally characterized by westfacing fronts that appear to be steeper than the eastfacing fronts, suggesting a possible thrust-fault origin. Ridges oriented radial to the mountain belt are observed at 64.5°N, 0°E. These ridges are similar in appearance to the ridges that parallel Maxwell; the reason for their peculiar orientation is not known.

Narrow, sinuous ridges and lineaments trending approximately N55°E parallel the ridges within Danu Montes northwest of the mountain belt (Figure 14). These features are less than 1 km wide and up to about 150 km long. Spacing varies from less than 2 to approximately 12 km, decreasing toward Danu. Extremely faint, closely spaced lineaments that parallel the trends of these ridges extend from near the base of Danu Montes 200 km into Lakshmi. These features are difficult to classify as ridges or troughs.

Closely spaced, linear to curvilinear troughs and lineaments are mapped along the border between Lakshmi and the South Scarp and Basin Province (Figure 10). These structures are oriented at large angles to the plateau edge, trending N30°-65°W (in contrast to the troughs which parallel the northern border of Lakshmi). These troughs occur in a region extending from 337°E to 2°E and south of about 64°N to the edge of Lakshmi (Figure 10). They are 75-270 km

in length and taper in width to the north. Widths range from 8 km to 600 m. Most of the troughs curve to the east near the edge of the plateau, although some curve to the west to form a complex, intersecting pattern of structures (e.g., 61.5°N, 343°E, Figure 11). These structures are best developed within local topographic highs along the southeastern edge of Lakshmi. Their spacing varies 1-10 km and is the most dense, with the narrowest widths, between longitudes 341° and 352°E (Figures 11 and 27). Troughs are widest and most distinctive within Rangrid Fossae (62.5°N, 358°E; Figure 10), and were previously observed in Venera imagery. The origin of these troughs may be related to relaxation of the unsupported plateau margin or deformation occurring at the plateau edge, either at Maxwell and/or south of Lakshmi within Danu Montes or the South Basin and Scarp Province [Ronca and Basilevsky, 1986; Vorder Bruegge *et al.*, 1990]. Some of these features resemble lava channels and sinuous rilles or are composed of chains of pits (e.g., 61.5°N, 340°E), suggesting an origin related to dike intrusion and eruption of lavas. Dike intrusion and surface fracturing also may be the cause of some of the other troughs, although this possibility seems inconsistent with the direction of taper; the troughs widen to the south, away from Colette and Sacajawea.

Two sizable calderas occur along the South Scarp, the southeastern border of Lakshmi Planum. Siddons, at 61.5°N, 341.5°E, is a nearly

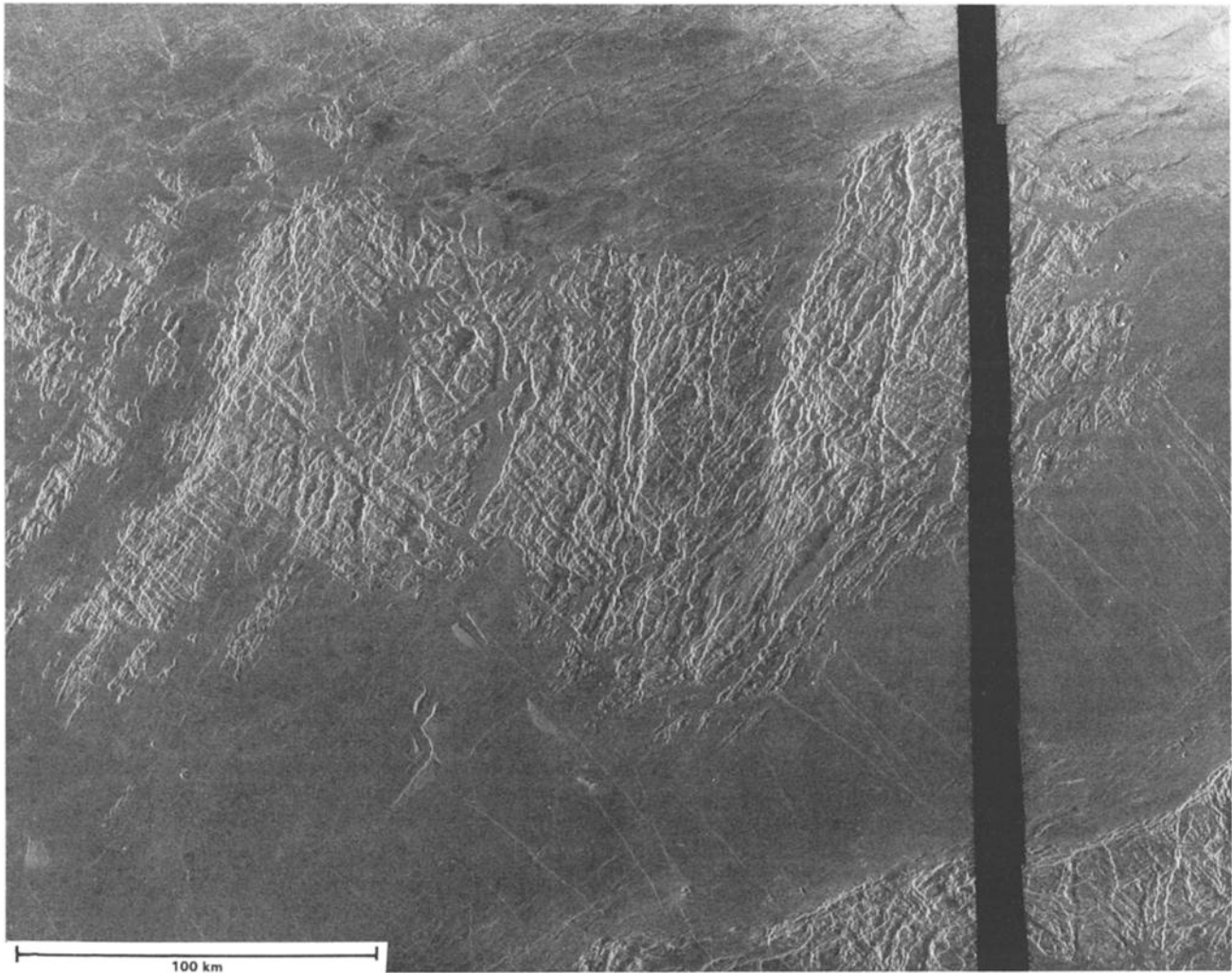


Fig. 9. Ridged terrain (Tr) and plains (Ps) in eastern Lakshmi Planum. Latitude 63.5° - 66.1° N, longitude 347.0° - 354.5° E = 270×337 km. From F-MIDRP.65N354.

circular depression 65 km in diameter (Figure 11). The northeast rim is well defined by multiple arcuate lineaments interpreted to be fault scarps; the southwest rim is not as well defined. Siddons has a dark interior from which radiate a series of very narrow lineaments. Siddons is not associated with any obvious flow features. The second caldera, at 61.4° N, 359° E, is an ellipse 40×20 km, with multiple concentric scarps and fractures (Figure 10). A number of smaller pits are distributed about the perimeter of this caldera, but there are no obvious flow features. Immediately to the south of this caldera is a quite featureless drop of about 2 km.

Kinematic Sequence (Figure 12). The relative ages of units mapped within Lakshmi Planum have been discussed by Roberts and Head [1990a]. Ridged terrain (Tr) units appear to be the oldest and form the underlying bedrock of the plateau. The formation of Sacajawea, Colette, and extensive plains units and the deformation of these plains units into fractured terrain and ridged plains appear to have overlapped in time. There appear to have been multiple stages of plains formation, deformation, and burial. Plains were emplaced and then deformed into ridges, fractures and troughs. Subsequent volcanism and plains formation partially embayed and flooded these structures (such as Tf). Continued deformation about the plateau margins produced additional ridges and troughs.

2.2. Danu

Danu Montes lies to the south of Lakshmi Planum and is the smallest mountain belt of Ishtar Terra. The scarp of Vesta Rupes bounds the westernmost edge of Lakshmi Planum as well as southwestern Danu Montes. Clotho Tessera is located to the southeast of Danu Montes. Below we describe and interpret the volcanism and deformation visible in radar images of southern Lakshmi Planum, Danu Montes, Clotho Tessera, and northern Sedna Planitia. Geomorphic units for this province are given in Figure 13.

Lakshmi Planum (Figure 14; F-MIDRP 60N334). As discussed in section 2.1, the portion of Lakshmi Planum just north of Danu Montes around 60° N, 334° E is remarkably smooth but not entirely featureless (Figure 14). Relevant to this subsection, there are flows that both cover and are cut by very narrow, anastomosing lineaments which roughly parallel ridges in western Danu Montes. These lineaments are up to 200 km in length and are spaced at 3-10 km (upper right of Figure 14).

Danu Montes (Figure 14; F-MIDRPs 60N334, 60N344). Danu Montes consists of a series of peaks which rise up to 2 km above Lakshmi Planum and drop steeply to the south, grading into Vesta Rupes and Clotho Tessera. The peaks are very radar-bright, probably

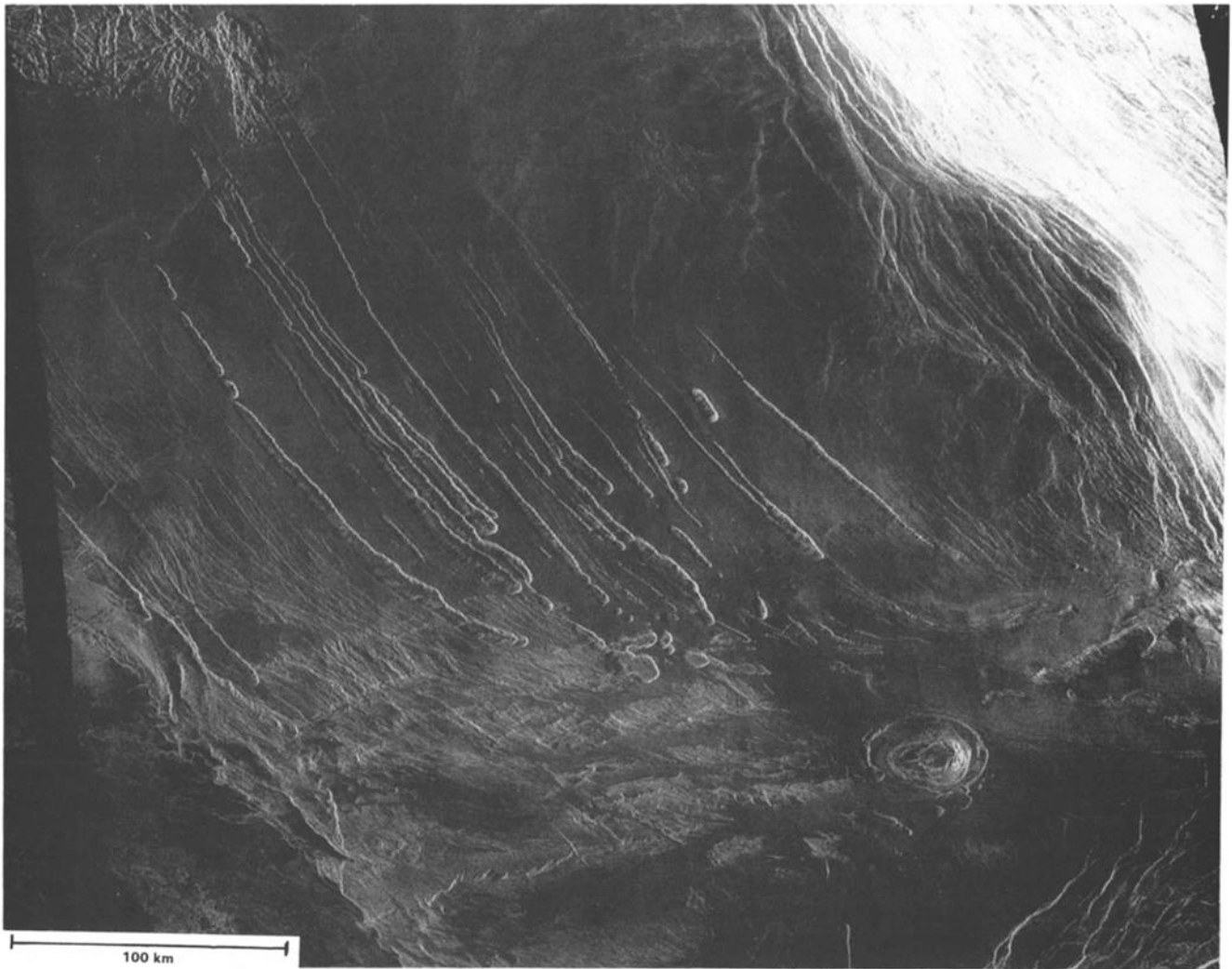


Fig. 10. Rangrid Fossae, troughs in southeastern Lakshmi Planum, and smooth plains (PI); also the South Scarp. Latitude 60.7°-64.0°N, longitude 354.0°-3.0°E = 350 x 450 km. From C1-MIDRP.60N347.

due to a combination of roughness and altitude-related changes in dielectric constant [Tyler *et al.*, 1991; Klose *et al.*, 1992]. The peaks consist of broad, curved, linear to lense-shaped ridges. Lenses are defined by either disrupted zones (bright, diffuse lineaments) or narrow, dark lineaments. The trend of the ridges curves from WNW-ESE in western Danu Montes to NE-SW to the east. Lens-shaped ridges are found at the intersection of the two trends, around 58.5°N, 334°E, with more elongated ridges to either side (Figure 14). These lenses range in size from 5 by 15 km to 10 by 30 km. There are also elongated ridges typically 5 km in width and up to 100 km in length e.g., at 60.5°N, 337°E. To the northeast, the ridges are cut by both EW-trending pit chains up to 100 km long and NW-SE trending troughs, with outflow channels, interpreted to be lava channels, approximately 50 km long [Solomon *et al.*, 1991]. Several pits, 1-5 km in diameter, are found in the range. These pits are probably volcanic in origin: they do not have ejecta deposits and often occur in a line. Possibly they are magma drains back into a dike below [Gundmanson, 1987; Burt and Head, 1991].

Vesta Rupes (Figure 14; F-MIDRP 60N334). *Vesta Rupes* is the steep slope southwest of Danu Montes. Within eastern *Vesta Rupes*, the dominant feature is a set of NWW-SEE trending faults spaced at 0.5-2 km with lengths of tens of kilometers. Several of these faults are

paired, forming narrow graben. Several longer scarps (about 100 km) with elevations of approximately several hundred meters parallel the smaller faults. One larger graben, 2 km wide and about 100 km long is centered at 58.6°N, 330°E. The trend of these faults is parallel to and, in one case, collinear with several pit chains which cut across *Clotho Tessera* and Danu Montes. A local, smaller set of NE-SW trending faults cut across the primary fault set. This secondary set of faults is similar in dimension to the small, numerous NW-SE trending features. In addition, near 58.2°N, 333.2°E there are two NNE-SSW trending graben, about 3 by 20 km. A degraded [Schaber *et al.*, this issue] 5 km impact crater, *Kartini* (57.8°N, 333°E; Figure 14), is located at the intersection of *Vesta Rupes* and *Clotho Tessera*: a remarkable coincidence with a change in tectonic trends.

Clotho Tessera (Figures 14 and 15; F-MIDRPs 60N334, 60N344, 55N337). *Clotho Tessera* is southeast of Danu Montes and is broader and gentler in slope than *Vesta Rupes*. It contains two regions with distinct morphologies. In southern *Clotho Tessera*, one linear trend is more pronounced than any other trend. This region is classified as ridged terrain (Tr, Figure 13). Just to the south of the lens-shaped ridges in Danu Montes, *Clotho Tessera* is highly disrupted, with no dominant trend. This area is mapped as disrupted terrain (Td, Figure 13). In this region, there is some continuation of the NW-SE and NE-

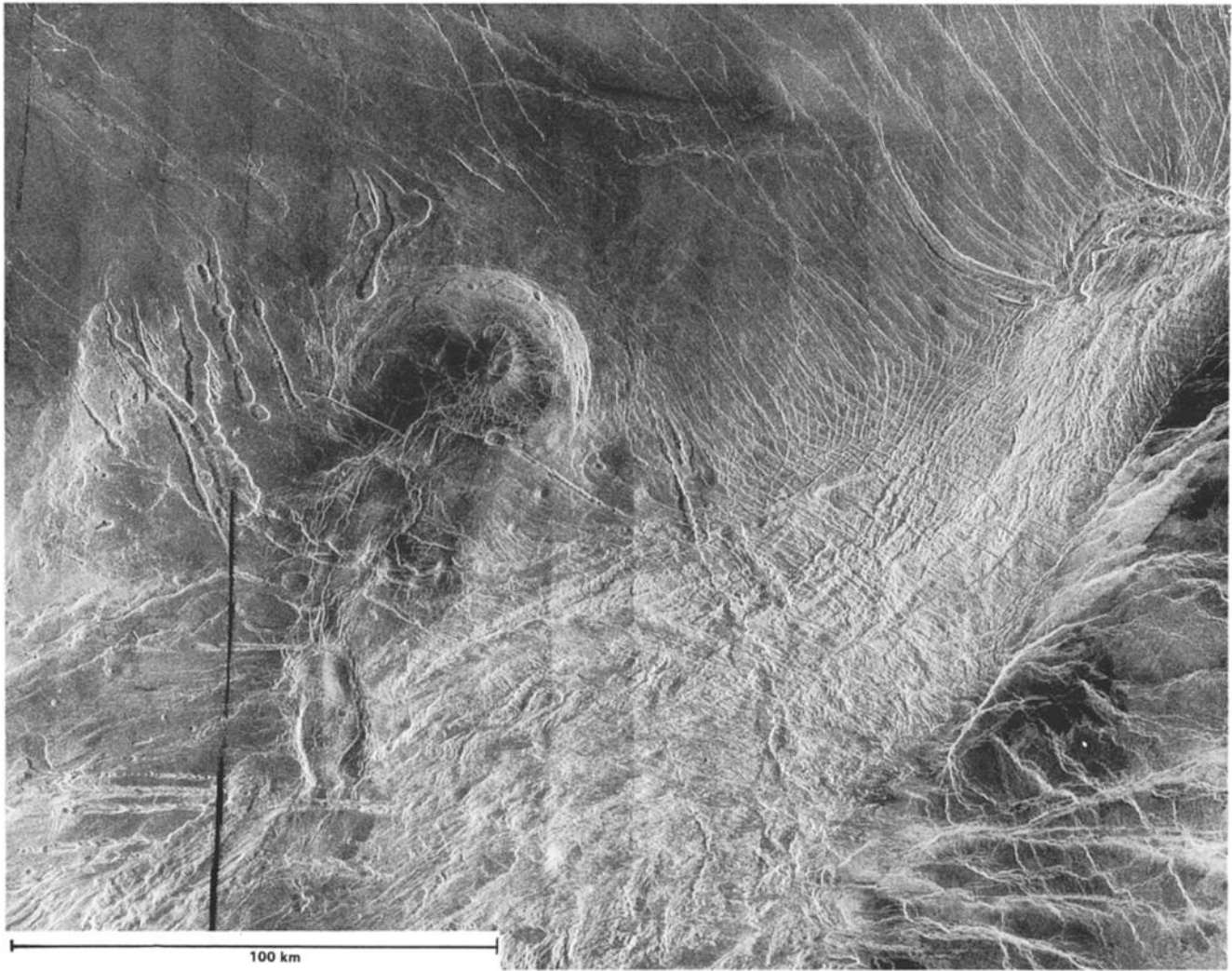


Fig. 11. Siddons Patera and lineaments in southern Lakshmi Planum. Latitude 60.6°-62.5°N, longitude 338.8°-345.0°E = 200 x 312 km. From F-MIDRP.60N344.

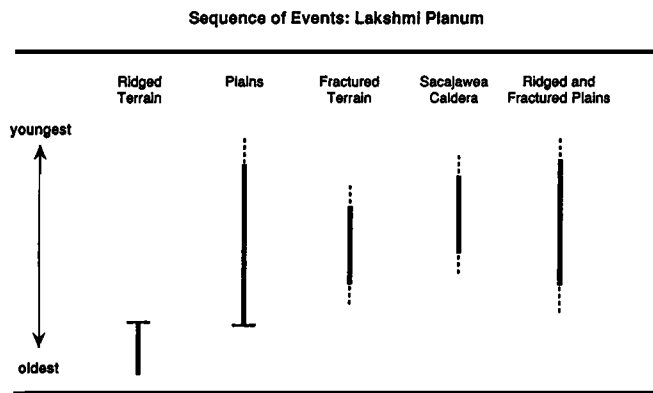
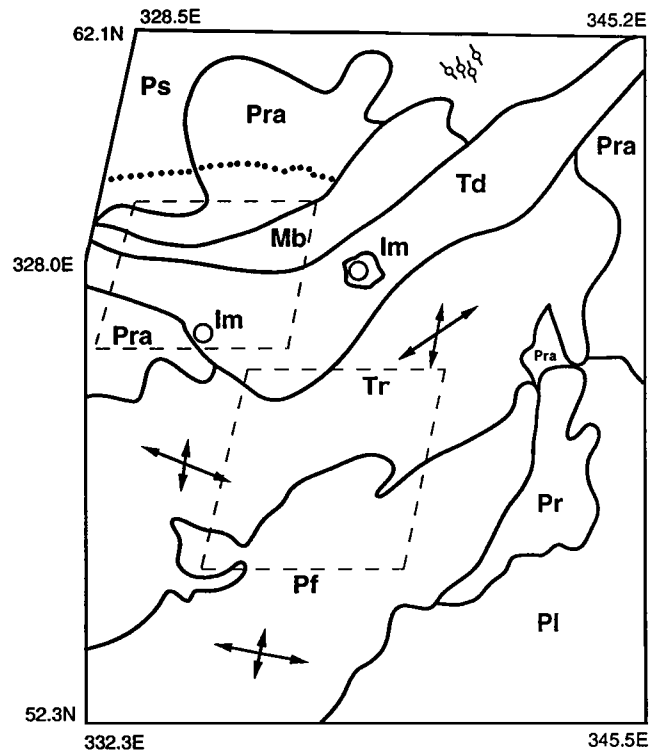


Fig. 12. Relative ages of features in Lakshmi Planum.

Fig. 13. Geomorphic map of Danu Province east of 330°E. Locations of figures 14-15 are outlined. See Table 1 for definitions of geomorphic units. The symbols around 65.7°N, 339.6°E indicate troughs 0.6-6 km wide; the dotted line at 60.1°N, 328.2°-335.5°E is the northern boundary of the very radar-dark plains; the arrows indicate lineament directions.



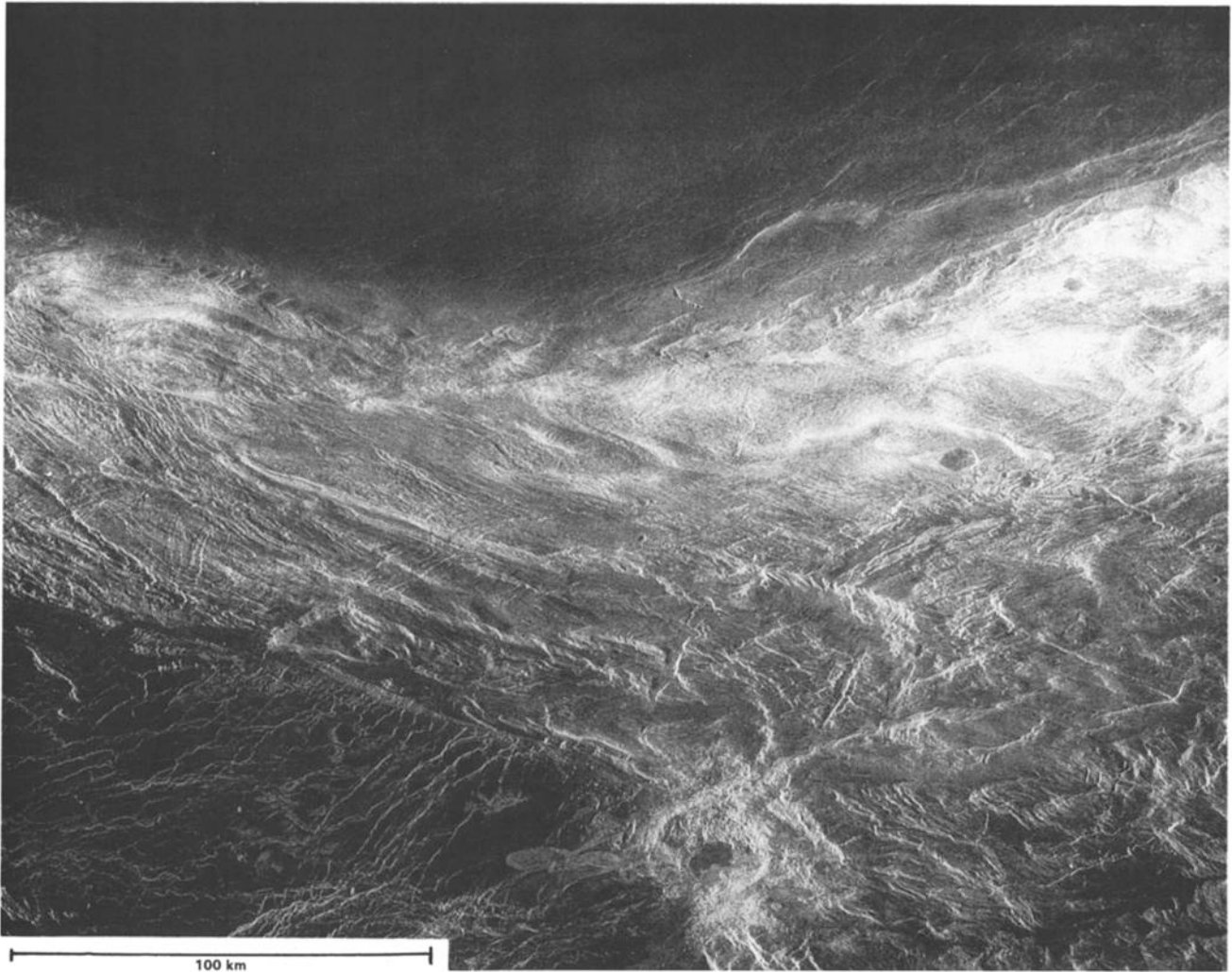


Fig. 14. Central Danu Montes and Vesta Rupes. Portions of units Ps, Pra, Mb, and Im are visible. Latitude 57.5°-59.7°N, longitude 330.0°-335.4°E = 232 x 297 km. From F-MIDRP.60N334.

SW trends found in Danu Montes, but lineaments also occur in a variety of other orientations. Lineaments are fairly short (<25 km) and tend to be curved and diffuse in their radar brightness. The only undisrupted features are several long (up to 100 km), NW-SE trending pit chains, e.g., at 58.4°N, 335°E (Figure 14). Numerous dark patches suggest that local volcanism has flooded parts of the region. The 20-km impact crater Magnani, 58.6°N, 337.2°E (Figures 1 and 2), has an interior covered with smooth, bright deposits. Its ejecta blanket is disrupted, more likely by emplacement on rough terrain than by subsequent deformation, since the floor and walls are undeformed.

In southern Clotho Tessera, the fine-scale fractures which cut the plains to the south (see plains) continue into the tessera and cut all of the older lineaments. In the tessera, their orientation is WNW-ESE. In many places, lows parallel to these fractures seem to be filled with volcanic flows. Numerous pits are also visible. A NS trend that also consists of a series of closely spaced fractures underlies the EW trend. Near the transition between the ridged terrain and the plains, NE trending fractures also occur (Figures 13 and 15). In southwestern Clotho Tessera, an elevated area of tessera, about 1 km above the surroundings, centered at 54.1°N and 332.5°E contains primarily NS fractures, along with other fractures which roughly parallel the topographic contours.

Within longitudes 337°-343°E, southern Clotho Tessera consists of a series of ridges cut by NS and NE-SW trending fractures which are

embayed by smooth material, probably lava flows. The ridges themselves form a grid in which NS-trending ridges are largely cut by EW fractures, and the EW ridges are largely cut by NE-SW fractures. The width of these ridges are commonly 20-40 km, and the spacing between them is approximately 25 km. The nature of the NS and NE-SW trends is difficult to determine because their interaction disrupts the pattern. In some cases these lineaments are narrow and fairly straight, occasionally occurring in pairs, suggesting that they are simple fractures or normal faults; in other regions they appear to be curved and domed, suggesting that they result from shortening.

Northern Sedna Planitia (C1-MIDRPs 60N319, 60N347). The plains immediately south of Clotho Tessera have a dense pattern of radar-bright lineaments which appear to be fractures. The average trend of the lineaments is EW, although sets thereof are slightly curved. The lineaments are long (60-100 km) and narrow (0.1-0.5 km). In a few cases, they occur in pairs, spaced at 0-3 km. In a few locations (e.g., 53.5°N, 336°E) NS to NE-SW trends are also visible. These lineaments are clearly cross cut by the EW lineaments. Smooth plains, looking like volcanic flows, are abundant in the region, and both embay and are cut by the lineaments.

Interpretation. In addition to the mantle upwelling and downwelling hypotheses suggested for the entire Ishtar Terra region [Pronin, 1986; Bindschadler et al., 1990; Grimm and Phillips, 1990, 1991], Danu Montes was suggested to have formed in response to northward

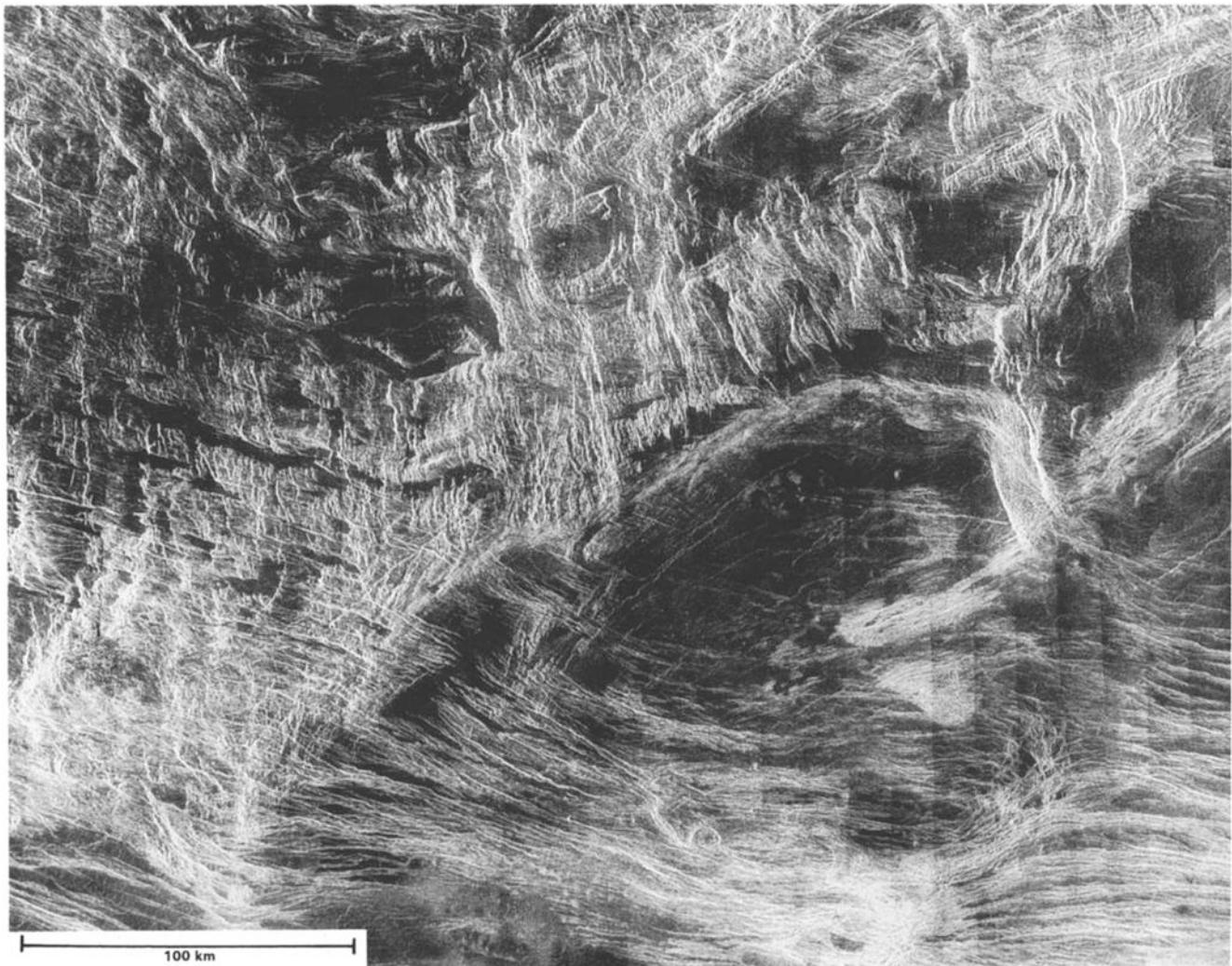


Fig. 15. Central Clotho Tessera. Units Tr and Pf are illustrated. Latitude 54.5°-57.3°N, longitude 334.4°-339.9°E = 296 x 326 km. From F-MIDRP.55N337.

subduction of the crust and lithosphere below Lakshmi Planum [Janle and Janssen, 1984; Head *et al.*, 1990].

The relatively low relief of Danu Montes suggests that either this area has undergone much less crustal shortening than other mountain belts in Ishtar Terra, or it is more extensionally relaxed. The curved, diffuse, and shorter ridges in Danu Montes appear more similar to those of Freyja Montes than to the sharply linear ridges of Maxwell Montes. There are several possible explanations for the curved morphology of the ridges. The curvilinear ridges may be a result of the interaction of a regional stress and either a preexisting tectonic fabric or simply variations in local topographic relief in the form of the edge of the plateau. Alternatively, the ridges may have been originally linear and were subsequently deformed into their current shape. As in Maxwell, Freyja, and Akna montes [Solomon *et al.*, this issue], deformation at Danu Montes seems to be moving out on to the plains of Lakshmi Planum. Several of the long, domed ridges which border the plains appear to be thrusts verging NW, as they are brighter on the NW side and have ends which curve back to the SE. The narrow, NE-SW trending, anastomosing ridges in the plains to the north of Danu Montes are approximately parallel to the ridges in Danu Montes and may be a result of the same tectonic event.

Numerous, low-strain extensional features appear to be approximately contemporaneous with shortening in Danu Montes. The

ridges in western Danu Montes (near 60.5°N, 339°E) are cut by several NW-SE trending pit chains, certainly volcanic, implying minor extension within the convergent regime [Burt and Head, 1991]. The southern end of the large graben located at 60°N, 338°E is overprinted by NE-SW trending ridges, implying (but not requiring) that extension near the peaks occurred before the stresses building the mountain belts completely ceased. Such extension could be the result of release of stress due to topographic relief [Solomon *et al.*, 1991]. Several pit chains that strike EW are collinear with some of the scarps in Vesta Rupes, suggesting that these scarps are most easily interpreted as normal faults. The narrow spacing of faults and graben in Vesta Rupes and their orientation perpendicular to the steep topographic slope suggest that they may be a result of extension above a shallow crustal detachment [Solomon *et al.*, 1991]. The presence of extensional features at right angles to the topographic slope in areas of high relief suggests gravitational spreading [Solomon *et al.*, 1991; Smrekar and Solomon, this issue; Burt and Head, 1991].

In the subparallel terrain (T1) of Clotho Tessera, the youngest tectonic trend appears to be the approximately EW set of lineaments which cut the plains and southeastern Clotho Tessera. The narrow width, great length, and apparent lack of relief of these lineaments imply that they are fractures. In a few cases, such as at 53°N, 336°E, the fractures appear to be graben sets, suggesting that all

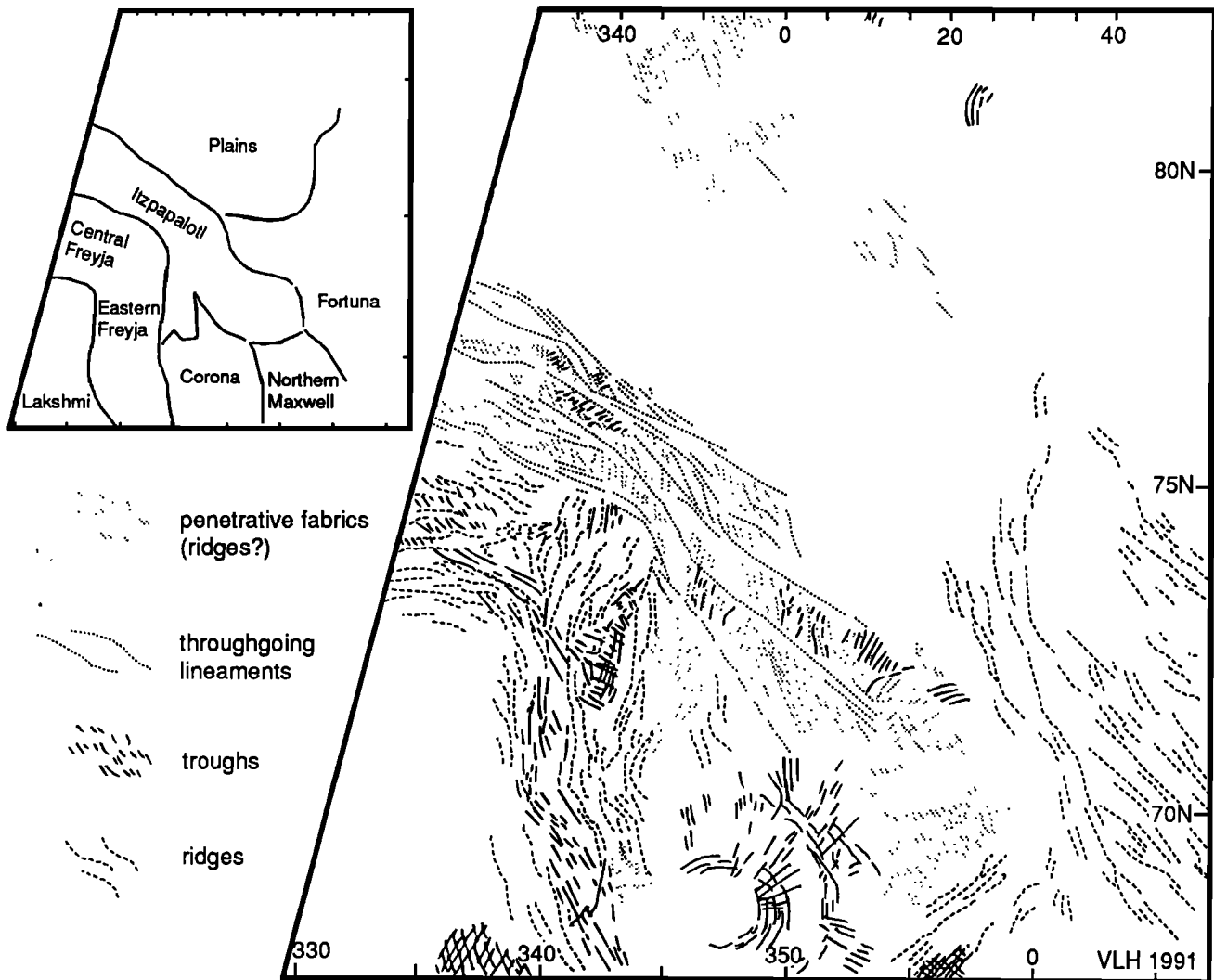


Fig. 18. Structural Map of Eastern Freyja Montes, Itzpapalotl Tessera, and North Scarp and Basin.

unit map, and Figure 18 is a structural map of this north side of Ishtar Terra 330°E-5°E.

Central Freyja Montes (Figure 19; F-MIDRP.75N332). This region is dominated by EW-trending, crosscutting bright and dark lineaments: the "banded terrain" originally seen by Earth-based radar [Campbell et al., 1983; Solomon and Head, 1984]. Often bands can be correlated with relatively broad wavelength (10-20 km) anastomosing ridges trend EW and dominate the EW structural fabric. Troughs (25-100 km long, 1-5+ km wide) parallel the ridges; they are best developed in the middle of central Freyja (73.5°N, 333°E) and correspond with the highest region of the mountain range. A second set of troughs is developed in the NW part of central Freyja (74°N, 332°E) which are thinner, shorter, and trend NW, roughly parallel to troughs which comprise a major fabric element in the inside (Lakshmi) corner of the central-eastern Freyja junction. The troughs in central Freyja appear locally to crosscut, and be crosscut by, the EW ridges. They also show numerous small offsets and curvatures, but we are unable to distinguish whether these latter features are due to structure or artifacts due to local relief.

Eastern Freyja Montes (F-MIDRPs 75N332, 75N351, 70N339). Eastern Freyja is similarly dominated by broad anastomosing ridges; here the ridge orientation is NS. This fabric is truncated to the north by Itzpapalotl Tessera, near 75°N. NW-trending troughs cross cut the ridges (e.g., 72.5°N, 339°E). Ridge-parallel troughs are more preva-

lent to the south, projecting out of the mountains and on and just above the scarp bounding Lakshmi Planum (71°N, 339°E to 67°N, 342°E). Ridges are found on both sides of this trough zone: widely spaced ridges occur farther westward into the plateau (e.g. 69°N, 338°E) and numerous sharp asymmetric ridges dominate to the east at the lower elevations of the North Basin (70°N, 341°E; Figure 22). These latter ridges in particular appear westward vergent, in contrast to the symmetric appearance of ridges in central Freyja. Note, however, that this effect could be due solely to radar foreshortening; apparent displacements would then indicate ridge heights of several hundred meters. As in central Freyja, a secondary set of troughs is also present in eastern Freyja. Two sets of troughs, WNW- and NNE trending, intersect in a NS-elongate low oval rise at 72°N, 343°E. The region of intersecting troughs correlates, at least in part, with a topographic high; its southern half is bounded by slopes of 5°-10°.

Freyja Montes Bend (Figure 19; F-MIDRP.75N332). The central and eastern arms of Freyja Montes are separated by a 100-km wide transition zone centered around 74°N, 336°E. This subdomain lies across a topographic saddle (up EW and down NS) and appears to be a zone of structural overprinting or culmination (i.e., the point away from which folds plunge). In the northern part of this zone, west-vergent apexes of cone-shaped ridges may represent refolded folds resulting from the interference of EW and NS trending ridges in central and eastern Freyja, respectively. The lengths (tens of kilome-

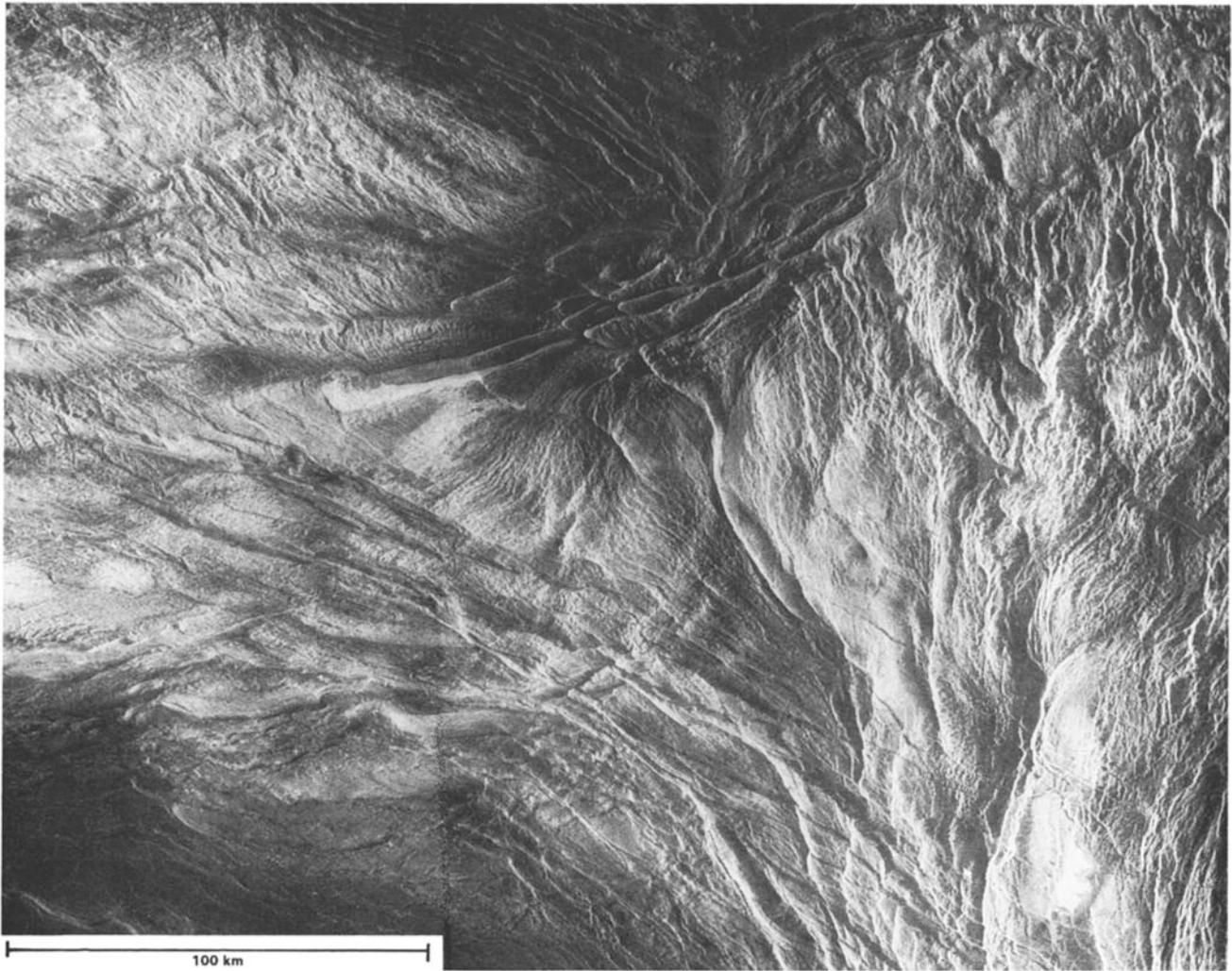


Fig. 19. Central Freyja Montes. Latitude 72.8°-75.0°N, longitude 330.0°-340.1°E = 232 x 296 km. The elevation changes from 4.5 km in Lakshmi Planum at the southern edge of the picture, to over 6.0 km above MPR at the crest, latitude 74°N, and then down to 4.0 km at the northern edge of the picture. From F.MIDRP.75N332.

ters) of the individual lineaments rule out layover as the principal cause of the apex-to-the-west appearance.

The structural fabrics of both central and eastern Freyja fade out toward Lakshmi Planum. The southern part of the transition zone is smooth and gradational: both ridges and troughs show a gradual change in orientation from EW to NS, parallel to the trends of their respective belts and the boundary with Lakshmi Planum.

Western Itzapalotl Tessera (Figure 20; F-MIDRPs 75N332, 75N351; C1-MIDRP.75N338). Forming the northernmost geomorphic unit of western Ishtar Terra, Itzapalotl Tessera is topographically and structurally divided into two regions; the boundary is transitional but centered at about 345°E. The western portion is bounded to the north by the steepest part of Uorsar Rupes, where slopes are 10°-20°. Interior slopes, however, are small, less than 2°. The scarp itself shows a number of Z-shaped offsets, near 77°N, 340°E, that become more closely spaced to the west, and individual structures along the scarp (such as the basal wrinkle ridges) show similar offsets (e.g., 77°N, 339°E). A single structural fabric comprised of two principal sets of structures dominates western Itzapalotl. A highly penetrative fabric, perhaps tightly spaced ridges, trends NNW; individual elements are spaced less than 1 km apart. This fabric occurs mainly in the interior of radar-bright blocks (e.g., 76°N, 339°E). Separating these blocks are throughgoing lineaments or

flooded lows trending WNW (e.g., 75.5°N, 340°E); these features are separated by several tens of kilometers. The penetrative ridge fabric is apparently rotated into parallelism with the throughgoing lineaments (75.5°N, 343°E); see Figure 21. The spatial development of these two families of structures defines a regionally consistent asymmetric fabric geometry which defines the Itzapalotl domain. A third set of structures, locally developed troughs, completes the structural fabric of this domain. These troughs are 5-20 km long and about 2 km wide. They developed perpendicular to the penetrative ridge fabric and are best observed in westernmost Itzapalotl (76°N, 333°E; Figure 20).

The transition zone to eastern Itzapalotl begins near 340°E, where the penetrative NNW fabric is obscured by a rougher NS fabric that is part of the northernmost structural expression of Freyja Montes. The WNW throughgoing lineaments generally truncate the NNW fabric, however. Across the width of the transition zone, these lineaments are continuously displaced 50-100 km to the south. The transition zone is also marked by a change in topography as well as structural fabric. The northernmost extension of Freyja, marked by a broad rise at 344°E above elevation 3.0 km, falls off to the east by 1 km on a 2°-5° slope. To the north, Uorsar Rupes is no longer distinguishable by 353°E as its slope has fallen to less than 2°.

Eastern Itzapalotl Tessera (F-MIDRP 75N351; C1-MIDRP

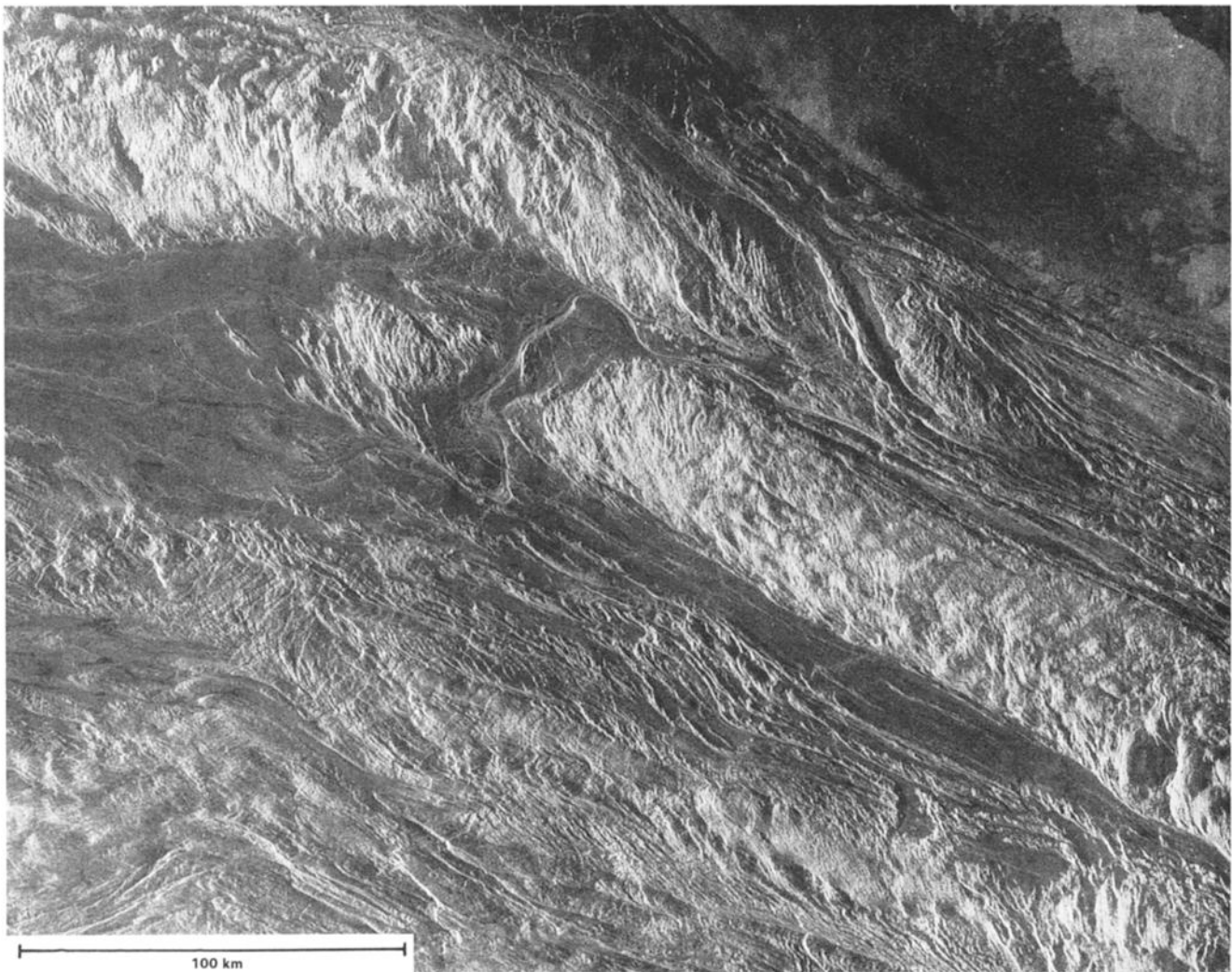


Fig. 20. Western Itzapaplotl Tessera. Latitude 75.1°-77.5°N, longitude 330.6°-343.6°E = 253 x 325 km. From F-MIDRP.75N332.

75N338). This region is characterized by larger (100x300 km) tessera blocks standing higher than the surrounding northern basin; parts of these blocks lie at heights similar (2.5-3.0 km) to those of the more uniformly elevated western subdomain. Structural trends here are variable; NNW orientations are visible in the north and south center, but north to NNE structures occur in the SW and an orthogonal ENE/NNW pattern is seen in the SE. This orthogonal pattern is similar to structures observed elsewhere on Venus (e.g., Laima Tessera) and appears to have been overprinted by NNW-trending structures.

Interpretation. Freyja Montes, together with the other mountain belts surrounding Lakshmi Planum, represents some of the most severe crustal shortening observed on Venus [Head, 1990]. The principal manifestations of this shortening are the high topography of the mountain ranges and the ridges within them. Ridge-parallel troughs may have formed as a result of high-level extension of shortened crust. Troughs south of Freyja Montes are probably related to steep slopes of the North Scarp. In southcentral Freyja and eastern Freyja, troughs generally parallel the outline of Lakshmi Planum, suggesting a structural control due to lithospheric heterogeneity. Although numerous crosscutting relationships exist, we are unable to assign a consistent offset or sense of shear within Freyja [cf. Solomon *et al.* 1991]. If ridge-parallel troughs formed as a result of earlier crustal shortening, then ridge development, topography, and cross-

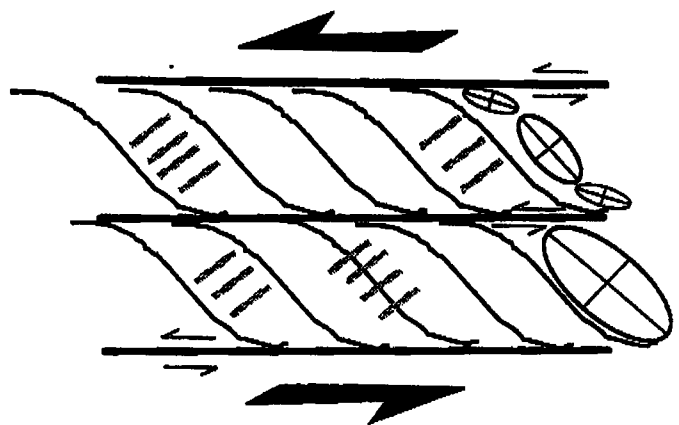


Fig. 21. Kinematic interpretation of western Itzapaplotl structures illustrating sinistral noncoaxial deformation. Curved lines represent the trace of the penetrative ridge fabric, heavy lines mark throughgoing lineaments, and short grey lines mark the trend of troughs. Strain ellipses with principal axes illustrate the average strain associated with the structures. Small arrows show displacement along throughgoing lineaments, large arrows show bulk displacement direction. The family of structures may be kinematically akin to S-C structures [Berthe *et al.*, 1979; Hansen, 1992].

cutting relations may indicate temporal relations for different parts of Freyja. Southeastern and eastern Freyja may have formed early with ridge and boundary parallel troughs reflecting advanced states of postshortening collapse. The corner of Freyja (transition zone) may have formed next with ridge formation earlier than NW-striking ridge-parallel troughs. Locally, NW troughs appear to truncate NS structures of East Freyja. Eastwest boundary-parallel ridges of central Freyja may have formed later, folding previously formed NW-trending troughs of the transition zone. The relative dearth of EW-ridge parallel troughs in central Freyja may reflect a less mature stage in the crustal shortening in this region. Magellan images of western Freyja may be used to test this hypothesis of progressive Freyja deformation from east to central. We expect to see a lack of NW-trending troughs and good development of EW-trending ridges in western Freyja.

The family of structures in western Itzpapalotl Tessera, consisting of penetrative ridges (?), throughgoing lineaments (apparently marking local topographic lows), and the perpendicular troughs, are interpreted as the result of distributed noncoaxial sinistral shear across Itzpapalotl [e.g., Berthe et al., 1979; Corsini et al., 1991; Shimamoto, 1989]. The undulations in Uorsar Rupes, if not altimeter artifacts, are also consistent with left-lateral shear with a westward increase in intensity. North-trending structures of Freyja to the south appear to be overprinted by, and locally rotated into parallelism with, the Itzpapalotl fabric, and hence deformation of northern Freyja structures is viewed as dominantly older than Itzpapalotl deformation, although the structural domains of these two regions are mostly well separated. Furthermore, the superposition of composite sinistral structures on the orthogonal fabric of eastern Itzpapalotl suggests two deformation events, the former responsible for the original formation of the tessera and the latter a left-lateral shear across the northern boundary of western Ishtar Terra.

In summary, preorogenic deformation included the formation of tessera, relict structures of which can be found in eastern Itzpapalotl, and the Corona region (69°N, 349°E; Figure 23). Freyja and Maxwell Montes formed in major orogenies, perhaps contemporaneously, in a bulk strain regime with principal axes of shortening probably controlled by preexisting lithospheric heterogeneity associated with Lakshmi Planum. Central Freyja appears to postdate Eastern Freyja. Left-lateral shear dominates West Itzpapalotl and appears to be the youngest structural style in the region.

An age sequence joint with the North Scarp and Basin Province is given at the end of section 2.4.

2.4. North Scarp and Basin

This province is less marked in topographic variation than the mountain belts to the west or east, but nonetheless has strong structural trends. We divide it into western, central, and eastern regions.

Western North Scarp and Basin (Figure 22; F-MIDRP.70N339). The 400-km portion of the North Scarp running roughly NS at 340°E, from 71°N to 67°N, is remarkably smooth, despite a topographic drop of more than 1.0 km. All along this boundary are fine troughs, less than 2 km wide, with lengths of 50-100 km and spacings of 5-20 km. In places, there are broader down slope troughs, most notably around 68.5°N, 342°E. Downhill from this scarp, centered at 70°N, 341°E, there is a complex of bright, anastomosing lines. These lines become straighter to the south. The most recent, crosscutting other features, runs 280 km, straight as a taut cable, from 70.1°N, 340.2°E to 68.1°N, 344.5°E, where it ends abruptly in a T-shaped intersection with a lineament 15 km long. Most of this length it is hardly 1 km wide.

Central North Basin and Corona (Figure 23; F-MIDRPs70N353,

65N342, 65N354). The Central North Basin contains a nearly circular topographic depression 500 km in diameter centered near 68°N, 348°E standing about 2.8 km above MPR and 1.5 km lower than adjacent Lakshmi Planum. It has some of the features of a corona [Stofan et al., this issue]. The depression is structurally bounded to the east by discontinuous grooved units of intermediate radar backscatter. The grooves appear to be roughly radial and concentric to the basin outline; however, some NW-SE and NE-SW structural control is evident in the southern and northern parts of the basin, respectively. A second smaller partial arc, about 150 km across, lies at the center of the basin (68.5°N, 348°E). Although individual grooved units appear to have low positive relief, emphasized by plains embayment, the centers of units to the north and NW are lower than the basin proper and slopes here are 2°-5°. The larger, northern depression contains arcuate troughs. The southernmost grooved unit (67.5°N, 353°E) lies on the northwest slope of Maxwell Montes.

Eastern North Basin and Maxwell Slope (Figure 24; F-MIDRP 70N353). The easternmost corner of this region grades into the north slope of Maxwell Montes, described in section 2.6. Here the discussion is confined to elevations below 5.0 km.

A NW-sloping zone of severe distortion runs from 67°N, 350°E to 69°N, 2°E, widening to >100 km around 68°N, 358°E. It is predominantly radar-dark, with its most marked lineaments running SW-NE. These lineaments are spaced 3-5 km apart and have a rough, ropey appearance. In a few places, they are interrupted by more NS trends, particularly at 68.2°N, 358°E, where the predominant lineaments bend 90° around a brighter apex. North of this zone, there are embayed tesseræ, with a finer NW-SE trend cutting across the SW-NE. The region of lowest elevation, 2.5-3.0 km, from 70.2°N, 355°E to 71°N, 2°E, is very smooth and radar-dark. The higher terrain north of 71°N has a much more marked tessera structure.

Interpretation. The throughgoing lineaments and ridges trending NE-SW could be thrust faults, either due to gravity sliding or to "extrusion" perpendicular to the principal axis of Maxwell shortening. Alternatively, these lineaments could be shear zones; the orientations of subordinate structures, if not artifacts of radar foreshortening on the steep slope, then indicate right-lateral displacement [Vorder Bruegge et al., 1990; Hansen, 1992].

The partial radial and concentric groove pattern suggests a corona [Stofan et al., this issue] formed contemporaneously with plains volcanism (embayments appear to dominate to the south, whereas fractures form on the plains to the north). The corona appears to be older than Maxwell Montes, because it is embayed by smooth material overthrust by Maxwell, but clear indicators of its age relative to Freyja are lacking. Greater age is also consistent with its apparent lack of dynamical relation to the structural development of either Maxwell or Freyja.

Kinematic Sequence (Figure 25). The structural trends of Itzpapalotl clearly postdate those associated with central and eastern Freyja Montes (Figure 18). The trends of eastern Freyja Montes appear to parallel those of Maxwell Montes (Figure 1), suggesting contemporary formation, as mentioned above. Thus from the imagery of the area north of Lakshmi Planum alone, the sequence given in Figure 25 is indicated. However, eastern Freyja Montes and the NNW trending region of Maxwell Montes are more than 600 km apart, and other factors discussed below suggest that Maxwell Montes is more recent.

2.5. South Scarp and Basin

The South Scarp and Basin Province has largely been ignored in examinations of Ishtar Terra based upon Arecibo and Venera 15/16 data, and thus the major topographic and structural features of the

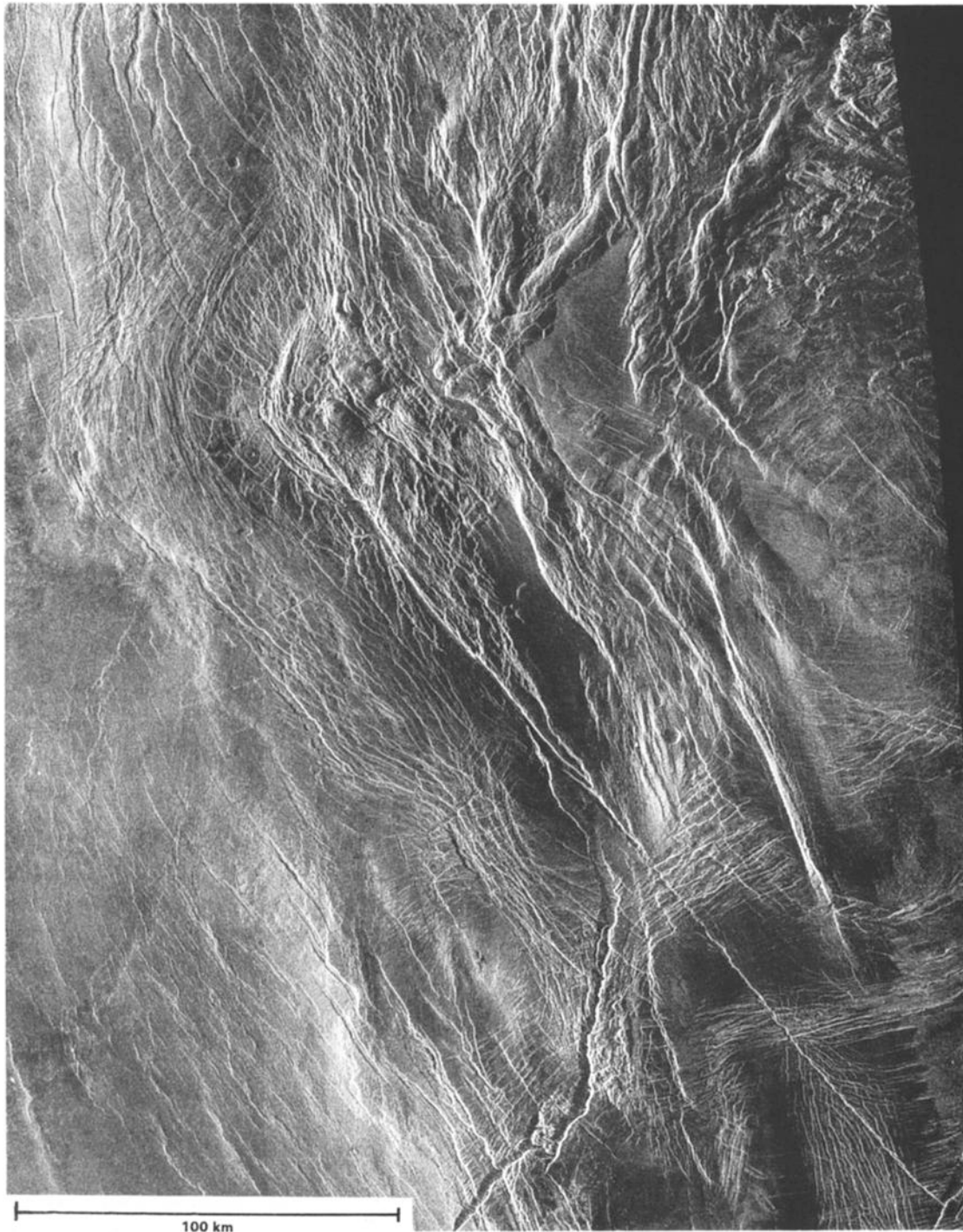


Fig. 22. Western North Scarp and Basin. Latitude 68.1°-71.2°N, longitude 338.0°-344.5°E = 327 x 250 km. From F-MIDRP.70N339.

region are unnamed. The most topographically distinct features (Figures 3 and 26) consist of the following:

1. The South Scarp which separates Lakshmi Planum from the lowlands to the south. This scarp can be considered continuous with Vesta Rupes; however, because of the interruption by the SWNE trending portion of Danu Montes and Clotho Tessera, 335°-342°E, we adopt the separate designation of South Scarp (until an appropriate goddess of hearth and home is found).

2. Two basins are clearly visible in both the topography and imagery. They are referred to as the West and Central basins, respectively. They appear in images as two scallops in an otherwise

eastwest trending South Scarp and their surfaces are dominated by plains. A third, less topographically distinct basin is centered at 61°N, 359°E in the plains south of South Scarp near a set of NE-SW trending ridges in the plains and is referred to as the East Basin.

3. A pair of topographic highs extend south from South Scarp. The West Ridge (343°E) separates Clotho Tessera from the West Basin and the Central Ridge (350°E) separates the West and Central basins. Both are characterized by the presence of complex ridged terrain.

4. A discontinuous set of topographic highs run approximately parallel to South Scarp, approximately 500 km to the south. These constitute the Outer Rise (58°N) and are located in approximately the

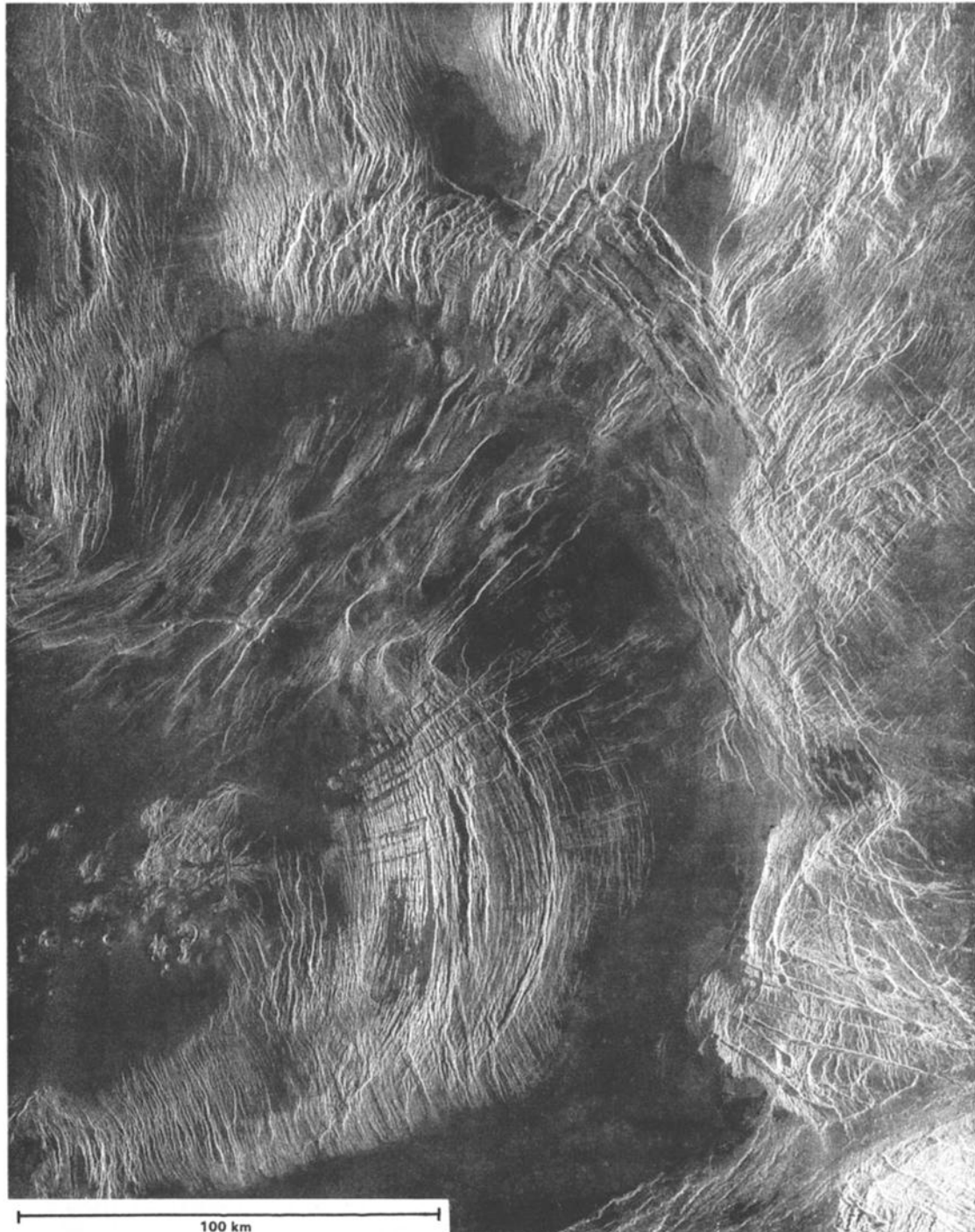


Fig. 23. Central North Basin and Corona. Latitude 67.6°-70.42°N, longitude 346.2°-353.4°E=296 x 271 km. From F-MIDRP.70N353.

same position relative to South Scarp as Ut Rupes (55°N, 322°E) with respect to Vesta Rupes.

The geomorphic units used in this discussion are given in Table 1. The linear ridged terrain designated T1 therein is the same as the subparallel ridged terrain Tsr of *Bindschadler and Head* [1991].

South Scarp (Figures 10, 11 and 27; F-MIDRPs 65N342, 65N354, 60N344, 60N355, 60N005). The scarp separating Lakshmi Planum from the lowlands to the south is 2-3 km high. It is steepest in the vicinity of the West Basin (Figures 11 and 27), with slopes approaching 10° over a horizontal distance of 25 km, widens somewhat near the Central Ridge, narrows again near the Central Basin (slopes more than

10°), then widens by more than a factor of 2 until it approaches Maxwell Montes. From the West Basin through the Central Basin, the topographic scarp coincides with disrupted terrain (Td). As many as three distinct structural trends are present within the Td along South Scarp. The first is a set of gently sloping ridges which parallel the scarp. They are most clearly visible along the northwestern (near 61°N, 344°E, Figure 11) and northeastern edges of the West Basin (63°N, 349°E, Figure 27). The ridges appear approximately symmetric and tend to exhibit cusped shapes. They are interpreted as compressional structures and may be thrust faults. The second and third sets of structures consist of steep-sided valleys which either

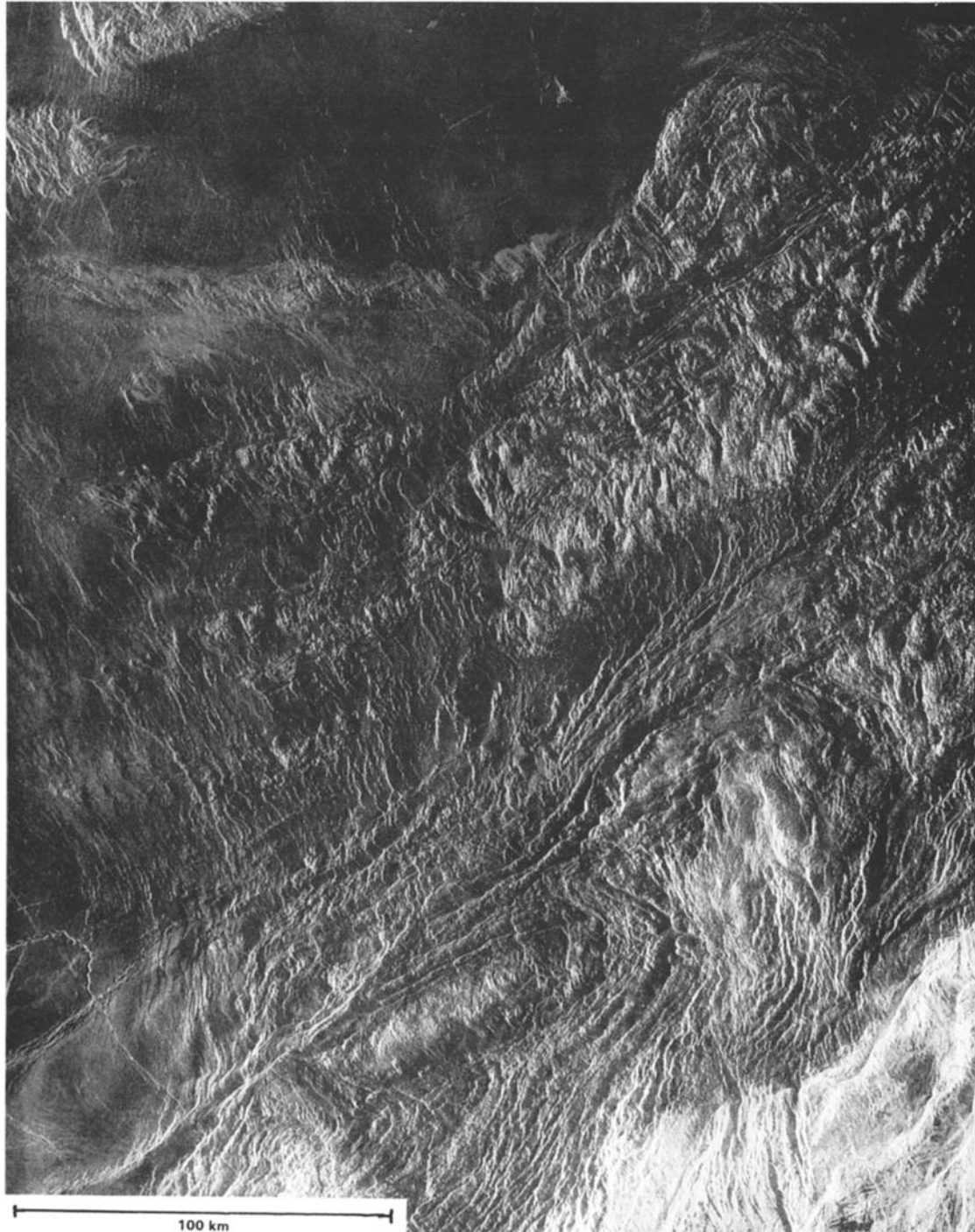


Fig. 24. Eastern North Basin. Latitude 67.4°-70.5°N, longitude 353.8°-0.4°E = 327 x 250 km. From F-MIDRP.70N353.

trend parallel or perpendicular to the strike of South Scarp (Figures 10 and 11). In some cases, these steep-sided troughs are collinear with or lie parallel to steep-sided, flat-floored troughs with rounded ends and pit chains. These latter features are interpreted as collapse features associated with movement of subsurface magma.

Structures are most prominent in the portion of South Scarp that lies above the West Basin. Here, broad ridges are clearly the oldest structures along the scarp and are extensively crosscut by extensional features which both parallel and trend at high angles to the scarp. Troughs parallel the scarp tend to be prominent where slopes are steepest or where the trend of the scarp is approximately NW-SE. This

NE-SW orientation brings the scarp into alignment with a set of steep-walled troughs observed on Lakshmi Planum (Figures 10 and 27), which include Rangrid Fossae. Most scarp-perpendicular troughs also align with this regional trend. Thus, most troughs appear to reflect regional NE-SW extension, while the less common scarp-parallel troughs generally reflect a local deformation associated with the steep slopes of South Scarp. Such a hypothesis explains the complex pattern of curvilinear troughs near 61°N, 343°E (Figure 11). In this area, the northwesternmost scarp-parallel troughs curve away from the scarp until they are approximately aligned with the more regional set of features. Crosscutting relationships between sets of troughs are com-

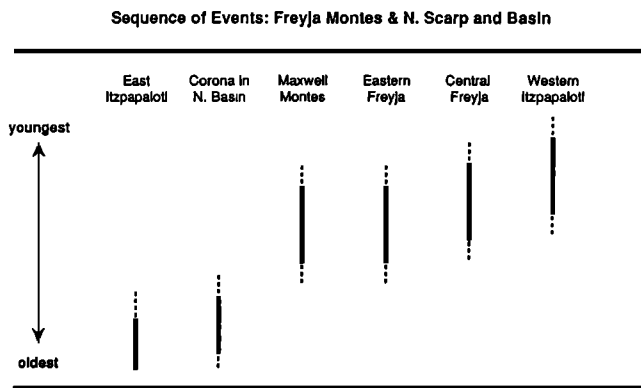


Fig. 25. Relative ages of features in Freyja Province and the North Scarp and Basin.

plex, although in general, NW-SE trending troughs tend to crosscut slope-parallel (typically NE-SW trending) troughs. This is the steepest part of the South Scarp: 10° over 17 km near 60.9°N , 343.6°E .

From the Central Basin eastward, the structural character of South Scarp changes significantly. Both scarp-parallel and NW-SE trending structures become less common and less pronounced. The scarp widens and has more smooth terrain and flat-floored troughs are more common. The 50×30 km caldera located near the top of South Scarp, at approximately 61.5°N , 359.5°E (described in section 2.1) may be the source of much of the plains deposits that have embayed the fractured terrain to the west.

West Ridge (Figure 28; F-MIDRP.60N344). The broad West Ridge rises 1.0-1.5 km above the plains to the east and consists of a system of roughly NS-trending ridges. The ridges are approximately continuous between 57.5°N and 58.5°N , where they are interrupted by an EW-trending zone of diffuse deformation that extends westward into Clotho Tessera. Ridges resume approximately 50 km to the north with a more westerly trend, and 100 km farther north they become progressively more disrupted over a 75-km-wide zone until their NNW-SSE trend is supplanted by a NE-SW trend which parallels Danu Montes. South of 57.5° ridge structures appear to become progressively more embayed by plains until they are completely buried south of 55°N . Ridges within the Pr to the east of the West Ridge predominantly trend EW but near the boundary with the complex-ridged fractured terrain (Tf), they curve into alignment with the plains-Tf boundary. No structures within the plains can be clearly traced into the fractured terrain of Clotho Tessera.

West Basin (F-MIDRP60N344). The West Basin sits at an elevation between 2.5 and 3.5 km below the level of adjacent Lakshmi Planum. Its surface is primarily characterized by a network of radar-bright lineaments that appear to be marelike ridges set in smooth, radar-dark plains. Most ridges in the basin trend EW to ESE-WNW, as do most ridges throughout the plains south of South Scarp. A secondary set of such ridges trend NS to NNW-SSE and are found in the northern and southwestern parts of the basin. In the northwest portion of the basin, near the scarp, both sets of ridges tend to curve so that they parallel the scarp. Within the horizontal resolution of the altimetry data (~ 10 km), these scarp-parallel ridges appear to lie at the topographic base of the scarp. In the NE portion of the basin, ENE-trending ridges can be traced up to 1.5 km above the basin itself. Numerous similarly trending ridges are visible on Lakshmi Planum directly to the NE of the West Basin, although none can be traced as continuous features into the basin. The southern quarter of the basin is dominated by a group of ridges that trend EW to ESE and extend as far as 355°E .

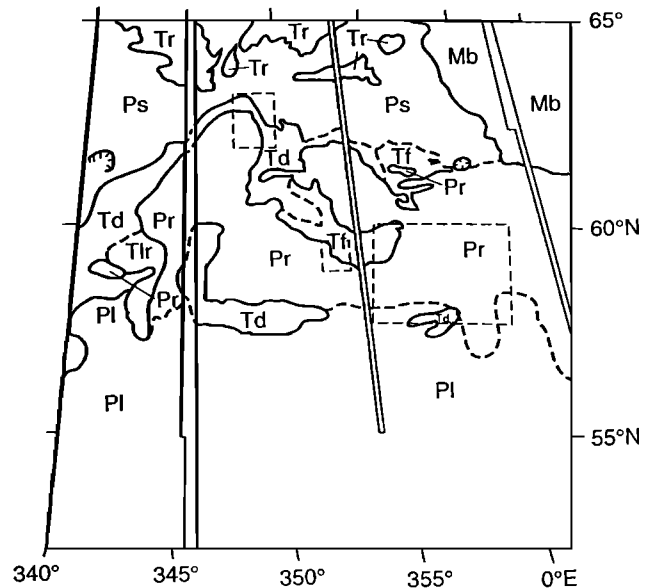


Fig. 26. Geomorphic map of South Scarp and Basin. Dashed lines represent uncertain or transitional contacts. Locations of Figures 27-29 are outlined. See Table 1 for definitions of geomorphic units.

Central Basin (F-MIDRP.60N355). The Central Basin sits at a nearly uniform elevation, approximately 3.5 km below adjacent parts of Lakshmi Planum. It exhibits fewer ridges than the West Basin. Ridges trend EW and, as in the West Basin, climb upward toward Lakshmi Planum in the NE corner of the basin. Some ridges curve so as to parallel South Scarp in the northern and northeastern portions of the basin.

Central Ridge (Figure 28; F-MIDRP.60N355). The West and Central basins are separated by a broad topographic ridge that extends south from a 0.5-1.0 km high along South Scarp and wraps around to the east to nearly enclose the Central Basin. The ridge consists of disrupted terrain in the north and fractured terrain in the south. As in South Scarp, ridges are crosscut by steep-sided troughs. Within the fractured terrain, a set of NS trending steep-sided troughs are crosscut by scarps trending approximately ENE and WNW over an area $70 \text{ km} \times 70 \text{ km}$ centered on 59.5°N , 353°E (Figure 28). Walls of the NS troughs are offset in a right-lateral sense along the ENE-trending scarps and in a left-lateral sense along the WNW-trending scarps. This set of relationships is consistent with conjugate strike-slip faulting related to EW directed contraction and/or NS-directed extension. Neither style of deformation is evident in any of the surrounding terrain and both sets of features (scarps and troughs) truncate abruptly at the plains-fractured terrain contact.

Outer Rise (Figure 29; F-MIDRPs 60N344, 60N355, 55N346). A discontinuous topographic high rises 0.5 to 1.5 km above the plains and runs roughly EW along 58°N . Along this rise lies a region of Td located south of the West Basin and consisting of an L-shaped region of deformed terrain. Most of the northern arm of this region of Td lies in a gap in the Magellan imagery but can be seen clearly in Venera 15/16 images of the region. Along the southern border with the plains, a set of linear, anastomosing ridges, about 5 km wide, trend EW, parallel to marelike ridges within the adjacent plains. The northern boundary is characterized by indistinct lineaments which parallel the boundary and a few narrow (less than 5 km) ridges and troughs which trend approximately NS. These small ridges parallel a set of three large (about 15 km) ridges within the interior of the region. The large ridges are truncated by boundary-parallel structures both to the north

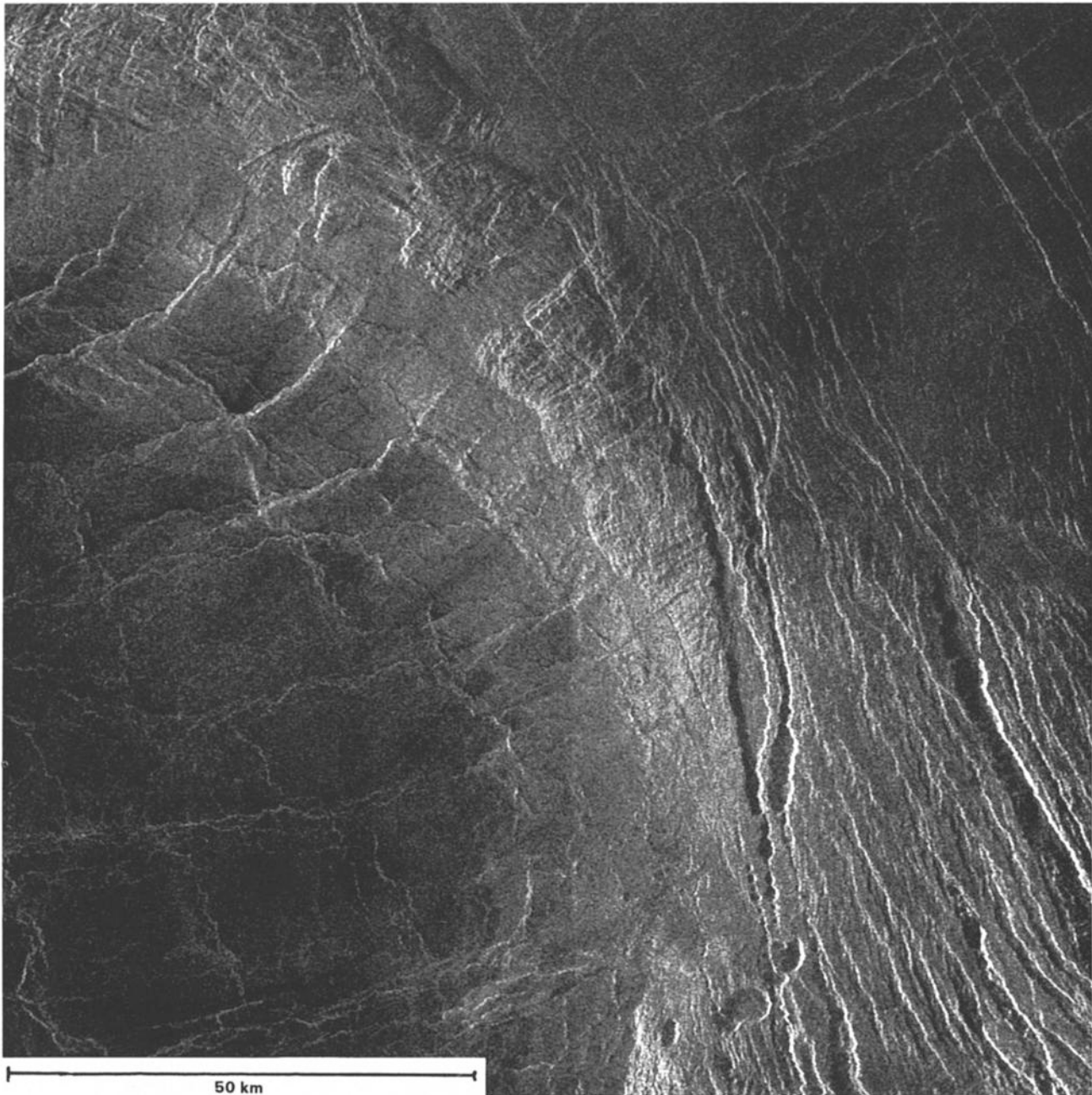


Fig. 27. South Scarp: northeast side of West Basin. Latitude 61.9° - 63.0° N, longitude 347.7° - 350.0° E = 116×112 km. From F-MIDRPs 60N347 and 65N342. A single broad ridge (20 km wide) runs NW-SE to NS through the center of the image and is extensively crosscut by both scarp parallel and perpendicular troughs and fractures. Lakshmi Planum lies to the NE (upper right) and the West Basin to the SW (lower left). Note also the colinearity of NE-SW trending ridges on either side of the broad ridge.

and south and thus appear relatively old. Approximately 250 km to the east, near 57.7° N, 356.8° E (Figure 29), portions of a few small ridges and troughs, oriented NS, appear near a local topographic high. These structures may represent an extensive region of Td which has been buried by plains deposits.

Ridged plains (Figure 29; FMIDRPs 60N344, 60N355). A region of ridged plains extends south and east of the West Basin, between the Central Basin and the Outer Rise, and to the south of Maxwell Montes. The strike of ridges in this region is predominantly EW to SSE, but near 355° E, some turn to the NE, while others turn to a more SE trend. The northeast trending ridges occupy part of the East Basin, then proceed NE to climb approximately 4.5 km onto Lakshmi Planum and

turn to a more NW trend along the western slope of Maxwell Montes, near 357° E (Figures 10 and 29). Small regions dominated by EW-trending fractures are observed just north of the Td portion of the Outer Rise. Discontinuities in the fractures and fingerlike extensions of the zones of fractures suggest that they have been embayed by plains deposits.

Interpretation. Magellan images contain extensive information on the relative ages of features within the South Scarp and Basin Province. Below are listed some of the more important observations on relative age; a suggested sequence of events is listed below.

1. All ridge-form structures within units Td and Tl are abruptly truncated at boundaries with plains (both lowland and highland)

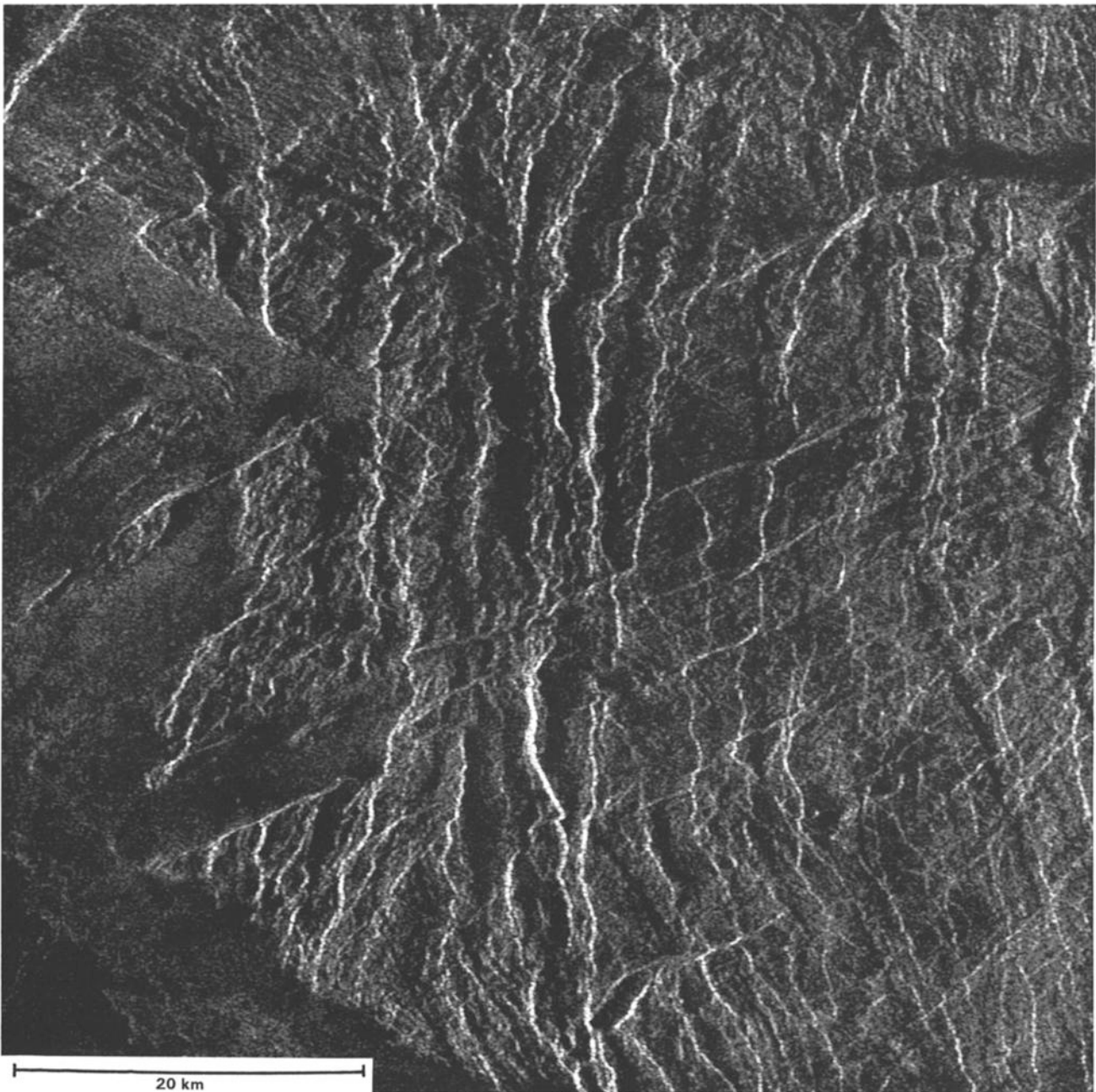


Fig. 28. West Ridge (Tf). Latitude 59.2°-59.8°N, longitude 351.9°-353.2°E = 63 x 70 km. From F-MIDRP.60N344. Small portion of fractured terrain (Tf) in West Ridge showing apparent offset of NS-trending troughs and NW-trending fractures.

unless they run parallel to the plains-Tf boundary. In this case, relative ages must be determined by other means or are indeterminate.

2. Steep-sided troughs and scarps in mapped regions of units Td or Tf are abruptly truncated or embayed at boundaries with lowland plains.

3. Relations between troughs and ridges within unit Td indicate that troughs postdate ridge formation. According to above interpretations of these features, this indicates that extension followed shortening in these regions.

4. Steep-sided troughs often crosscut plains-Tf boundaries on Lakshmi.

5. NW-trending fractures on Lakshmi crosscut (and thus postdate) plains ridges there.

6. Where crosscutting relationships can be determined at all, scarp-

parallel ridges along the base of South Scarp in some cases appear to truncate NW-trending fractures (e.g., 61°N, 344°E).

7. Crosscutting trends in Clotho Tessera suggest that scarp-parallel ridges postdate NS-trending ridges (in T1)

Kinematic sequence. A proposed sequence of events is given in Figure 30. The observed structural features, their crosscutting relationships, and the interpreted modes of origin suggest a scenario (described below) for the formation of the South Scarp and Basin Province. It is important to note that although individual "events" are described, the formation of the region most likely proceeded as a series of interleaving tectonic and volcanic events.

Initially, EW-directed shortening is manifested in the formation of shortening features oriented NS in Clotho Tessera and in the formation of a set of conjugate strike-slip faults in the Tf south of the Central

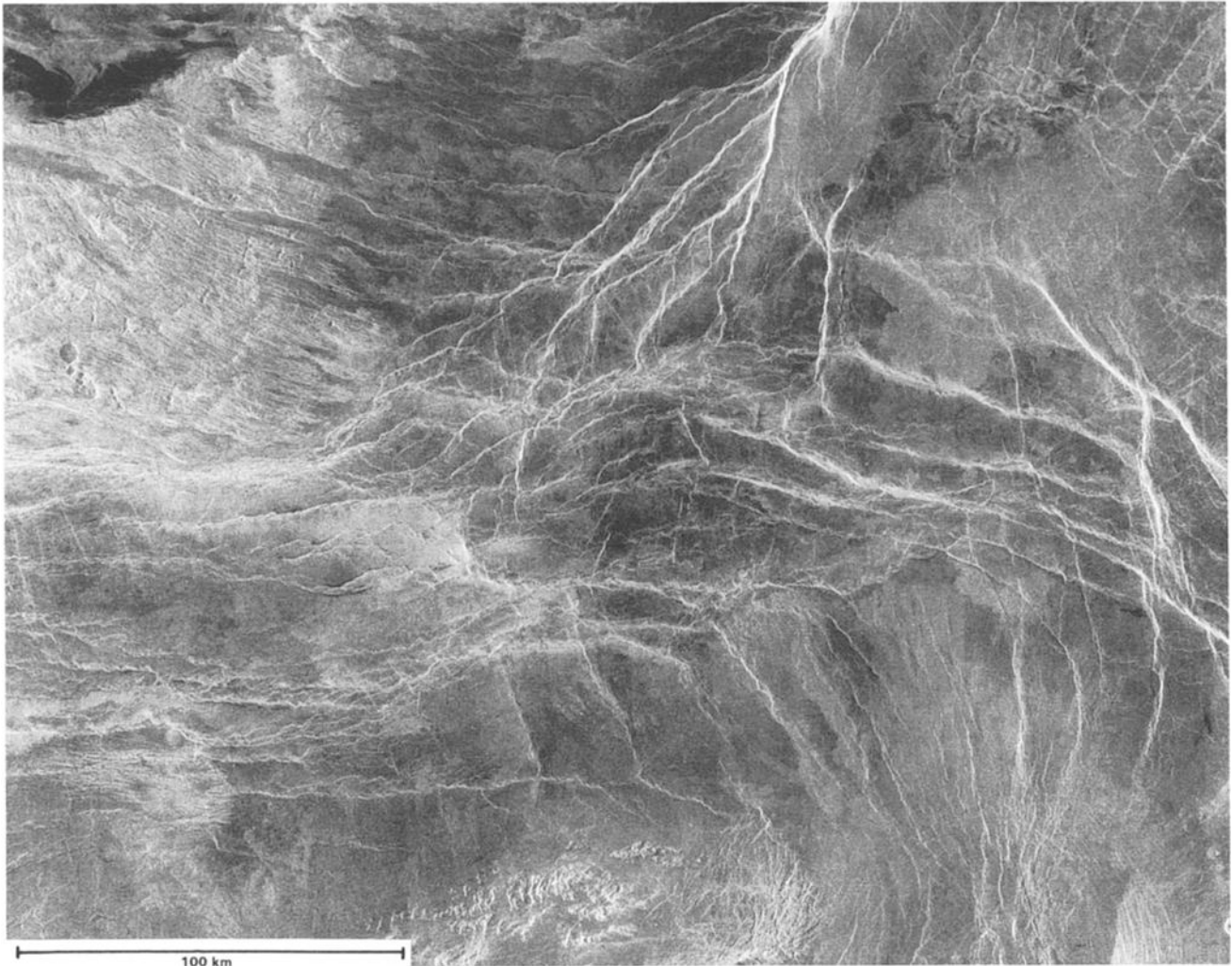


Fig. 29. Ridged Plains (Pr). 57.7°-60.1°N, longitude 354.0°±0.1°E = 253 x 332 km. From F-MIDRP.60N355. Many plains ridges turn from an EW trend (left) to a NE-SW trend near the upper center of the ridge. NE-trending ridges form a belt that merges with the western boundary of Maxwell Montes to the north.

Sequence of Events: South Scarp and Basin

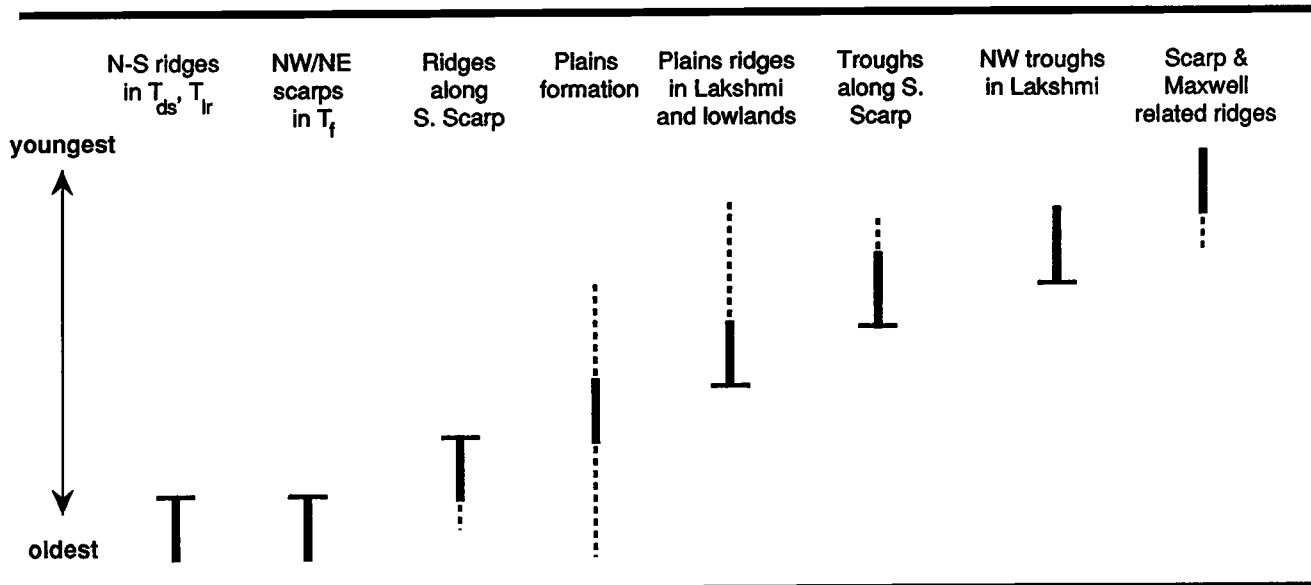


Fig. 30. Relative ages of features in the South Scarp and Basin.

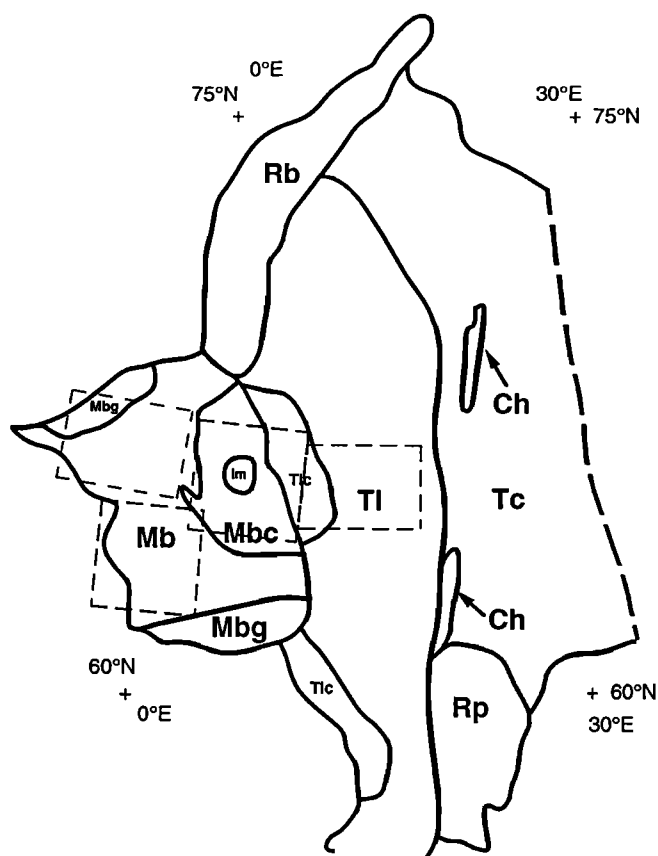


Fig. 31. Geomorphic map of Maxwell Montes and Western Fortuna Tessera. Locations of Figures 32-35 are outlined. See Table 1 for definition of geomorphic units.

Basin. (The NS-trending troughs would predate this event and are left unexplained under this scenario.) One possibility is that the more northwesterly trending portions of proto-South Scarp were formed during this time. Next, shortening directed approximately NW-SE led to the formation of proto-South Scarp and the scarp-parallel ridges observed there. Proto-South-Scarp may have been a mountain belt similar to Danu. This phase of deformation appears to have been followed by extensive plains volcanism, forming the bulk of Lakshmi Planum and the lowland plains. Unspecified modificational processes (gravitational relaxation or sliding) and volcanism combine to alter proto-South Scarp into a form similar to that seen today. Approximately NW-SE shortening continued, leading to formation of plains ridges in Lakshmi and the lowland plains. Variation in orientations of ridges in lowlands may be due to local variations in stresses caused by the topography of South Scarp. Either at roughly the same time or slightly later, gravitational stresses led to formation of scarp-parallel troughs in South Scarp NW of the West Basin. As indicated by crosscutting relationships along South Scarp, this was followed by the formation of NW-trending troughs form within Lakshmi. Orientations of these features are consistent with continued NW-SE shortening. The fact that they are only observed at high elevations suggests that gravitational stresses play a role in their formation. The final distinguishable event consists of continued NW-directed shortening, leading to the formation of some of the plains ridges running along the base of South Scarp and of the plains ridges SW of Maxwell Montes.

2.6. Maxwell

We define the Province of Maxwell as the terrain above 5.0 km in elevation, between 345°E in the west and 15°E in the east. We divide

the Province into four regions according to their characters in the imagery and altimetry: (1) Northwest Arm and Slope; (2) West Slope and Crest; (3) Cleopatra-Influenced; and (4) Southeast Slope (Figure 31).

Northwest Arm and Slope (Figure 32; F-MIDRPs 65N354, 70N353, 70N007). The boundary of this region on three sides is the 5.0-km elevation contour. On the fourth, east, side, there is a marked sinuous line that runs from 65°N, 0°E to 66.5°N, 359°E and then turns northeastward to run to 69°N, 4°E, beyond which it continues in the lowlands in a northerly direction to beyond 72°N, 3°E. Within Maxwell Montes, east of this sinuous line there are virtually no indications of gravitational modification, but to the west of it, there are appreciable indications.

Most of the western extremity of Maxwell Montes is very bright, except for a belt 20-60 km wide from 67°N, 356°E to 66°N, 0°E. This darker belt has no correlation with the topography. The southwest slope of the arm is marked by a series of ridges NW-SE of variable spacing, predominantly 3 to 10 km. On this slope, there are some narrow grabenlike features at a shallow angle to the main ridges (e.g., 65.9°N, 356°E) similar to those in Vesta Rupes, though much less marked. A sinuous feature about 0.5 km wide runs through this slope at about 66.3°N for 230 km. It is defined mainly by offsets of the ridges, but for some segments it looks like a terrestrial river valley.

On the steep north slope of Maxwell Montes, within 100 km of the North Scarp and Basin, there are troughs 1-2 km wide with an average spacing of about 15 km which trend SE-NW. In some cases, their upper ends are truncated by the ridge pattern; in others, they fade. At the 4.5-6.0 km elevation level these troughs cut across a series of ridges at 2-4 km intervals that parallel the contours, to create an orthogonal, blocky terrain. This pattern fades out in the west at about 353°E and in the east at about 359.5°E. On the western arm of Maxwell (67°N, 350°E), the fractures are wider, more broadly spaced, and less orthogonal; the overall pattern is fan shaped, closing downhill to the north.

The higher regions, above 7.5 km in elevation, are a series of ridges 10-20 km apart. Their sawtooth pattern, with the steeper slopes on the west side, suggests that they are thrust faults.

West Slope and Crest (Figure 33; F-MIDRP.65N006). The boundary of this region is the marked sinuous lineament on the west and north and approximately the 8.0 km elevation in the east (near 4°E) and south (near 62.5°N).

To the west of a line from about 67°N, 1°E to 63°N, 6°E, there are marked ridges at right angles to a SW-NE line. The most prominent ridges are 15-25 km apart, but in places the ridge pattern breaks down to a spacing as small as 3 km. This smaller spacing is particularly true of a belt 40 km wide all along the western boundary of the region. This belt is characterized by the steepest slopes: an average of 5°, or an elevation change of 3 km in 40 km. The belt extends from 66°N, 356°E to 62°N, 2°E. The elevation contours (Figure 3) do not coincide markedly with the ridge pattern, and in places there is an appreciable angle between the two: as much as 45° near 64.5°N, 0°E.

There are no apparent indications of either gravitational or impact modification throughout the region. In much of the higher parts, above 9.5 km elevation, there are bright sinuous lineaments, less than 0.5 km wide and 2-4 km apart, running NS, at about 45° to the main features, most marked near 64°N, 4°E, which might be caused by gravitationally influenced stress. They also could be interpreted as continuations of lineaments to the east of the crest, overlain on the west slope.

The eastern boundary of the region is ill defined. Centered on 65°N, 4°E is a bright, featureless region about 30 km x 90 km, but to the northeast of it are more marked ridges at 15-20 km spacing. The lineaments on the east slope of Maxwell Montes are more NS than

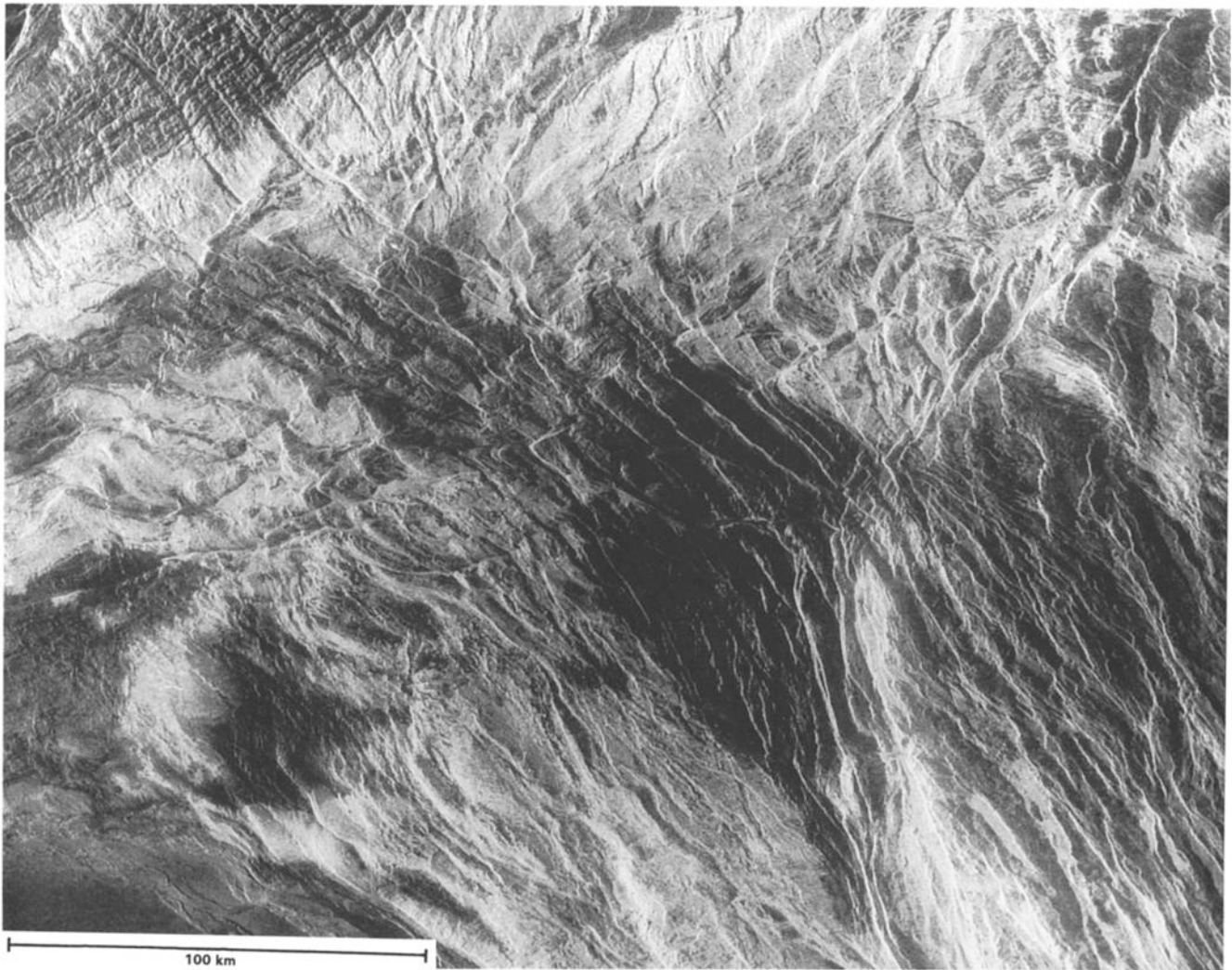


Fig. 32. Northwest Arm and Slope of Maxwell Montes. 65.3° - 67.5° N, 355.0° - 0.5° E = 232×251 km. The elevation change from the northwest corner of the figure to the eastern edge at 67.0° N is about 4.7 km. From F-MIDRP.65N354.

those on the west slope, thus aligning more with the faint lineaments described in the preceding paragraph.

Cleopatra-influenced (Figure 34; F-MIDRP.65N006). At 130 km (mainly EW) to 210 km (mainly NS) from the center of Cleopatra the uplands of Maxwell have a smooth appearance, as though covered by a layer some hundreds of meters thick. This smoothed upland region differs from the lower region to the east mainly in brightness. It is as reflective as the more distorted regions to the west and south, suggesting that the source of the brightness is a compositional effect associated with altitude [Klose *et al.*, this issue], rather than roughness. Embayments of the ridge pattern (not as obliterating as in Western Fortuna Tessera) suggest that the "Cleopatra influence" was subsequent to the tectonic deformations that created the ridges, probably associated with the uplift of Maxwell Montes. There is no absolute evidence that the smooth material is volcanic; it may be ejecta, similar to some highland regions on the moon.

Cleopatra itself has two marked rings: a central pit 45 km in diameter that is smooth, 1.5-2.0 km below the uplands to the west, and a surrounding shelf of a lighter shade, 15-35 km wide. The border between the central pit and the shelf appears to be much more hummocky than that between the shelf and the surrounding uplands, perhaps because the darker inner part affords more contrast. A pronounced sinuous channel, about 2 km wide, extends from the eastern edge of the pit at 66° N, 7.5° E, to the northeast, cutting through

the bright material at 66.2° N, 8.2° E. [Kirk *et al.*, manuscript in preparation]. There are *no* other impact features in the 500,000 km² of Maxwell Montes.

Southeast Slope (F-MIDRPs 65N006, 60N005). This crescent-shaped region is consistently bright but lacks the alternating pattern of the west slope and crest. This bland brightness seems not to be a result of a differing direction of slope with respect to the radar, since it looks the same in Arecibo and Venera imagery as well, indicative of a pervasive multioriented roughness [Vorder Bruegge *et al.*, 1990].

The boundary in the north with respect to the Cleopatra-influenced region, near 64° N, is indistinct. But south thereof are subtle but abundant lineaments, with 3-10 km spacing. North of 63° N these lines run mainly NS, but south thereof there are NW-SE trending features that in places cut across, and in other places are cut by, the NS features. There is no evidence of gravitational modification in this area on the Magellan imagery, but it could exist in a localized, interlaced manner.

The southern part of the slope, on F-MIDRP.60N005 west of 9° E, does indicate appreciable gravitational modification (as earlier inferred by Vorder Bruegge *et al.* [1990] and Vorder Bruegge and Head [1991]), though not as great as in the Northwest Arm and Slope. There are troughs running NW-SE, as much as 6 km wide at 30 km spacing. In the west, these troughs blend in the north to the lineaments of the West Slope and Crest. There also are subtle EW trends in the Southeast Slope that appear to underlie the troughs.

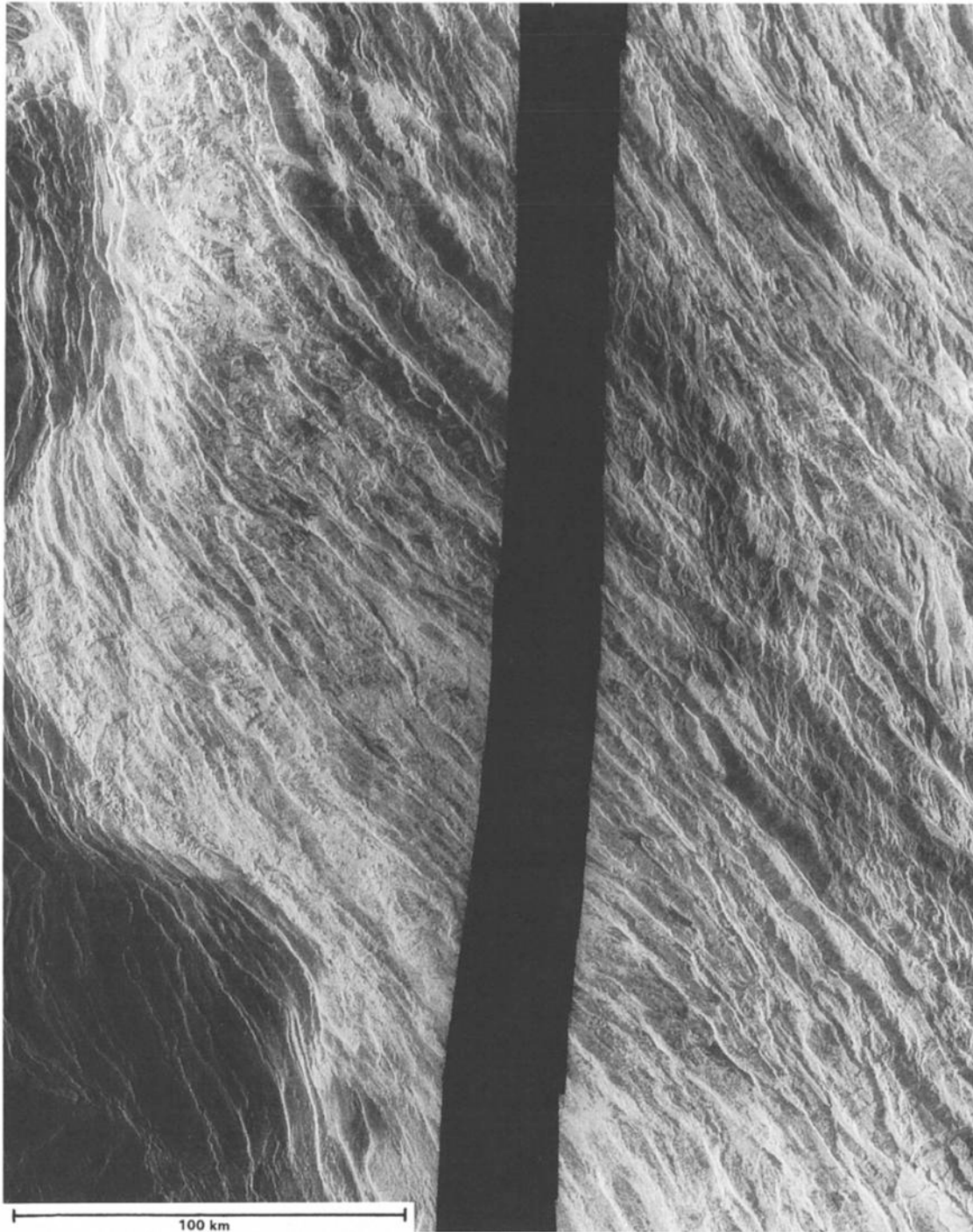


Fig. 33. West Slope and Crest of Maxwell Montes. Latitude 62.4° - 65.4° N, longitude 359.6° - 5.0° E = 317×251 km. The elevation change from the southwest to the northeast corner of the figure is about 4.5 km. From F-MIDRP.65N006.

Interpretation. Compensation of the great height of Maxwell solely by a stable crustal root is quite implausible. Even on Earth it would require temperature gradients well under $10^{\circ}/\text{km}$ [Bird, 1991]. The only way to obtain such a low gradient is a rapid strain rate [Vorder Bruegge and Head, 1991]: i.e., dynamic support. But low temperatures are inconsistent with the interpretation of the banded structure as arising from low viscosity at depths of a few kilometers [Solomon and Head, 1984; Zuber, 1987]. Crustal compensation would also require a fourfold thickening of crust beneath a 500-km width, and thence horizontal displacements of 2000 km [Solomon et al., this issue], for which there is little evidence.

The evident interpretation is that Maxwell Montes is undergoing severe contemporary compression, in a SWW-NEE direction. This compression (and associated downflow) must extend rather deep to account for the geoid high in the vicinity. We hope a much more detailed gravity field will be obtained to help examine this hypothesis. Across the main edifice of Maxwell this compression is manifested by overthrusting, faulting, and folding, with negligible indications of shear or gravitational modification. This need for contemporary compression does not rule out a long history of convergence and thickening of crustal blocks which contribute to compensation of the topographic high, involving both imbrication near the surface and

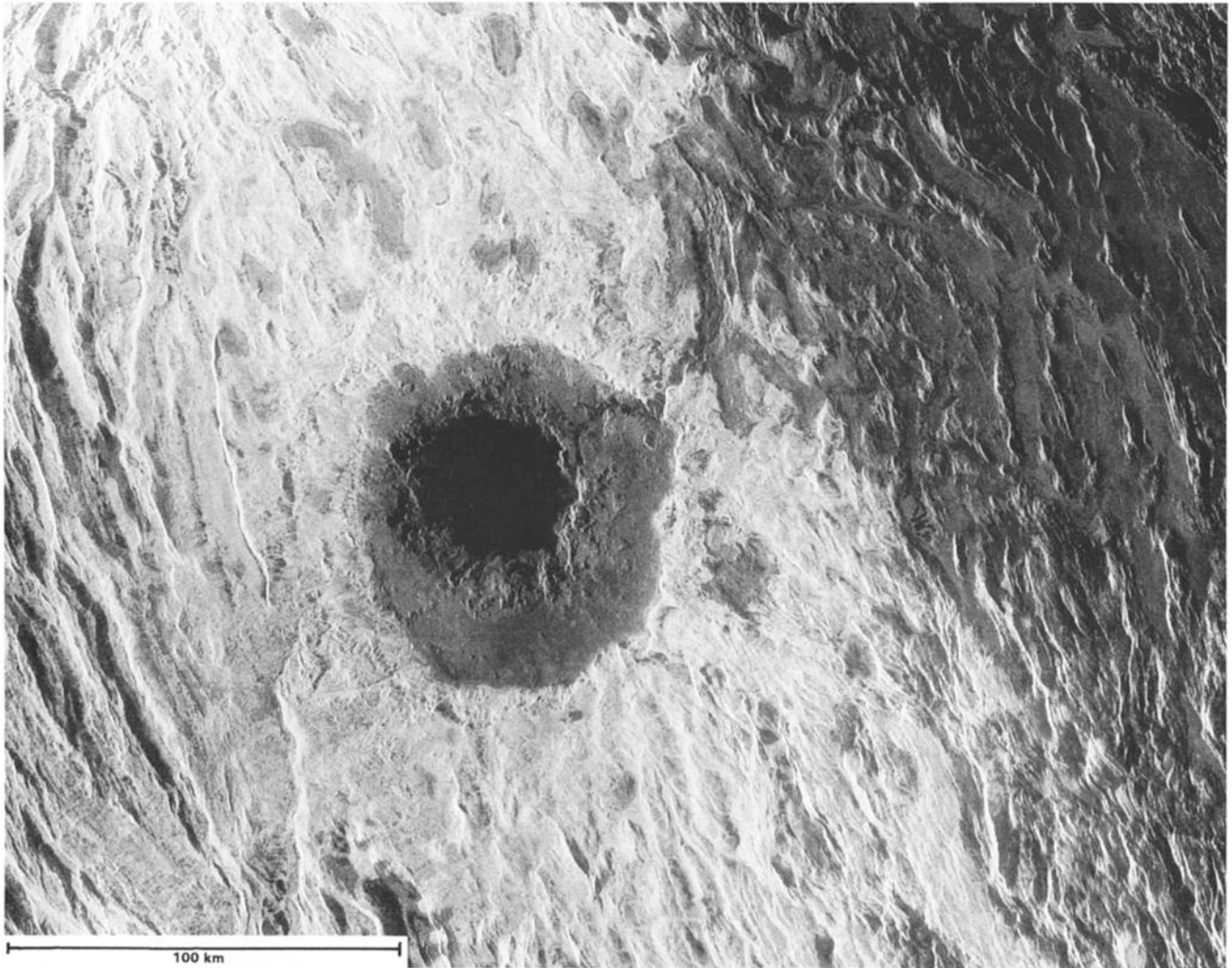


Fig. 34. Cleopatra Crater, plus areas of Maxwell Montes and Fortuna Tessera affected by it. Latitude 64.8°-67.1°N, longitude 3.7°-12.0°E = 243 x 357 km. From F-MIDRP.65N006.

plastic deformation at depth, as hypothesized by *Vorder Bruegge and Head* [1990]. However, we find no evidence that the imbrication is sequential.

An important increment from Magellan data is firmer evidence of extensional accommodation on the flanks: pronounced in the north, above 67°N, but slight in the south. In the lower Ridged Belt region to the north of Maxwell Montes there are similar NS ridge patterns. But in the eastern part of South Basin south of Maxwell Montes there is an almost total lack of any indication of structure related to Maxwell Montes, other than a moderate continuation of the sinuous front around longitude 0°, suggesting very recent volcanism since the uplift of Maxwell Montes.

Magellan has settled that Cleopatra is an impact crater [*Kirk et al.*, manuscript in preparation]. The superposition of its effects on what appear to be tectonic folds requires that this major infall be late in the sequence of events shaping Maxwell, as earlier inferred by *Vorder Bruegge and Head* [1990]. The amount of smooth material produced by Cleopatra is much more than normal impact melt. If it is such, it suggests that much crust under Maxwell Montes is close to melting. But such a heated state is inconsistent with the great height of Maxwell, which requires a high strain rate if crustal thickening is a major contributor thereto [*Vorder Bruegge and Head*, 1991].

However, the high geoid (Figure 3) requires that appreciable support be from the mantle: a downflow of convection. Supporting this conjecture is the depression running along the west side of the great sinuous line, resembling trenches at terrestrial subduction zones, though shallower: see Figures 3 and Figure 17 of *Solomon et al* [this issue]. The likely stiffness of Venus's upper mantle [*Kaula*, 1990] would seem to make Earthlike subduction of lithosphere unlikely, but finite element modelling indicates that lithospheric sinking can occur as a relatively shortlived event [*Lenardic et al.*, 1992]. A question is the horizontal scale of tectonic motions on Venus. The western slope of Maxwell Montes is consistent with a uniform flow over a span of 400 km NS, but the topography to the west indicates that the horizontal scale of upper mantle kinematics is not much longer. The finite element modelling indicates that a plume under Lakshmi would stimulate steep lithospheric underthrusting beneath Maxwell Montes [*Lenardic et al.*, 1992].

While Maxwell Montes probably has a long history, like terrestrial mountain belts, we did not find persuasive evidence of past differing kinematic patterns, such as the cross-strike discontinuities inferred from Arecibo and Venera imagery by *Vorder Bruegge et al* [1990].

A joint kinematic sequence of Maxwell and Western Fortuna is given in Figure 36 at the end of section 2.7.

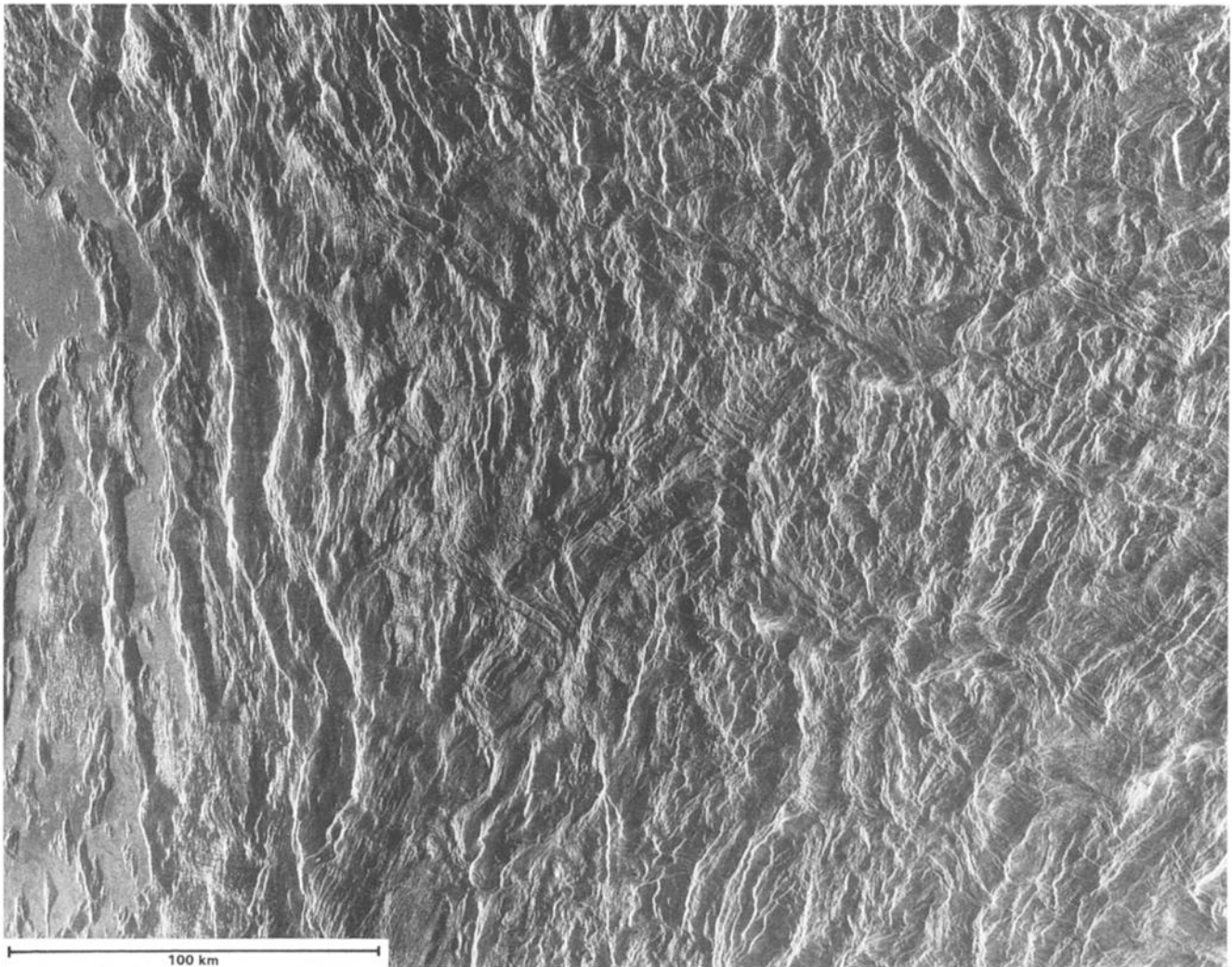


Fig. 35. Ridged TESSERA in Western Fortuna TESSERA. Latitude 64.7°-67.2°N, longitude 11.9°-19.9°E = 264 x 344 km. From F-MIDRP.65N018.

2.7. Western Fortuna

We define the province of Western Fortuna as the area of complexly deformed terrain between Maxwell Montes in the west and Varz Chasma in the east, 11E to 30E, and in latitude 76°N to 56°N. We divide Western Fortuna TESSERA into (1) Central Ridged TESSERA, (2) Ridged Belt, (3) Southern Ridged TESSERA, (4) Chevron TESSERA, and (5) Plumose Ridges. These regions follow *Vorder Bruegge and Head* [1989], with the exception that their "Arcuate Ridged TESSERA" is divided into central and southern parts.

Central Ridged TESSERA (Figure 35; F-MIDRPs 65N018, 70N007, 65N006, 60N016). We discuss this region first because it relates most closely to Maxwell Montes, discussed in the previous section. It also abuts on all the other regions of Fortuna TESSERA that we have defined for this study. The western boundary is defined by the 5.0-km level along Maxwell Montes, the line between bright and dark terrain. In the north, the region fades into the Ridge Belt, which has a greater variety of extensional as well as shortening features. South of 61.5°N there is a transition from steep ridges parallel to Maxwell's east front to a more heterogeneous terrain. In the east, the arcuate ridges give way at about 20°E to the less pronounced chevron tESSERA and plumose ridges. The northern, eastern, and southern boundaries all coincide with drops in elevation below 4.5 km.

The region is characterized mainly by subparallel arcuate ridges which roughly parallel the Maxwell front, with spacings of 15 to 25 km. They occur across the entire 950 km in longitude of the region. Not so marked, but still clear, are some crosscutting features. Most prominent is a curved pair of lineaments that extends about 400 km from 65°N, 14°E to 66.8°N, 21°E. Less prominent are straight lineaments that trend in a NW-SE direction, less than 5 km wide and spaced at intervals of about 60 km. The most marked are centered at 66.4°N, 17.4°E and 65.7°N, 17.9°E and extend about 160 km. The former of these crosses the curved lineaments and appears to offset them by about 5 km. Offsets of the arcuate ridges by the NW-SE lineaments occur but are smaller and unsystematic.

Within about 300 km of the center of Cleopatra there is much embayment of the arcuate ridges by smooth material. Around 66.4°N, 11°E, segments of the ridges disappear under this cover. An evident source of embaying material is the channel that comes out of the uplands at 66.4°N, 8.5°E. However, as in the Maxwell uplands south of Cleopatra, it cannot be ruled out that much of this cover is ejecta from the crater.

North of 68.2°N, the 20-km-spaced arcuate ridges become less marked, and there are both finer intertwining features in about the same orientation plus some straighter troughs in a SW-NE direction,

roughly radial from Maxwell Montes. There is no clear boundary with the Ridged Belt region.

In the south, there is a more marked boundary around 61.5°N.

Ridge Belt (F-MIDRP.70N007 to 72.5N; C1-MIDRP.75N029 north thereof). This region extends off the northeastern corner of Maxwell Montes in a NNE direction, sloping over 750 km from 5.0 km elevation to 3.0 km. Its western edge is the sinuous lineament described in section 2.6 on Maxwell Montes. Its eastern boundary is indistinct: a fading into the Central Ridged Tessera region.

North of 69°N, the sinuous lineament discussed in connection with Maxwell Montes becomes Semuni Dorsa: a bundle of bright lines against a darker background, about 30 km in width and undulating EW about 50 km, with a NS wavelength of about 200 km. East of the sinuous lineament the main trends are SSE-NNW, fading into smooth areas about 25 km wide in places. There also are fainter lineaments in a SW-NE direction, suggestive of earlier differently directed tectonics.

Southern Ridged Tessera (F-MIDRP60N016). As the terrain slopes down gradually south of 61.5°N, the arcuate ridges are much less marked. In a band between 13°E and 16°E, the ridges are embayed by smooth material., and south of 60°N there appears to be no preferred orientation. In an area 57°-60°N, 11°-13°E there appears a pattern of bright, fine NS lineaments: as many as 30 of them over a span of 105 km. A prominent EW graben 5 km wide cuts across them at 59.7°N. Starting at 12°E, NNE-SSW trending troughs become apparent, with one marked sinuous rille extending NNW around 60°N, 10.5°E.

Chevron Tessera (F-MIDRP.65N018 and C1-MIDRP.60N014). East of 20E, as the terrain starts to slope, there is a change in the imagery from the arcuate tessera: much less contrast and systematic orientation in the bright-dark alternations. From 62°N, 20°E to 66°N, 22°E Hina Chasma is a strongly delineated band about 60 km wide, within which there is a smooth, ropey texture. From 67°N to 70°N at 25°E Morana Chasma is a darker line, not more than 10 km wide, except for its northernmost 50 km. East of Hina Chasma there occurs

the chevron pattern in the tessera, but it is not marked, and south of 65°N it fades out. East of 26°E, where the elevation drops below 4.0 km, the tessera fade out completely into a smooth plain.

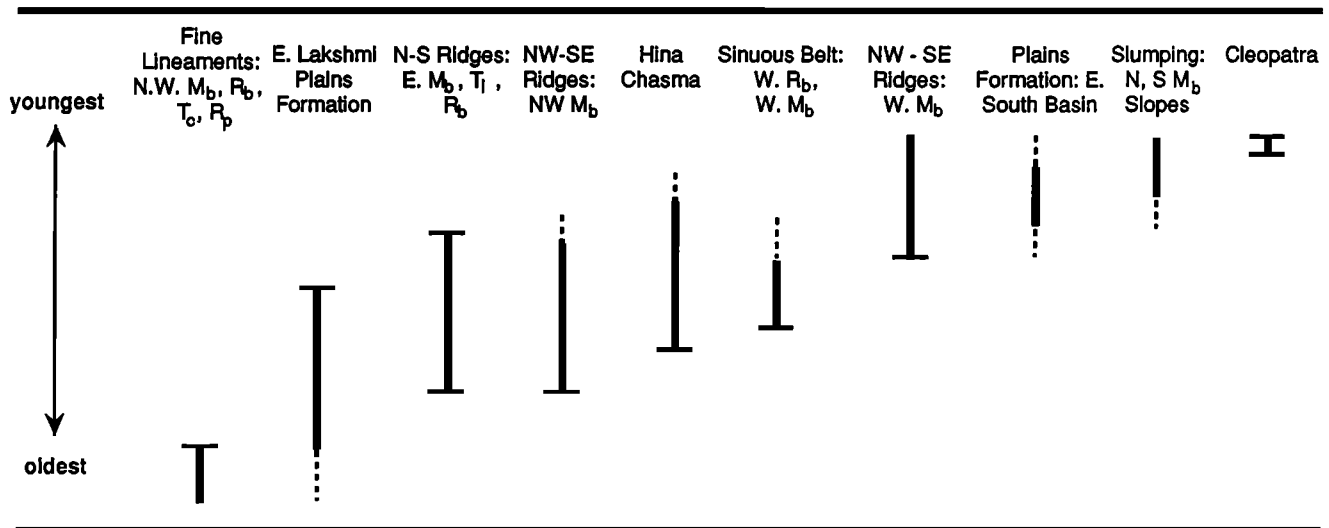
Plumose Ridges (F-MIDRPs 65N018, 60N016, 60N026). The area south of 65°N and between 16°E and 20.5°E is not typical tessera, but rather is marked by a welter of fine lineaments. These fine NNW-SSE striations at 2-3 km intervals become more prominent with distance from Maxwell Montes. East of 20.5°E there are some more arcuate ridges, roughly NS with spacings of 5-15 km. A smooth bay 25 km x 90 km, containing a 30-km-long rille, exists around 58.8°N, 21.4°E. East of 25°E and south of 63°E there appears another sinuous lineament bundle, about 15 km wide and extending about 500 km. But the whole region is cutoff sharply to the southeast by a smooth plains deposit along a SSW-NNE line from 56°N, 21°E to 61°N, 27°E.

Interpretation. The Magellan data appear consistent with the main conclusions of *Bindschadler and Head* [1991] and *Vorder Bruegge and Head* [1990], i.e., horizontal convergence, followed by some gravitational relaxation, particularly on the flanks. This is not surprising, since the dominant arcuate ridge features strongly indicate EW convergence in the Central Ridged Tessera, an outboard plateau of Maxwell Montes. Also identified are lineaments at angles of about 45° to the ridges, west of Hina Chasma more likely indicative of contemporary stress patterns than past convergence directions.

More questionable is where this EW convergence ends; it is irksome that the solar conjunction gap occurs over Central Fortuna Tessera, where *Vorder Bruegge and Head* [1990] hypothesized a different contemporary direction.

Kinematic sequence (Figure 36). As discussed above, the topographic and geoid highs of central Ishtar strongly suggest that it is a region of vigorous contemporary convergent tectonics. This contemporary vigor is most evident in the west slope of Maxwell Montes, which has a steep slope; marked parallel folding; and few indications of either earlier tectonic patterns or gravitational relaxation (except to the extreme flanks). The northwest arm and the east slope of Maxwell Montes also are much deformed, but they have more variety, sugges-

Sequence of Events: Maxwell Montes and Western Fortuna Tessera



*Note: N.W. Mb = Northwest Arm and Slope region;
 E. Mb = Maxwell East Slope region;
 W. Mb = Maxwell West Slope region;
 W. Rb = Samuni Dorsa

Fig. 36. Relative ages of features in Maxwell and Western Fortuna Tessera provinces. Abbreviations in the headings: N.W.Mb = Northwest Arm and Slope Region; E.Mb = Maxwell East Slope Region; W.Mb = Maxwell West Slope Region; W.Rb = Samuni Dorsa.

tive of greater age. The east slope is marked by the great impact crater Cleopatra, of a size that occurs at intervals of more than 100 m.y. It is thus ambiguous as to whether the physiographic modification by Cleopatra predates or is essentially contemporaneous with the tectonics giving the observed form to the west slope.

Sharing the kinematic patterns of the Maxwell West Slope and Crest are two regions within Fortuna Tessera: the Central Ridged Tessera and the Ridge Belt. Semuni Dorsa is also shaped by the sinuous west margin, and the dominant ridges in the central region parallel Maxwell's folds. But both these regions have underlying patterns indicative of different tectonic patterns in the past. Finally, the lower regions of Western Fortuna Tessera are less marked by contemporary tectonics, and have more evidence of volcanism and gravitational relaxation.

3. SYNTHESIS OF OBSERVATIONS AND INTERPRETATIONS

The Magellan imagery enables a more accurate and detailed geomorphic mapping, settling debates generated by the Venera data (e.g., Cleopatra is clearly an impact feature, not a caldera [Kirk *et al.*, manuscript in preparation]). This geomorphic mapping also contributes significantly to the broader scale interpretation of the major features: the relative roles of constructional and modificational tectonic processes, volcanism, and impacts. But it is desirable to synthesize the contemporary kinematics and, beyond that, a history of Ishtar. Such a synthesis must draw together the indications of current and past deformations from different provinces. The ability to reconstruct the past varies greatly among the provinces, probably being least in the most intensely folded mountain belts and greatest in the relatively smooth lowland basins.

In this section, we collect the various parts into terrain types, identify common features of a type, plus variations within them. These types are (1) upland plains; (2) mountain belts; (3) outboard plateaus; (4) smooth scarps; and (5) basins. The order of presentation is from the center outward. The one great upland plains feature, Lakshmi Planum, does have a quite central character and thus a central role, while the mountain belts and smooth scarps are peripheral thereto and the outboard plateaus and basins in turn are peripheral to the belts and smooth scarps. Furthermore, the belts and plateaus are appropriately considered before the scarps and basins because they are more closely related to contemporary tectonics.

Placing the upland plain first gives an orientation for the most difficult task, the inference of structural patterns cutting across provinces: to first order, radial in-or-out, tangential clockwise-or-counter, but not neglecting either secondary internal patterns or broader patterns reflecting processes influencing areas even larger than Ishtar.

3.1. Upland Plains

As discussed in section 2.1, there appears to be a well-defined age sequence from the ridged terrains (centering near 65°N, 345°E) to the smooth plains to caldera-associated and margin-associated deformations.

The most pronounced of the margin-associated deformations are those paralleling the most prominent features, most notably, the Rangrid Fossae paralleling the western front of Maxwell Montes near 62°N, 357°E. Those paralleling the North and South scarps are narrow but distinct; paralleling Danu Montes, rather faint.

Markedly absent are (1) major rifts, comparable to those in Beta Regio and Atla Regio; and (2) any embayment by the upland plains material of the three mountain belts, Maxwell Montes, Freyja Montes, and Danu Montes.

3.2. Mountain Belts

All the mountain belts thus appear to be thrust over the plains, indicating compressive shortenings later than the lava flows. But the altimetry indicates that only Maxwell and Freyja Montes have trenches [Solomon *et al.*, this issue], less than a kilometer deep, mild compared to island arcs on Earth. A better terrestrial analogue might be the Ganges trough associated with the continent-continent collision of India and Asia, except that Maxwell Montes is associated with a marked geoid high, rather than a low, as is the Himalayan-Tibetan complex.

Of the three belts, only Danu Montes has lava channels extending down slope into the plains (except possibly the sinuous lineament running EW through Maxwell Montes near 66°N). Danu Montes (including Vesta Rupes) also has the most extensional features, suggestive of gravitational modification, among the three belts.

All mountain belts have more indications of volcanism on their outboard slopes, although in the case of Maxwell Montes it appears confined to flows triggered by the Cleopatra Impact. Magnani (58.6°N, 337.1°E), 25 km in diameter (thus created by a bolide much less massive than Cleopatra's), has no indication of impact-associated melt: even its central floor is radar-bright, thus rough. Both Danu Montes and Freyja Montes have pits on their outboard slopes, some of them aligned, indicative of volcanism facilitated by extensional tectonics.

The three belts all have two arms forming shapes concave to the upland plain. At the bends between the arms there appear to be appreciably greater deformations than in the arms in all three cases, although generally the folding and faulting in Danu Montes is less intense than in Freyja or Maxwell Montes. Within each of the three belts, one arm appears to have more intense folding: the eastern, in Danu and Maxwell Montes; the western, in Freyja Montes, suggesting that it is more recent. Overlaps confirming this suggestion are hard to define in Danu and Maxwell but exist in Freyja.

In the more intensely folded parts of all belts, the ridge spacing is quite variable. These spacings are mainly 3-10 km but in places are as close as 1 km or as wide as 20 km. These spacings are consistent with a shallow depth, a few kilometers, to a weak layer of accommodation [Zuber, 1987].

All mountain belts have very bright crests. In Maxwell Montes, the brightness extends over a wide area, about 500 x 500 km, covering a fairly wide range of image textures. One thing in common over this area is an elevation greater than 5.0 km, suggesting that the brightness is a chemical effect. But the crest of Danu is inferred to have appreciable intrinsic reflectivity, as well as roughness, even though it does not reach this elevation. In general, the correlation of brightness with elevation is not as systematic as it appears to be for most of Maxwell; the cause of intrinsic brightness is still not understood [Klose *et al.*, this issue].

3.3. Outboard Plateaus

Maxwell Montes, Freyja Montes, and the eastern arm of Danu Montes all have highly deformed regions on the side away from Lakshmi Planum. These regions are appreciably lower in elevation than the mountain belt crests and extend 100-1000 km before a final descent to the lowland plain. The widths of these plateaus vary with the heights of the mountain belts, from 100-200 km for Clotho Tessera, southeast of Danu Montes, to almost 1000 km for Western Fortuna Tessera, east of Maxwell Montes.

Also correlated with mountain belt characteristics are the intensity of deformation and degree of modification in these outboard plateaus. Most intense and monotonous among the plateaus is the Central

Ridged Tessera of Western Fortuna. Although there are many finer lineaments in directions other than the NS arcuate ridges 15-25 km apart, few cut across the ridges. Itzpapalotl Tessera, north and northeast of Freyja Montes, has more variety: within 200 km of the crest, there exist radar-dark, hence smooth, areas 30 km in width, including a marked sinuous rille about 1 km wide and more than 100 km long (76.5°N, 336°-340°E) [see *Baker et al.*, this issue]. But beyond this smooth embayment there is yet more rugged tessera, until the abrupt drop of 2 km at Uosar Rupes (near 80°N). See Figures 35 and 20.

In all the outboard plateaus there are lineaments at appreciable angles to the main trends. In some cases, these crosscutting trends can be traced into the adjacent lowlands. They are much less marked than the strike-slip trends seen in imaging radar of Asia north of the Himalayan orogeny on Earth, and they are not as readily relatable to features likely to be due to contemporary tectonics, such as the dominant banded terrain of Maxwell Montes. Hence, in view of the lack of erosion, they are more likely relicts of earlier kinematic patterns.

3.4. Smooth Scarps

The margins of Lakshmi Planum 338°-353°E in the north and 340°-5°E in the south are strikingly smooth compared to the mountain belts, despite being topographic drops of 2-3 km within 40-70 km. The smooth scarps also contrast with the mountain belts in that their horizontal shapes are convex toward the upland plain, see Figures 1 and 3.

In the north, the convexity is one great sweep over about 900 km, making a smooth bend of slightly more than 90°, centered near 67°N, 344°E. The north-south arm of this sweep is the smoother, but nonetheless marked throughout by fine troughs less than 1 km wide, over a width of 40-80 km, contrasting with the radar dark plains of the plateau and the anastomosing lineaments of the basin. The only prominent crosscut of these trends is an irregular trough 5 km wide 68°-69°N, 343°E. But in the east-west arm, east of 345°E, the downslope of the scarp is cut by many more rilles 1-3 km wide at 4-12 km intervals.

In the south, the convexity is broken up into three scallops, varying from a 180° semicircle 180 km in diameter in the west to a smooth bend of only 20° over 270 km in the east. There also is a marked decrease from west to east in the number of troughs parallel to the scarp. But the topographic drop remains the same, and near 359°E, just south of a caldera, the imagery is uniformly dark. The number of upland troughs at appreciable angles to the scarps increases appreciably from west to east.

The scarps are not entirely without areas of disrupted terrain. In the north, there occur a series of troughs at the eastern extreme, 345.5°-348°E, at the apex of the northwest arm of Maxwell Montes. In the south, there occur severe lineaments and two large troughs in the cusp between the Central and West basins. In both north and south, these distorted terrains are of limited extent, less than 150 km, and do not appear to be related to trends in the basins below. However, those in the south scarp are among the features paralleling the Maxwell front, 500 km to the east.

3.5. Basins

The basins below the scarps are similar in appearance to the lowland plains that dominate the surface of Venus. However, they do have appreciable elevation: about 2 km above MPR in the south and 3.5 km in the north. Like most of the lowland plains, they contain a variety of patterns, suggestive of long geological histories with

changes in trends from one epoch to another. In both cases, sequences of events can be inferred. In the north basin, the more recent events appear associated with either Itzpapalotl to the northwest or Maxwell to the southeast, but in the south basin they seem more local and not so directly related to whatever forces raise the major features of Ishtar. In particular, there is a striking absence of any continuation of the structural patterns in the imagery of Maxwell Montes to the plains to its south.

4. SUMMARY AND INFERENCES

Ishtar Terra is one of five regions on Venus that contain elevations more than 4.0 km above MPR. The other four regions are all at low latitudes and appear to fall into two pairs on the basis of imagery and gravimetry, as well as altimetry.

One pair of highland regions appear to be mantle upflows surmounted by volcanic constructs: Atla Regio (0°N, 195°E) and Beta Regio (30°N, 185°E) are characterized by extensive areas of lava flows, with little thrust faulting or folding, the main deformations being rifts [*Head et al.*, this issue]. Atla and Beta are the two greatest geoid highs in the gravity field of Venus, over 120 in the solution by *Smith and Nerem* [1992], correlating very closely with the topography. These geoid: topography ratios yield apparent compensation depths over 200 km deep [*Smrekar and Phillips*, 1991], suggestive of deep mantle plumes.

The other two highlands appear to be belts of convergence, leading to topographic uplift and downflow: Ovda Regio (5°S, 90°E) and Thetis Regio (10°S, 130°E) are characterized by extensive distorted mountain belts and tesserae, with little or no extensional deformation and only occasional patches suggestive of volcanism [*Bindschadler et al.*, this issue]. Ovda and Thetis are also geoid highs, but appreciably milder, with peaks of 40 and 75 m, respectively. These geoid highs have greater lateral extent than those of the volcanic constructs, and do not correlate as closely with the topography. These geoid signatures suggest shallower, more complicated density variations in the convergent belts than in the volcanic uplifts [*Bindschadler et al.*, this issue].

Ishtar Terra appears to have characteristics in common with both the volcanic uplifts and convergent belts: the imagery contains extensive areas of both volcanic flows and tectonic deformations. The volcanic flows of Lakshmi could be several 100 m.y. old. But even with a stiff upper mantle, a major geoid high could not be maintained without contemporary mantle convection. Unfortunately, Ishtar is too far north to obtain an accurate geoid from the Pioneer Venus data: the 36th degree field yields a high of about 65 meters 500 km south of the crest of Maxwell Montes, with a bland positive area over all of Lakshmi, Freyja, and Western Fortuna provinces, as well as Maxwell: see Figure 3. The true geoid high could be appreciably greater, perhaps over 100m, and centered farther north (the eighth degree field does center over Maxwell Montes), but this is not necessarily so. The regional solutions of *Grimm and Phillips* [1991] get apparent depths of compensation of 130-180 km, more easily explained by upwelling. The problem is to reconcile this finding with the absence of large rifts and strongly convergent appearance of the mountain belts [*Roberts and Head*, 1990a,b; *Bindschadler et al.*, 1990, this issue; *Grimm et al.*, 1992]. Two-dimensional finite element modelling of a convergent flow in a crust and stiff mantle reproduces the topography in a rather complex evolution taking several 100 m.y. [*Lenardic et al.*, 1991, 1992].

It is tempting to suggest that Ishtar contains a combination of flows: not only convergence, leading to downflow, but also an upflow. Ishtar is probably similar to the Earth in that the recent-to-contemporary dynamics, which have the dominant influence on topographic

and geoidal elevations, are strongly influenced by the past, mainly through old relatively stable blocks.

The Magellan imagery contributes by constraining likely kinematic patterns and their sequence. The volcanic flows of Lakshmi Planum are more recent than the ridged terrain they embay, suggesting that the latter is relict of a craton whose resistance to deformation led to the transfer of deformation elsewhere. All three mountain belts appear to have had tectonism continuing since the volcanic flows in the adjacent parts of Lakshmi Planum, since all of them appear to be thrust over the upland plain. Among the three mountain belts, there appears to be a sequence youngest-to-oldest of Maxwell-Freyja-Danu. This sequence is based mainly on the abundance, least-to-most, of indications of gravitational modification in these mountain belts. But this may be an oversimplification; details in the structural patterns of the mountain belts and their outboard plateaus suggest shifts in the magnitude and direction of thrusting affecting all the belts: north-to-south in Maxwell, with perhaps a clockwise rotation in the main direction; east-to-west in Freyja, with a counterclockwise rotation; and, most speculative, west-to-east in Danu. But structural patterns in the outboard plateaus and lowlands appear to be younger than the deformations forming Freyja and Danu. In the south basin, these patterns seem related to Maxwell Montes, but in the north, in central Itz'papatol' and beyond, they seem unrelated to Ishtar Terra.

The smooth scarps are enigmatic; Venus lacks Earthlike erosion to remove the irregularities expected with such marked topographic jumps. Smoothing by flow in the weak layer of the lower crust seems most plausible, since it would have obliterated small features much faster than large [Bird, 1991]. Even so, the scarps are surprisingly steep. Also this mechanism would have left a fractured terrain, like the hill at 72°N, 342°E. Hence it seems covering up by lava flows is required. Corroborative of this suggestion is that the areas on each scarp pointed out as more deformed locally (347°E in the north; 350°E in the south) both have higher elevations than the rest of their respective scarps. There also is no constraint that the volcanism of Lakshmi Planum all occurred in one epoch; indeed, there are several evidences of more than one episode, such as the cutoff of the fractured terrain (Tf) near 68°N, 337°E.

The scarps, as well the secondary structural patterns in the outboard plateaus, emphasize that Ishtar is definitely not uniformly young. The only available estimator of age is crater density [Phillips *et al.*, this issue]. In the 5×10^6 km² bounded by 57°N, 75°N, 330°E, 30°E, there are 10 impact craters identified, close to the global average density, which corresponds to a mean surface age of about 500 My. More germane to the question raised here is the distribution of crater ages for an area of extent much larger than the average crater spacing. The Ishtar area studied in this paper is about 36 times the maximum volcanic patch area in the random volcanism steady-state model of Phillips *et al.* [this issue]. From this model, the median likely age for the oldest crater in a 5×10^6 km² area with ten craters is about 1.4 Ga, with a 50% probability range of 1.0-1.9 Ga and a 90% range of 0.7-2.3 Ga [Kaula, manuscript in preparation]. Thus Ishtar has a high probability of containing relicts going back more than 1.0 Ga in age. In this time, there could have been considerable shift of the tectonic and volcanic forces affecting Ishtar. Just how, and why, these shifts occur is obscure, compared to Earth, because Venus lacks an asthenosphere [Kiefer *et al.*, 1986; Phillips, 1990]. This lack leads to changes being generated much more by conditions within the upper mantle that can be quite regional, rather than by conditions associated with large tectonic plates generated by global scale flow. In other words, tectonics on Venus cannot be expected to occur in clearly defined belts and zones as it is on most of Earth, because there is not a well-defined pattern of plates. Possibly similar on Earth are continental areas of thick crust [Solomon *et al.*, this issue]. But even there

conditions hidden at depth on Venus have greater effect on surface tectonics because of the lack of an asthenosphere: there is a tighter coupling of the layer immediately below the crust, which determines the regional patterns seen in imagery, to the interior.

Ishtar's structure evidences that the pattern of flow can vary appreciably over a few hundred kilometers within Venus: a contrast to Earth (certainly to Earth's oceans), where patterns are controlled over thousands of kilometers by the tectonic plates. Because of the high upper mantle viscosity required by the high geoid: topography ratios, Venus probably gets rid of its heat in a style that is more regional, i.e., shorter wavelength, than does Earth [Kaula, 1992]. Probably both the material velocities and rates of change in the pattern are somewhat slower than Earth's. The result for a complex of heterogeneities generated in earlier times, such as Ishtar Terra, is a marked variation of characteristics over distances of a few hundred kilometers.

Doubtless there is vigorous contemporary convergence contributing a major share to the uplift of Maxwell Montes. Aspects of contemporary dynamics that are more in doubt are whether there is continued strong underthrusting under Freyja and whether there is an upflow under Lakshmi Planum. If there is, then there can exist marked variations in the flow pattern of Venus's upper mantle over distances of a few hundred kilometers, as in some convergent zones on Earth, despite the high viscosity. It seems clear that over the long past of Ishtar Terra there has been a shifting around of tectonic and volcanic activity, much influenced by structures relict from earlier phases. The time scale of these shifts is unsure, but it is likely, from the complexity of Ishtar structures as well as crater density, that they have gone on for more than 1.0 b.y., as well as generating structures that are relatively new. But we cannot hope to resolve conclusively the contemporary density structure, and thence the flow patterns, without a more detailed gravity field, which requires circularization of the orbit of Magellan.

Acknowledgments. We are very grateful to Richard W. Vorder Bruegge for performing an extremely thorough review, which greatly influenced revision of the paper. This work was supported by the NASA Magellan Project through JPL contracts 957088 (Brown), 958497 (UCLA), 975072 (SMU), and 957070 (MIT).

REFERENCES

- Baker, V.R., G. Komatsu, T.J. Parker, V.C. Gulick, J.S. Kargel, and J.S. Lewis, Channels and valleys on Venus: Preliminary analysis of Magellan data, *J. Geophys. Res.*, 97, 13,421-13,444, 1992.
- Barsukov, V.L., et al., The geology and geomorphology of the Venus surface as revealed by the radar images obtained by Venera 15 and 16, *Proc. Lunar Planet. Sci. Conf. 16th, Part 2, J. Geophys. Res.* 91, suppl., D378-398, 1986.
- Berthe, D., P. Choukroune, and P. Jegouzo, Orthogneiss, mylonite and noncoaxial deformation of granite: The example of the South American shear zone, *J. Struct. Geol.*, 1, 31-42, 1979.
- Bindschadler, D.L., and J.W. Head, Tessa terrain, Venus: Characterization and models for origin and evolution, *J. Geophys. Res.*, 96, 5889-5907, 1991.
- Bindschadler, D.L., G. Schubert, and W.M. Kaula, Mantle flow tectonics and the origin of Ishtar Terra, Venus, *Geophys. Res. Lett.*, 17, 1345-1348, 1990.
- Bindschadler, D.L., G. Schubert, and W.M. Kaula, Coldspots and hotspots: Global tectonics and mantle dynamics of Venus, *J. Geophys. Res.*, 97, 13,495-13,532, 1992.
- Bird, G.P., Lateral extrusion of lower crust from under high topography in the isostatic limit, *J. Geophys. Res.*, 96, 10,275-10,286, 1991.
- Burt, J.D., and J.W. Head, Types and occurrences of volcanic features and their relations to tectonics of Freyja and Danu Montes, *Lunar Planet. Sci. Conf.*, 22, 159-160, 1991.
- Campbell, D.B., J.W. Head, J.K. Harmon, and A.A. Hine, Venus: Identification of banded terrain in the mountains of Ishtar Terra, *Science*, 221, 644-647, 1983.

- Corsini, M., A. Vaquez, C. Archanjo, and E.F.J. de Sa, Strain transfer at continental scale from a transcurrent shear zone to a transpressional fold belt: The Patos-Serido system, northeastern Brazil, *Geology*, **19**, 586-589, 1991.
- Grimm, R.E., and R.J. Phillips, Tectonics of Lakshmi Planum, Venus: Tests for Magellan, *Geophys. Res. Lett.*, **17**, 1349-1352, 1990.
- Grimm, R.E., and R.J. Phillips, Gravity anomalies, compensation mechanisms, and the geodynamics of western Ishtar Terra, Venus, *J. Geophys. Res.*, **96**, 8305-8324, 1991.
- Grimm, R.E., R.H. Herrick, and R.J. Phillips, Highlands, III, On the origin and evolution of large uplands on Venus, *Lunar. Planet. Sci. Conf.*, **23**, 453-454, 1992.
- Gundmundsson, A., Geometry, formation, and development of tectonic fractures on the Reykjanes Peninsula, southwest Iceland, *Tectonophysics*, **139**, 295-308, 1987.
- Hansen, V. L., Regional non-coaxial deformation of Venus: Evidence from western Itzppalodl Tessera, *Lunar. Planet. Sci. Conf.*, **23**, 479-480, 1992.
- Head, J.W., The formation of mountain belts on Venus: Evidence for large-scale convergence, underthrusting, and crustal formation in Freyja Montes, Ishtar Terra, *Geology*, **18**, 99-102, 1990.
- Head, J.W., and L. Wilson, Magma reservoirs and neutral buoyancy zones on Venus: Implications for the formation and evolution of volcanic landforms, *J. Geophys. Res.*, **97**, 3877-3904, 1992.
- Head, J.W., R.W. Vorder Bruegge, and L.S. Crumpler, Venus orogenic environments: architecture and origin, *Geophys. Res. Lett.*, **17**, 1337-1340, 1990.
- Head, J.W., D.B. Campbell, C. Elachi, J.E. Guest, D.P. McKenzie, R.S. Saunders, G.G. Schaber, and G. Schubert, Venus volcanism: Initial analysis from Magellan data, *Science*, **252**, 276-288, 1991.
- Head, J.W., L.S. Crumpler, J.C. Aubele, J.E. Guest, and R.S. Saunders, Venus volcanism: Classification of volcanic features and structures, associations, and global distribution from Magellan data, *J. Geophys. Res.*, **97**, 13,153-13,197, 1992.
- Janle, P., and D. Jannsen, Tectonics of the southern escarpment of Ishtar Terra on Venus from observations of morphology and gravity, *Earth Moon Planets*, **31**, 141-155, 1984.
- Kaula, W.M., Venus: A contrast in evolution to Earth, *Science*, **247**, 1191-1196, 1990.
- Kaula, W.M., Compositional evolution of Venus, in *Chemical Evolution of the Earth and Planets*, Geophys. Monogr. Ser., edited by E. Takahashi, E. Jeanloz, and D. Rubie, AGU, Washington, D.C., in press, 1992.
- Kaula, W.M., Implications of crater distribution for surface ages on Venus, *Geophys. Res. Lett.*, manuscript in preparation.
- Kiefer, W.S., M.A. Richards, B.H. Hager, and B.G. Bills, A dynamic model of Venus's gravity field, *Geophys. Res. Lett.*, **13**, 14-17, 1986.
- Kirk, R.L., G.G. Schaber, O.V. Nikolayeva, B.A. Ivanov, A.V. Potapov, and A.T. Basilevsky, Cleopatra Crater, Venus: The Magellan view, *J. Geophys. Res.*, manuscript in preparation.
- Klose, K.B., J.A. Wood, and A. Hashimoto, Mineral equilibria and the high radar reflectivity of Venus mountaintops, *J. Geophys. Res.*, this issue.
- Lenardic, A., W.M. Kaula, and D.L. Bindschadler, The tectonic evolution of western Ishtar Terra, Venus, *Geophys. Res. Lett.*, **18**, 2209-2212, 1991.
- Lenardic, A., W.M. Kaula, and D.L. Bindschadler, Maxwell and the Andes: analogous structures?, *Lunar. Planet. Sci. Conf.*, **23**, 773-774, 1992.
- Masursky, H., E. Eliason, P.G. Ford, G.E. McGill, G.H. Pettengill, G.G. Schaber, and G. Schubert, Pioneer Venus radar results: Geology from images and altimetry, *J. Geophys. Res.*, **85**, 8232-8260, 1980.
- Pettengill, G.H., P.G. Ford, and R.J. Wilt, Venus surface radiothermal emission as observed by Magellan, *J. Geophys. Res.*, **97**, 13,091-13,102, 1992.
- Phillips, R.J., Convection-driven tectonics on Venus, *J. Geophys. Res.*, **95**, 1301-1316, 1990.
- Phillips, R.J., R.F. Raubertas, R.E. Arvidson, I.C. Sarkar, R.R. Herrick, N. Izenberg, and R.E. Grimm, Impact crater distribution on Venus: Implications for planetary resurfacing history, *J. Geophys. Res.*, this issue.
- Pronin, A. A., The structure of Lakshmi Plateau, an indication of asthenosphere horizontal flows on Venus, *Geotectonics*, **20**, 271-280, 1986.
- Roberts, K.M., and J.W. Head, Lakshmi Planum, Venus: Characteristics and models of origin, *Earth Moon Planets*, **50/51**, 193-249, 1990a.
- Roberts, K.M. and J.W. Head, Western Ishtar Terra and Lakshmi Planum, Venus: Models of formation and evolution, *Geophys. Res. Lett.*, **17**, 1341-1344, 1990b.
- Ronca, L.B., and A.T. Basilevsky, Maxwell Montes and Tessera Fortuna: A study of Venera 15 and 16 radar images, *Earth Moon Planets*, **36**, 23-39, 1986.
- Schaber, G.G., R.G. Strom, H.J. Moore, L.A. Soderblom, R.L. Kirk, D.J. Chadwick, D.D. Dawson, L.R. Gaddis, J.M. Boyce, and J. Russell, Geology and distribution of impact craters on Venus: What are they telling us? *J. Geophys. Res.*, **97**, 13,252-13,301, 1992.
- Shimamoto, T., The origin of S-C mylonites and a new fault zone model, *J. Struct. Geol.*, **11**, 51-64, 1989.
- Smith, D. E., and R. S. Nerem, Gravity field modeling of Mars and Venus at NASA/GSFC, in *Gravity Field Determination from Space and Airborne Measurements*, edited by O. L. Colombo, Springer-Verlag, New York, in press, 1992.
- Smrekar, S. E. and R. J. Phillips, Geoid to topography ratios and their implications, *Earth Planet. Sci. Lett.*, **107**, 582-597, 1991.
- Smrekar, S.E., and S.C. Solomon, Gravitational spreading of high terrain in Ishtar Terra, Venus, *J. Geophys. Res.*, this issue.
- Solomon, S.C. and J.W. Head, Venus banded terrain: Tectonic models for band formation and their relationship to lithosphere thermal structure, *J. Geophys. Res.*, **84**, 6885-6987, 1984.
- Solomon, S.C., J.W. Head, W.M. Kaula, D. McKenzie, B. Parsons, R.J. Phillips, G. Schubert, and M. Talwani, Venus tectonics: Initial analysis from Magellan, *Science*, **252**, 297-312, 1991.
- Solomon, S.C., S.M. Smrekar, D.L. Bindschadler, R.E. Grimm, W.M. Kaula, G.E. McGill, R.J. Phillips, R.S. Saunders, G. Schubert, S.W. Squyres, and E.R. Stofan, Venus tectonics: An overview of Magellan observations, *J. Geophys. Res.*, **97**, 13,199-13,255, 1992.
- Stofan, E. R., J. W. Head, and D. B. Campbell, Geology of the southern Ishtar Terra/Guinevere and Sedna Planitia region of Venus, *Earth Moon Planets*, **38**, 183-207, 1987.
- Stofan, E.R., V.L. Sharpton, G. Schubert, G. Baer, D.L. Bindschadler, D. M. Janes, and S.W. Squyres, Global distribution and characteristics of coronae and related features on Venus: Implications for origin and relation to mantle processes, *J. Geophys. Res.*, **97**, 13,347-13,578, 1992.
- Tyler, G.L., P.G. Ford, D.B. Campbell, C. Elachi, G.H. Pettengill, and R.A. Simpson, Magellan: Electrical and physical properties of Venus's surface, *Science*, **252**, 265-270, 1991.
- Vorder Bruegge, R.W., and J.W. Head, Fortuna Tessera, Venus: evidence of horizontal convergence and crustal thickening, *Geophys. Res. Lett.*, **16**, 699-702, 1989.
- Vorder Bruegge, R.W., and J.W. Head, Tectonic evolution of eastern Ishtar Terra, Venus, *Earth Moon Planets*, **50/51**, 251-304, 1990.
- Vorder Bruegge, R.W., J.W. Head, and D.B. Campbell, Orogeny and strike-slip faulting on Venus: Tectonic evolution of Maxwell Montes, *J. Geophys. Res.*, **95**, 8357-8391, 1990.
- Vorder Bruegge, R.W., and J.W. Head, Processes of formation and evolution of mountain belts on Venus, *Geology*, **19**, 885-888, 1991.
- Zuber, M. T., Constraints on the lithospheric structure of Venus from mechanical models and tectonic surface features, *Proc. Lunar Planet. Sci. Conf.*, Part 2, *J. Geophys. Res.*, **92**, suppl., E541-551, 1987.

D. L. Bindschadler and W. M. Kaula, Department of Earth and Space Sciences, University of California, Los Angeles, CA 90024-1567.

R. E. Grimm, Department of Geology, Arizona State University, Tempe, AZ 85287.

V. L. Hansen, Department of Geological Sciences, Southern Methodist University, Dallas, TX 75275.

K. M. Roberts, Department of Geological Sciences, Brown University, Providence, RI 02912.

S. E. Smrekar, Department of Earth, Atmospheric, and Planetary Sciences, Massachusetts Institute of Technology, Cambridge, MA 02139-4307.

(Received October 16, 1991;

revised July 13, 1992;

accepted July 13, 1992.)